

**Flanders**  
State of  
the Art

21\_091\_1  
FH reports

## ShorelinesS Knokke-Heist model

Set up of the numerical model

DEPARTMENT  
MOBILITY &  
PUBLIC  
WORKS

[www.flandershydraulics.be](http://www.flandershydraulics.be)

# ShorelineS Knokke-Heist model

## Set up of the numerical model

Trouw, K.; Verwaest, T.; Dujardin, A.; Dan, S.

### Legal notice

Flanders Hydraulics is of the opinion that the information and positions in this report are substantiated by the available data and knowledge at the time of writing.

The positions taken in this report are those of Flanders Hydraulics and do not reflect necessarily the opinion of the Government of Flanders or any of its institutions.

Flanders Hydraulics nor any person or company acting on behalf of Flanders Hydraulics is responsible for any loss or damage arising from the use of the information in this report.

### Copyright and citation

© The Government of Flanders, Department of Mobility and Public Works, Flanders Hydraulics 2024  
D/2024/3241/295

This publication should be cited as follows:

**Trouw, K.; Verwaest, T.; Dujardin, A.; Dan, S.** (2024). ShorelineS Knokke-Heist model: Set up of the numerical model. Version 4.0. FH Reports, 21\_091\_1. Flanders Hydraulics: Antwerp

Reproduction of and reference to this publication is authorised provided the source is acknowledged correctly.

### Document identification

Customer:	DELTAIRES	Ref.:	WL2024R21_091_1
Keywords (3-5):	Coastline changes, beach evolution, ShorelineS, Knokke-Heist		
Knowledge domains:	Coastal Protection> erosion protection coast>beach>numerical modelling		
Text (p.):	47	Appendices (p.):	70
Confidential:	<input checked="" type="checkbox"/> No	<input checked="" type="checkbox"/> Available online	

Author(s):	Trouw, K.; Verwaest, T.; Dujardin, A.; Dan, S.
------------	--

### Control

	Name	Signature
Reviser(s):	Verwaest, T.	Getekend door:Toon Verwaest (Signatur Getekend op:2024-12-10 11:46:00 +01:0 Reden:Ik keur dit document goed  
Project leader:	Dan, S.	Getekend door:Sebastian Dan (Signature Getekend op:2024-12-10 11:51:28 +01:0 Reden:Ik keur dit document goed  

### Approval

Head of Division:	Bellafkih, K.	Getekend door:Abdelkarim Bellafkih (Sig Getekend op:2024-12-10 17:58:54 +01:0 Reden:Ik keur dit document goed  
-------------------	---------------	---

# Abstract

Deltares and IHE Delft Institute for Water Education developed ShorelineS (Roelvink et al, 2020), a 1 line open source code to model longshore transport and coastline changes. Led by Deltares, an international partnership conducted a research project aimed at transforming the existing academic shoreline model ShorelineS (open source code in MATLAB) into a user-friendly engineering tool for long-term shoreline morphology using open software over a period of two years (2022 – 2024). The ambition is to develop this tool into a global community, analogous to XBeach, following the principles of open-source software. Through the Dutch TKI program (TKI stands for Top Consortia for Knowledge and Innovation), co-financing has been granted, based on the in-kind and cash contributions of the partners. Flanders Hydraulics conducted a case study for the Belgian coast, providing feedback that has been useful for the further development of ShorelineS. Among other things, the Belgian case study will allow testing the incorporation of tidal currents, as tides are relatively important for the evolution of the Belgian coastline.

Another important aspect was the incorporation of submerged groins. Up to now, coastline models were only able to model emerged groins.

# Contents

Abstract .....	III
Contents .....	IV
List of tables.....	VI
List of figures .....	VII
1 Introduction.....	1
2 Bathymetry .....	2
3 Groynes.....	6
4 Hydrodynamic boundary conditions .....	7
4.1 Wave conditions.....	7
4.2 Tidal velocities.....	12
4.2.1 Introduction .....	12
4.2.2 Effect on longshore sediment transport.....	14
4.2.3 Comparison with Scaldis-Coast.....	25
5 Adaptations to the ShorelineS modules.....	27
5.1 Run_shorelineS.m .....	27
5.2 ShorelineS.m .....	27
5.3 Transport.m.....	27
5.4 Tide_wave_transport.m.....	28
5.5 Wave_current.m .....	28
5.6 soulsy_van_rijn.m .....	28
5.7 transport_bypass .....	28
5.8 Prepare_transport.m .....	28
5.9 Prepare_structures.m .....	29
5.10 Initialize_defaultvalues.m .....	29
5.11 get_timesteps .....	29
6 Run_shorelineS -parameters .....	30
7 Final simulations.....	33
7.1 Introduction .....	33
7.2 Observed volume changes .....	33
7.3 Modelled volume changes .....	37
7.4 Other observations .....	43
8 Recommendations.....	46

9	References .....	47
Appendix 1	Groynes Knokke-Heist .....	A1
Appendix 2	Bypass over low crested, sloping groynes in ShorelineS - Memo .....	A14
Appendix 3	Generation of tidal input files for ShorelineS.....	A51
Appendix 4	Kustlijnveranderingen te Knokke-Heist in de afgelopen 50 jaar – Memo (deel 1) .....	A53
Appendix 5	Kustlijnveranderingen te Knokke-Heist in de afgelopen 50 jaar – Memo (deel 2) .....	A62

## List of tables

Table 1. Output parameters for different directions with and without tide. ....	22
Table 2. Influence of profile shape on longshore transport.....	23
Table 3. Observed erosion/sedimentation trends (in m <sup>3</sup> /m/y) in the period 1999-2004/2007) (based on data of Houthuys et al, 2022). ....	37
Table 4. Modelled erosion/sedimentation rates (m <sup>3</sup> /m/year) for a period of 3 years starting from 1 <sup>st</sup> of October 1999.....	38
Table 5. Modelled erosion/sedimentation per year (scenario with real groynes).....	40

# List of figures

Figure 1. Bathymetry (m TAW) NJ2019. ....	3
Figure 2. Cross shore profiles (m TAW) NJ2019. (legend: e.g. 73 means at X= <b>73</b> .000 m Lambert72 .....	3
Figure 3. Beach slopes. ....	4
Figure 4. Example of smoothed coastline. ....	5
Figure 5. Coast line and groynes.....	5
Figure 6. Example of a groyne representation. ....	6
Figure 7. Locations of wave climates (DTM in m TAW).....	7
Figure 8. Longshore sediment transport for different years (ShorelineS model April 2023, without groins); positive is towards NL.....	8
Figure 9. Wave climates 2000 and 2001. ....	9
Figure 10. Distribution of longshore transport over the wave directions (e.g. the wave direction $-45^{\circ}$ ( $+2.5^{\circ}$ ) contributes for 3.5% of the total eastward transport at $x=78.000$ m).....	9
Figure 11. Distribution of wave height and longshore transport over the wave directions at $x=74.000$ m)..	10
Figure 12. Distribution of wave height and longshore transport over the wave directions at $x=78.000$ m)..	10
Figure 13. Wave rose for the period 1999-2004. ....	11
Figure 14. Wave height non-exceedance curve. ....	11
Figure 15. Wave rose Scaldis-Coast model.....	12
Figure 16. Cross shore distribution of the tidal velocity (right axis: elevation, in m MSL).....	13
Figure 17. Tidal velocity as function of the water depth during a tidal cycle at MSL. ....	13
Figure 18. Effect of tide on the annual sediment transport.....	14
Figure 19. Variation of tidal velocities (blue: max/min: red: mean and stand. Dev). ....	15
Figure 20. Effect of tide on the cross shore distribution of longshore sediment transport. ....	15
Figure 21. Effect of tide on the cross shore distribution of longshore sediment transport (Scaldis-Coast model). Simulations MO6_004, MO6_003, MO6_005, MO6_009, MO6_011, MO6_014, MO6_012 respectively.....	16
Figure 22. Coastline and location of the studied profile. ....	16
Figure 23. Annual sediment transport at location $X=76150$ m with the ShorelineS Knokke model with and without the tide.....	17
Figure 24. Annual sediment transport per direction for $H_m0 = 1$ m on the foreshore. ....	18
Figure 25. Annual sediment transport per direction for $H_m0 = 2$ m on the foreshore. ....	18
Figure 26. Velocities across the cross-profile.....	19
Figure 27. Tidal velocities during the tide. ....	20
Figure 28. Velocity profiles. ....	20

Figure 29. Wave-driven velocity at the location of maximum transport (absolute values; location of max transport).....	21
Figure 30. Water depth at the location of maximum transport.....	21
Figure 31. Extra sediment transport due to the tide.....	22
Figure 32. Longshore transport over the profile for $H_m0=1$ m, direction $300^\circ$ at maximum low tide and maximum high tide (at the point of maximum transport). ....	23
Figure 33. Net transport (per year) for $H_m0=1$ m for different directions. ....	24
Figure 34. Net transport (per year) for $H_m0=2$ m for different directions. ....	24
Figure 35. Comparison between longshore velocity Scaldis-Coast model vs ShorelineS model. ....	26
Figure 36. Effect of ddeep and beach slope. ....	32
Figure 37. Sections (red numbering), coastline (blue line) and groynes (green). ....	34
Figure 38. Observed volumes ( $m^3/m$ ) for Duinbergen (sections 225-226). ....	34
Figure 39. Observed volumes ( $m^3/m$ ) for Albertstrand (sections 227-232).....	35
Figure 40. Observed volumes ( $m^3/m$ ) for Knokke-Zoute (sections 233-241).....	35
Figure 41. Observed volumes ( $m^3/m$ ) for Knokke-Lekkerbek (sections 242-249). ....	36
Figure 42. Observed volumes ( $m^3/m$ ) for Zwin (sections 250-255) (the seabed data point for 2003 is -190 $m^3/m$ ).....	36
Figure 43. Modelled longshore transport. ....	38
Figure 44. Modelled longshore transport with Scaldis-Coast (full lines) and Flemco (dotted). Orange:without wind, blue with wind. ....	39
Figure 45. Coastline after 3 years for the 3 different scenarios.....	39
Figure 46. Google Earth image of the effect of the most eastward groyne.....	40
Figure 47. Comparison between observed erosion/sedimentation rates and modelled (scaled).....	41
Figure 48. Temporal variation of in and out flux of stretch 4 (Lekkerbek).....	41
Figure 49. Longshore transport per year (case without groynes). ....	42
Figure 50. Temporal variation of $H_m0^{\cos(\alpha)}\sin(\alpha)$ .....	42
Figure 51. Time evolution of the coastline near the eastward boundary of stretch Lekkerbek. ....	43
Figure 52. Longshore transport between 2 groynes for 1 time step with oblique waves. ....	44
Figure 53. Longshore transport for a location in between 2 groynes. ....	44
Figure 54. Ratio of maximum transport during tidal cycle (westward) over minimum transport (eastward) (absolute values). ....	45
Figure A2.1 Comparison of longshore velocity at deep water (-5m TAW).....	A15
Figure A2.2 Comparison of longshore velocity at -1m TAW. ....	A16
Figure A2.3 Max ebb velocities (full lines) and max flood velocities (dotted). ....	A16

# 1 Introduction

This document describes the modelling of coastal morphology for the area east of the port of Zeebrugge to beyond the mouth of the Zwin using ShorelineS. ShorelineS is a modelling tool developed in Matlab by IHE Delft and Deltares. It is essentially a one-line model but includes additional functionalities (e.g., adding tide-induced currents in the cross-profile, making the model quasi-2D). In this study, the model has been extended to include the ability to model submerged groynes (whereas the base version assumes groynes extend above the water surface). The modelling is applied to the period 1999-2004, as no nourishments were carried out during this time, meaning the volume changes have entirely morphological causes. The document describes the model input: the bathymetry, wave and tidal climate, and the groynes. Additionally, it details where and how the model/script was adjusted and with which settings the model was run. The results are then described and compared with the measured volume changes during the considered period. Finally, some recommendations are formulated.

The area of interested stretches from just east of Baai van Heist (Duinbergen) up to Knokke-Lekkerbek (around the most eastward groyne). The computation domain stretches from the harbour groyne of Zeebrugge up to Cadzand. E.g. Baai van Heist and the mouth of Zwin are not suitable for ShorelineS modelling, but it needs to be incorporated in the model for a correct modelling of the area of interest.

## 2 Bathymetry

The bathymetry of end 1999 ("NJ1999") is used. In the period 1999-2004 no nourishments were carried out in the study zone, making it the best period for hindcasting. In spring 1999 a large nourishment is carried out. In Tabel 1 the nourishments since 1986 until 2019 are summarised. (Houthuys et al, 2020).

Tabel 1. Volumes supplied during maintenance nourishment and rand new nourishments at Knokke-Zoute.

Jaar	Plaats	Kust- lengte (m)	Volume in beun (m <sup>3</sup> )	"rende- ment"	Effectief volume (m <sup>3</sup> )	Deel boven LW	Deel onder LW
<b>voorjaar 1986</b>	secties 232-243	2963	1000000	85%	850000	85%	15%
<b>maart-mei 1999</b>	secties 233-243	2728	486418	85%	413500	85%	15%
<b>juni 2004</b>	secties 232-243	2800	389940	85%	331400	85%	15%
<b>2006</b>	secties 236-240	1318	(vrachtwagens)	100%	55500	100%	
<b>2007</b>	secties 232-237 en 239-240	1517	(vrachtwagens)	100%	55076	100%	
<b>2007</b>	secties 232(helft)- 236	1076	(vrachtwagens)	100%	12435	100%	
<b>2009</b>	secties 231-237 en 239-240	1770	(vrachtwagens)	100%	55785	100%	
<b>2010</b>	232-237, deel 239- 240	1651	(vrachtwagens)	100%	101600	100%	
<b>2010</b>	234-236, deel 239- 240	1052	(vrachtwagens)	100%	15400	100%	
<b>2011</b>	232-237, deel 239- 240	1651	(vrachtwagens)	100%	50920	100%	
<b>2011</b>	233-237, delen 239-240	1533	(vrachtwagens)	100%	60810	100%	
<b>2012, voor VJ</b>	s231-240	2466	100840	85%	85700	100%	
<b>2012, voor VJ</b>	s232-237, 239-240	1557.5	(vrachtwagens)	100%	63550	100%	
<b>2013, net na VJ</b>	s. 232-240	2231	132113	85%	112300	100%	
<b>2014, voor VJ</b>	s. 232-240	2121	175322	85%	149000	100%	
<b>2015, voor VJ</b>	s. 232-237	1451	252789	85%	204900	100%	
<b>voor 31-03-2017</b>	s 232-240	2231	309642	85%	233200	100%	
<b>23/02/2019 t.e.m. 17/03/2019</b>	s 234-243	2131	292802	85%	218900	100%	

In the 4<sup>th</sup> column, the reported volume of nourished sand ("beun") is given, unless there were nourishments done by trucks: in that case, the volume is considered a 100% contribution to beach morphology.

The bathymetry (in m TAW) is shown in Figure 1.

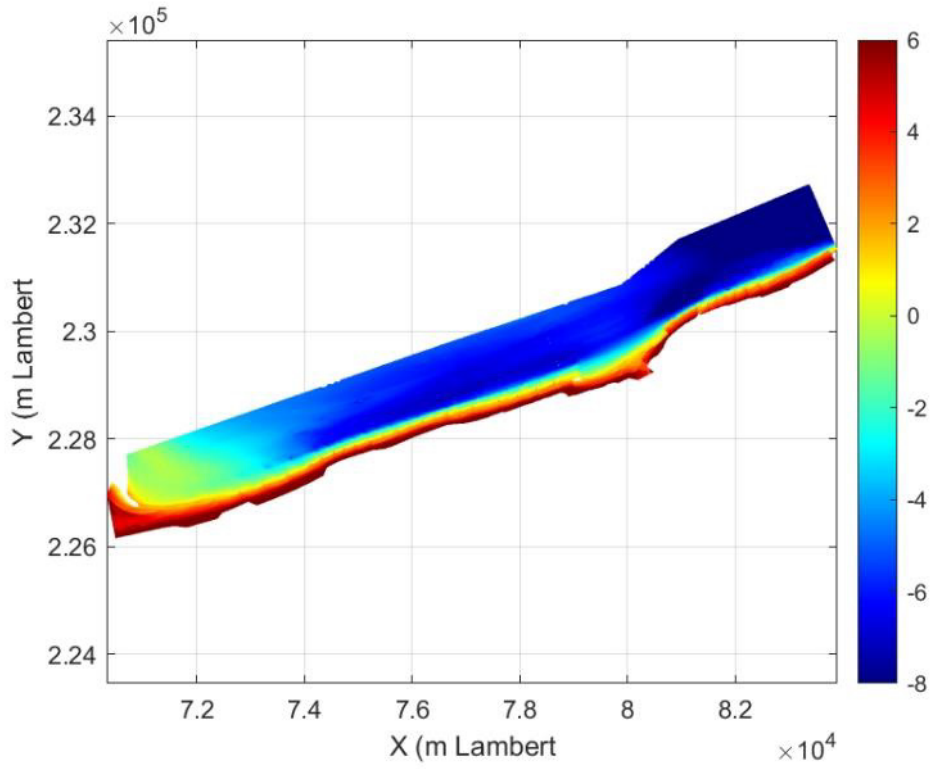


Figure 1. Bathymetry (m TAW) NJ2019.

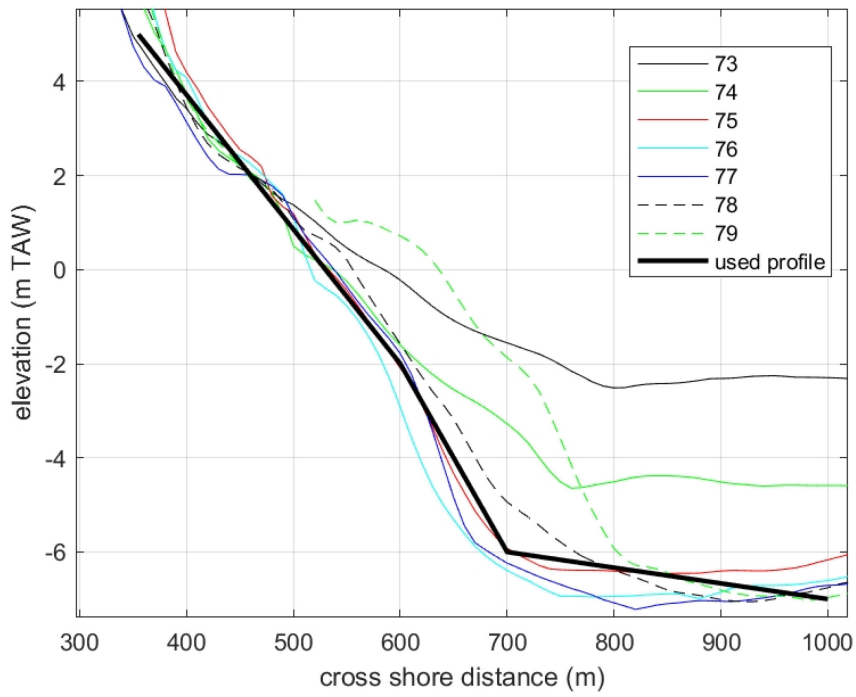


Figure 2. Cross shore profiles (m TAW) NJ2019. (legend: e.g. 73 means at X=73.000 m Lambert72)

Cross shore profiles every km are shown in Figure 2. The most important profiles (at  $x=74.000$  till  $78.000$ ) can be represented by a profile with slope 1/35 between +5 and -2 m TAW, slope 1/25 between -2 and -6 m TAW, and slope 1/300 between -6 and -7 m TAW. The shape of the cross shore profile is only important below the highest water level: dune processes are not incorporated in this version of the model. The profile is relevant for the hydrodynamics and sediment transport. The movement of the shoreline is based on gradients in longshore transport and the depth of closure/active height of the profile. These parameters have to be imposed in the ShorelineS – input file (cf. chapter 6). After conversion to MSL, this profile is used in ShorelineS for the entire model domain.

Recently the beach slopes (calculated between 1 m TAW and 4.5 m TAW) became milder as illustrated in Figure 3 (steeper in 2004 compared to 2023).

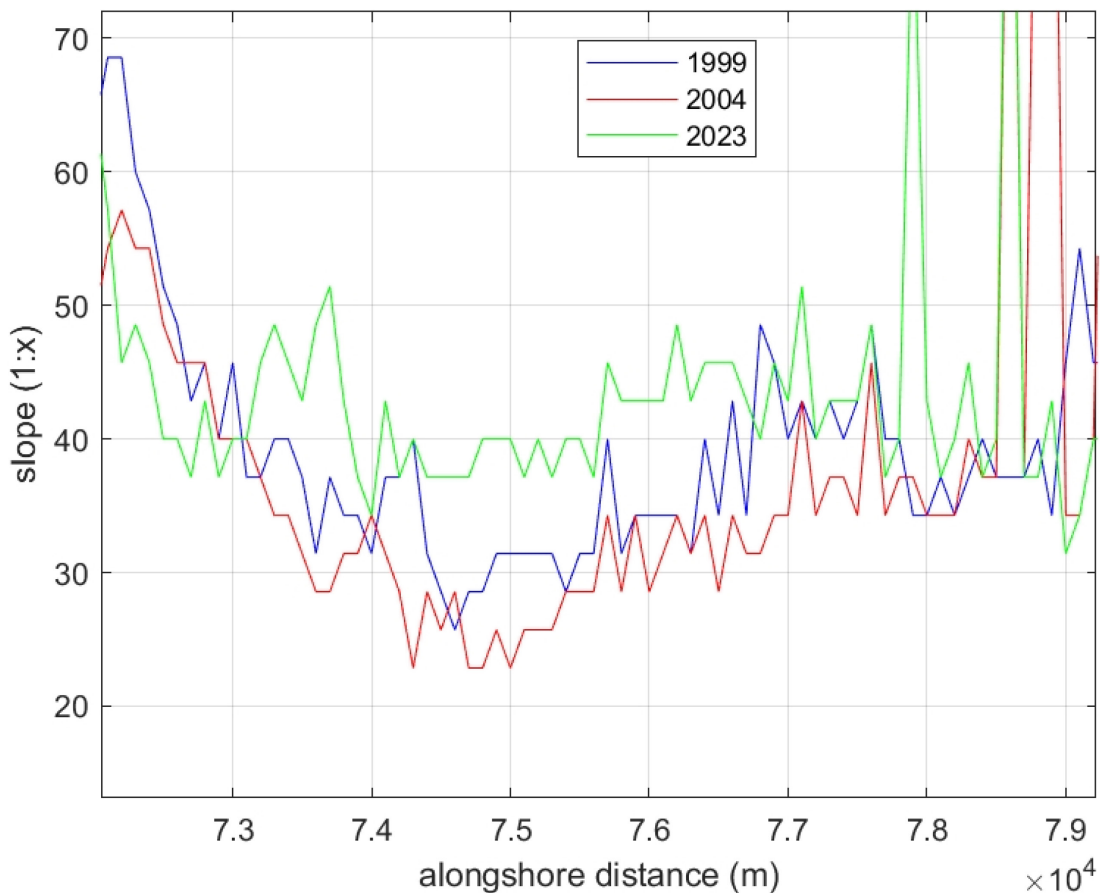


Figure 3. Beach slopes.

The coastline is obtained by using the contour at +2.3 m TAW (= MSL, the vertical reference system of ShorelineS). Some smoothing is applied (window of 50 m): an averaged x and y value are looked up over a distance of 50 m, which smooths out partly the effect of the groyne on the coastline. An example is shown in Figure 4. For Baai van Heist and west of Zeebrugge an artificial coastline is used in combination with an artificial groyne to represent the harbour of Zeebrugge. (cf. Figure 5).

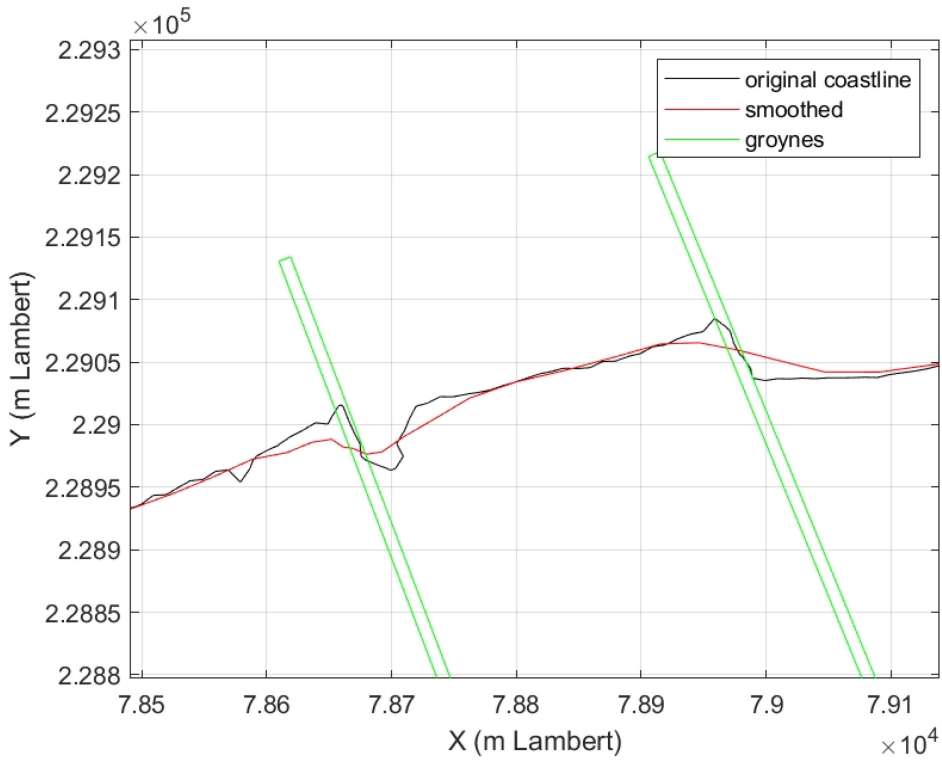


Figure 4. Example of smoothed coastline.

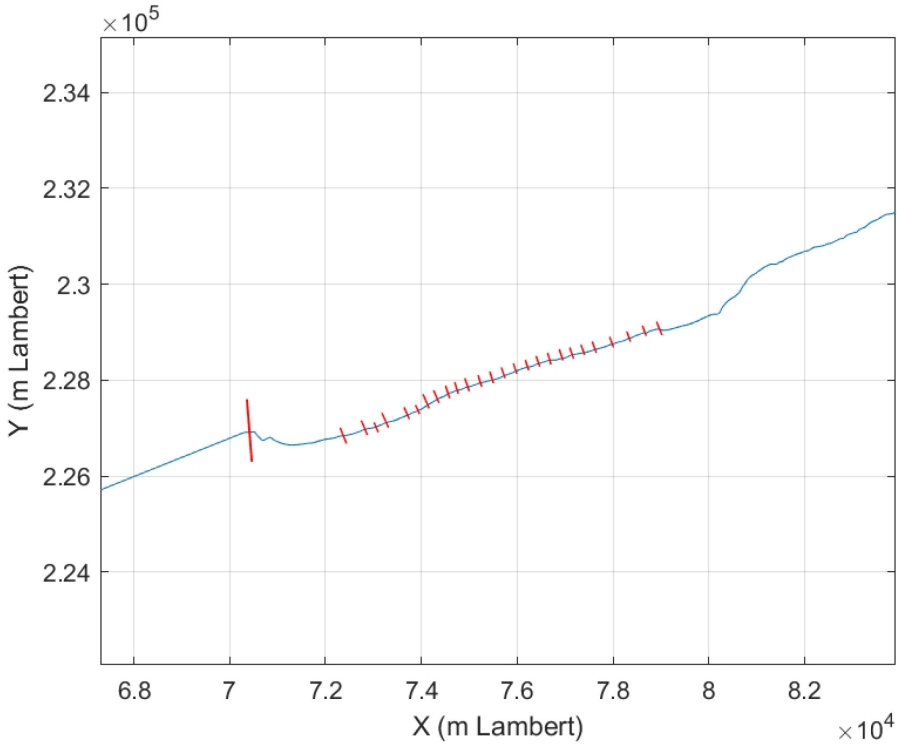


Figure 5. Coast line and groynes.

### 3 Groynes

In ShorelineS (Roelvink et al. 2020) it is assumed that the groyne crest of the submerged groyne has a constant height relative to the beach. So the crest slope is equal to the beach slope. The groynes of Knokke are inventorised (Montreuil et al, 2024 - P:\19\_118-EvlrgCstNrsh\3\_Uitvoering\GroynesExtraction). The crest lines are represented with x,y,z coordinates.

A representative groyne is obtained by starting at the real groyne level of +2 m TAW and extend it landward and seaward with the beach slope (1/35) as assumed in ShorelineS. +2 m TAW has been chosen to be most representative in the breaker zone where most transport occurs. The groyne implemented in the model ends offshore at the location where the real groyne becomes very steep. This is illustrated in Figure 6. The black lines are representative for the situation in 1999 (start of modelled period). Two beach profiles (one at the location of the groyne, the other 20 m eastward) are shown in thin lines. ShorelineS will use the thick black dotted line (it is the input profile of ShorelineS as described in chapter 2; the profile has been shifted so that it aligns with the coastline at an elevation of 2.3 m TAW). The crest line of the groyne is parallel with the beach profile while the offshore end is situated at a x-coordinate 30 m. The blue and green line show the maximum and minimum elevation in a 20 m box around the center line of the groyne. It is remarkable that these lines are below the groyne crest (under investigation in other projects). Appendix 1 shows all the groynes. Please note that groyne "Heist 51" still existed until 2010, but was not implemented in the ShorelineS Knokke model.

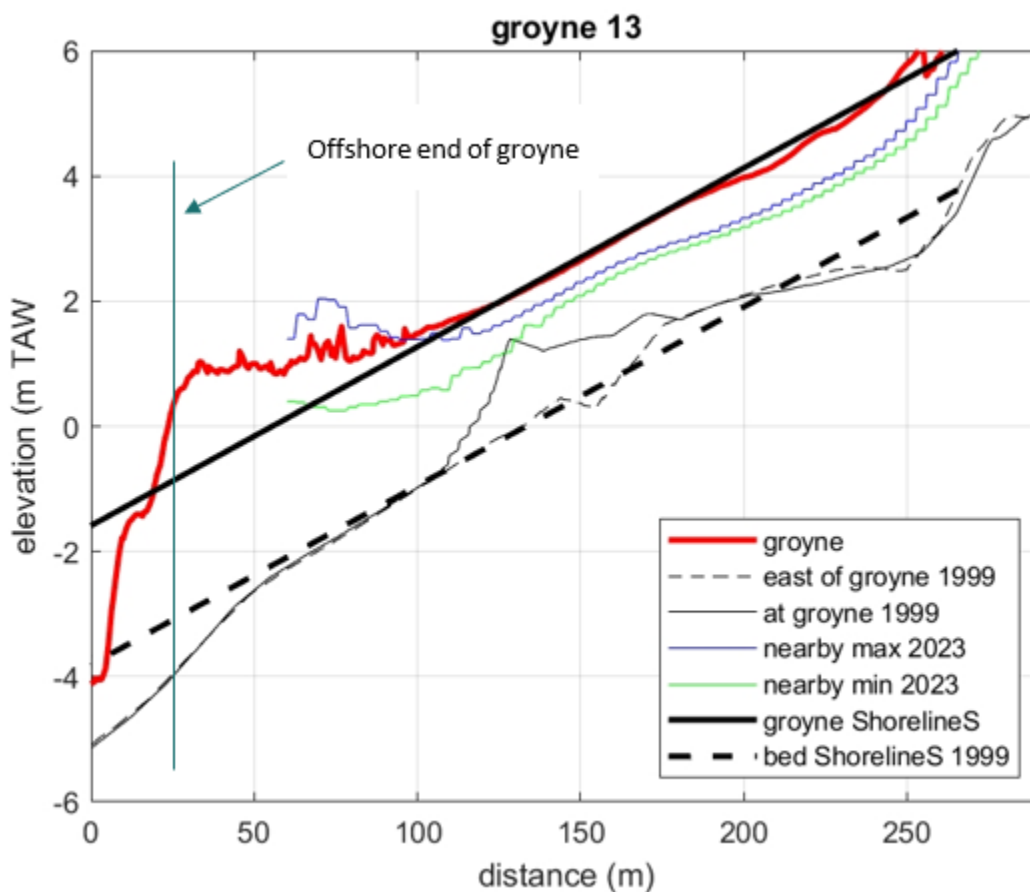


Figure 6. Example of a groyne representation.

## 4 Hydrodynamic boundary conditions

### 4.1 Wave conditions

At 5 locations the wave climate is defined. These locations are situated around the -5 m TAW line (Figure 7). The climates are obtained from the project “Golfklimaat Vlaamse Kust” (FHR project 769\_01; IMDC, 2009), where detailed research with SWAN was done in order to transform the offshore wave climate to the coast. The modelled period is 1996-2005. The difference in wave climate between the 3 most eastward locations is very small, refining (more locations) does not make a difference. The 2 most westward locations are outside our area of interest.

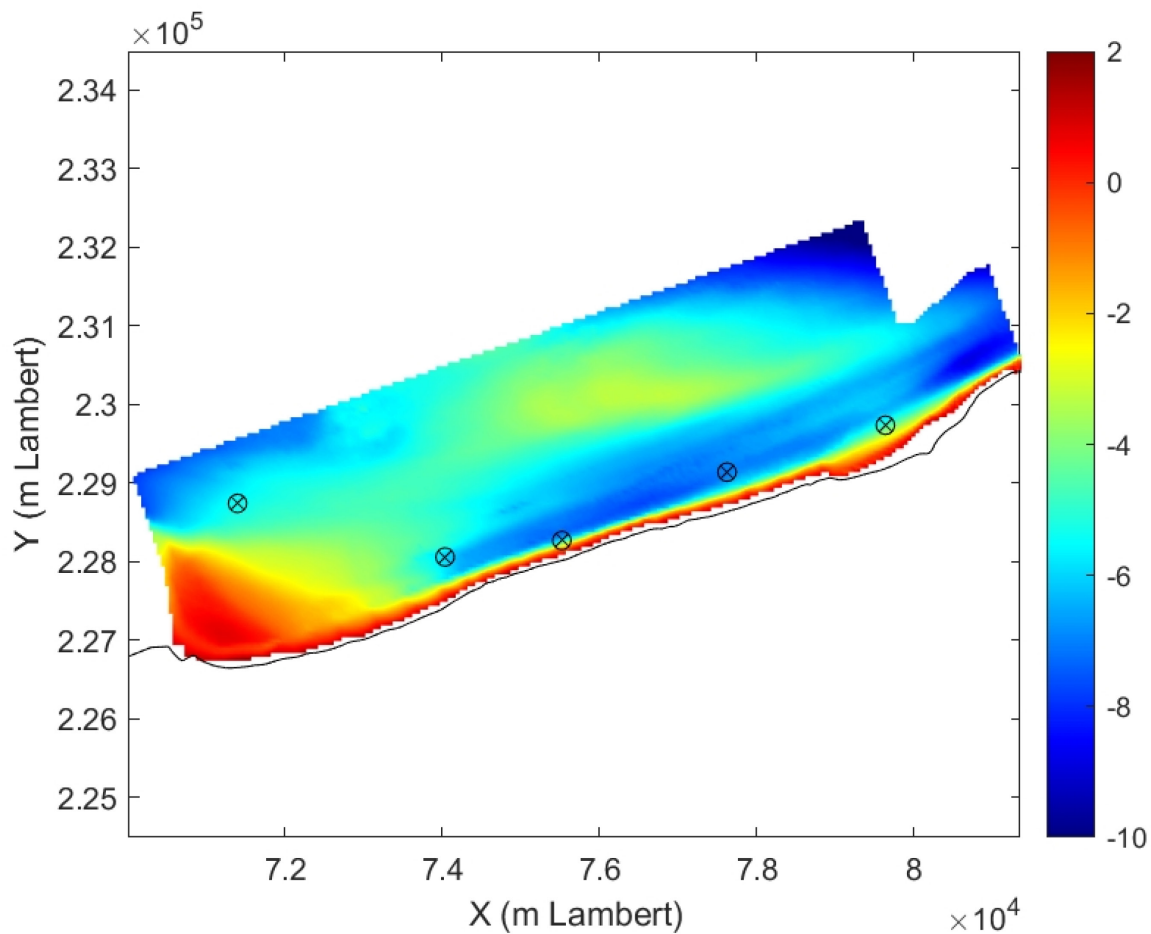


Figure 7. Locations of wave climates (DTM in m TAW).

Time series are used. In the older versions of ShorelineS, the use of wave climates resulted in very large time steps for small wave heights and high wave events were not used. This is probably fixed in the latest version, but not tested yet at the study zone.

The time series contain gaps, therefore time series were compiled for specific years. Small gaps are filled up, larger gaps not. Gaps are moved to the end of the time series in order to obtain continuous time series. Thus, the time series of e.g. 1997 ends at November 16<sup>th</sup> (10.5 months available). To obtain yearly transport rates, the simulated transport is thus multiplied by a factor 12/10.5.

In Figure 8 the longshore sediment transport for different years is compared. The differences are significant. As illustrated in Figure 9 this is due to the different weight of the wave direction classes.

These figures show the effect of the used modelling period. For hindcasts, the real occurred climate should be taken, for predictions, at least a period of 7 years is necessary (rule of thumb).

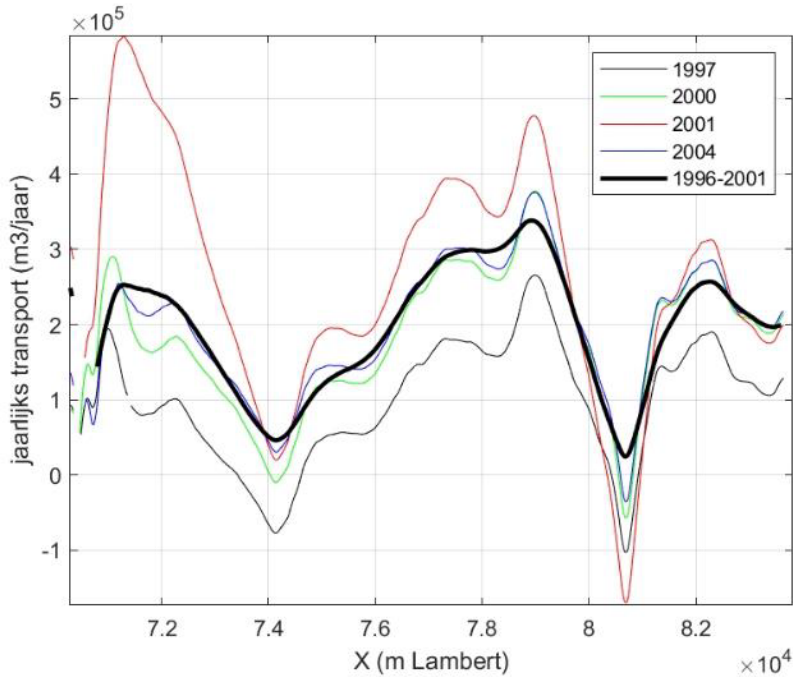


Figure 8. Longshore sediment transport for different years (ShorelineS model April 2023, without groins); positive is towards NL.

As can be observed, the longshore sediment transport increases between a minimum at  $x=74.000$  and a maximum at  $x=79.000$  m Lambert.

Figure 10 shows that this is explained by the higher contribution at  $x=78.000$  of the westward directions (negative directions), which are more sheltered at  $x=74.000$  (closer to the harbour of Zeebrugge). This is detailed in Figure 11 and Figure 12.

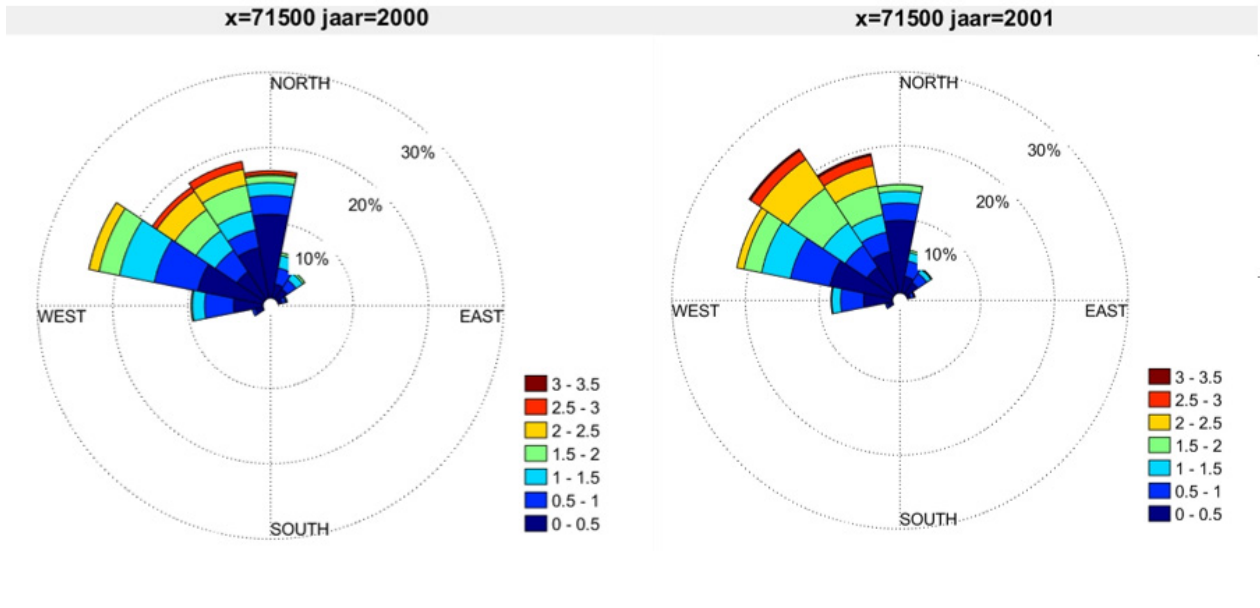


Figure 9. Wave climates 2000 and 2001.

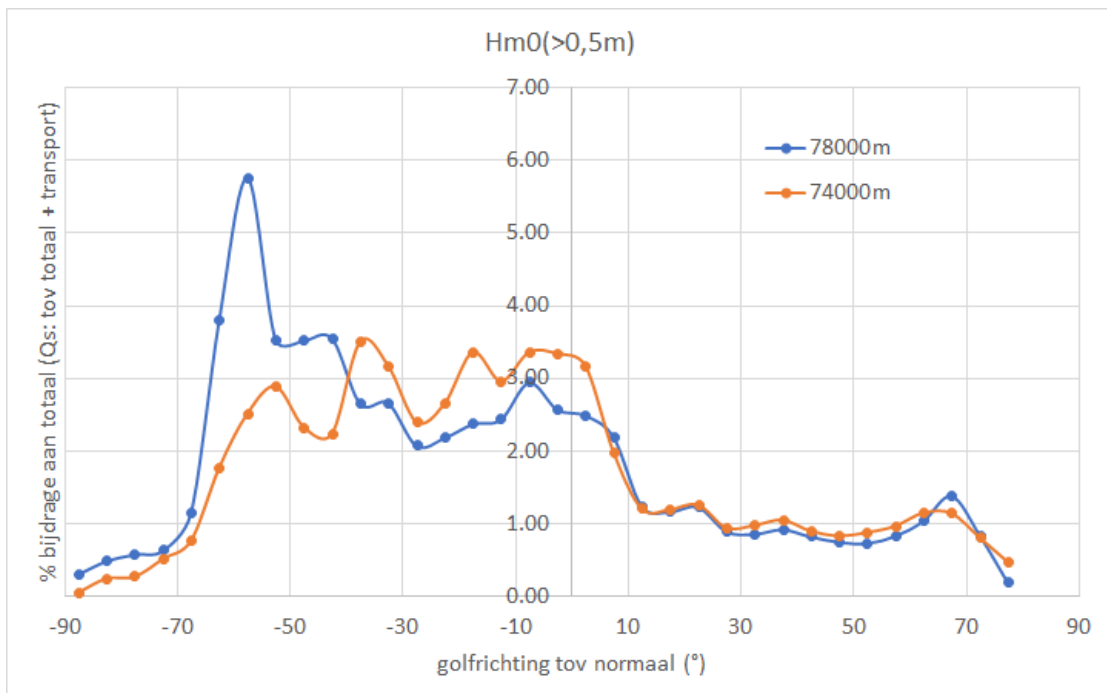


Figure 10. Distribution of longshore transport over the wave directions (e.g. the wave direction  $-45^{\circ}$  ( $+2.5^{\circ}$ ) contributes for 3.5% of the total eastward transport at  $x=78.000$  m).

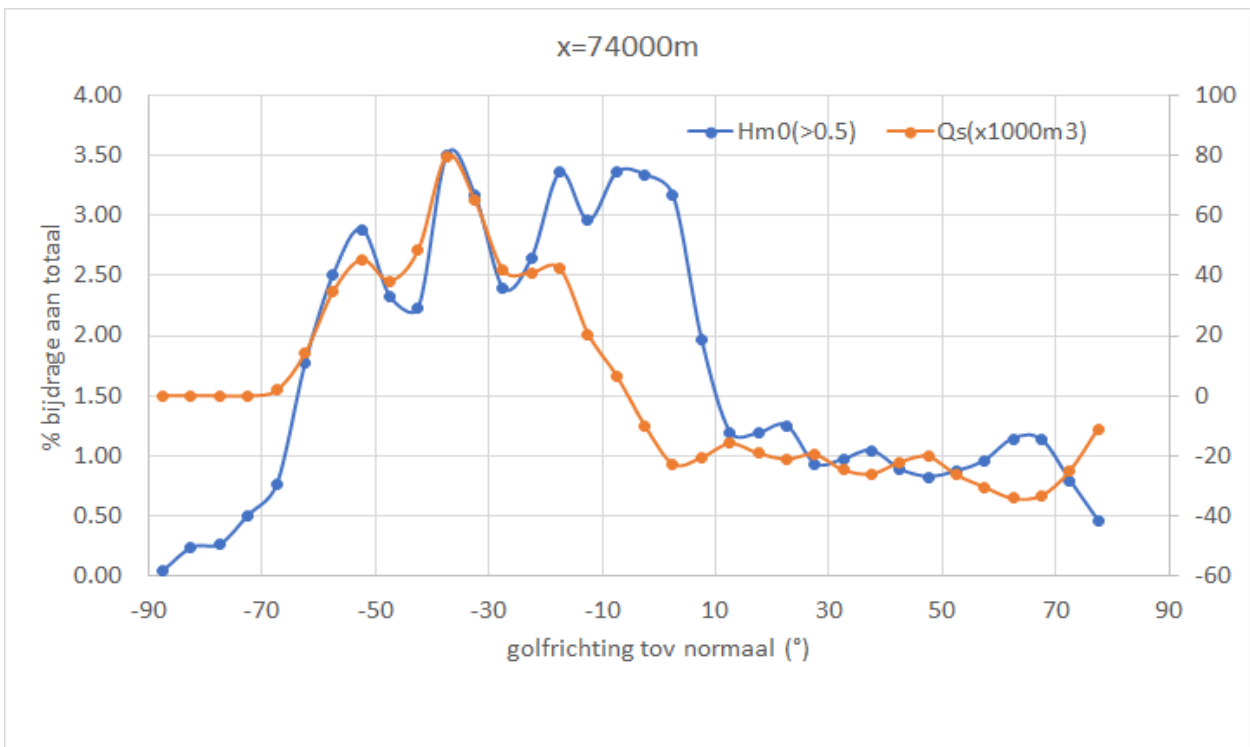


Figure 11. Distribution of wave height and longshore transport over the wave directions at x=74.000 m).

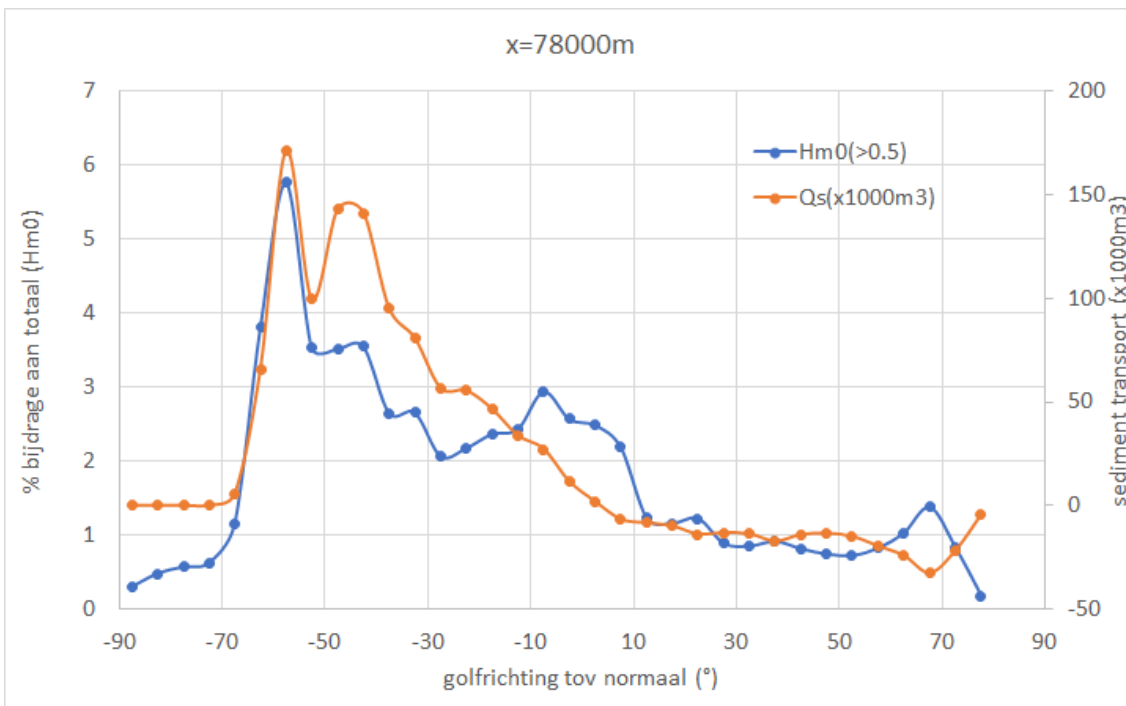


Figure 12. Distribution of wave height and longshore transport over the wave directions at x=78.000 m).

For the period October 1999- 2004 the wave rose for the location in the middle of the model is given in Figure 13. The wave height non-exceedance curve is given in Figure 14. It is remarkable that the wave directions differ from the wave climate as simulated in Scaldis-Coast run MO6\_009 (Figure 15). The different considered time period cannot explain the bi-directionality visible in Scaldis-Coast and not in the 1996-2005-wave climate data. The lack of directional spread in the Scaldis-Coast model is still under investigation.

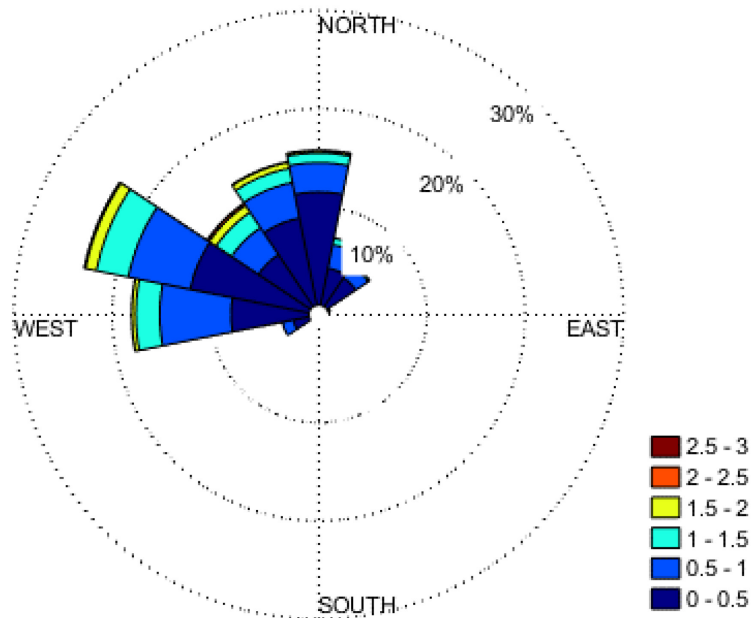


Figure 13. Wave rose for the period 1999-2004.

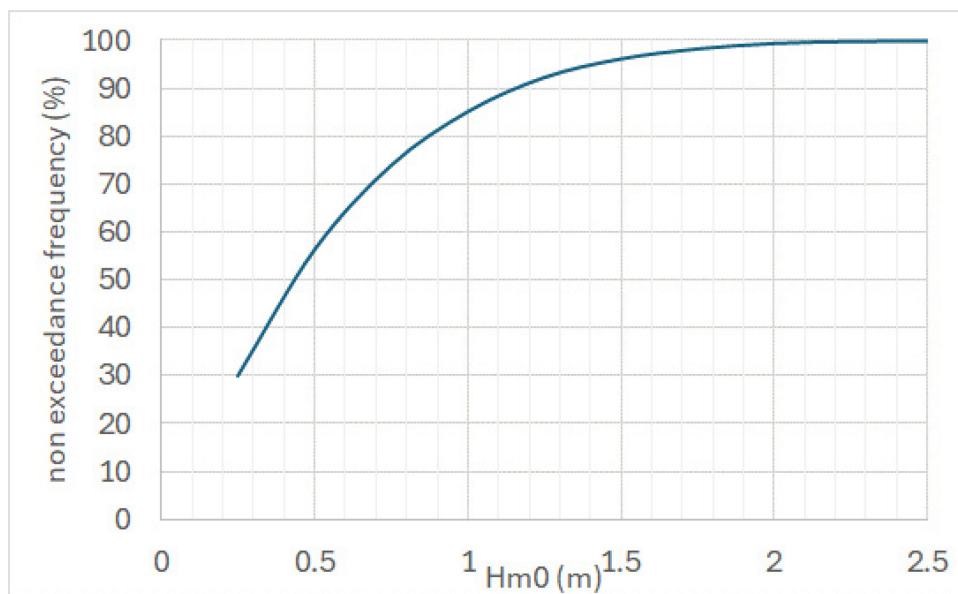


Figure 14. Wave height non-exceedance curve.

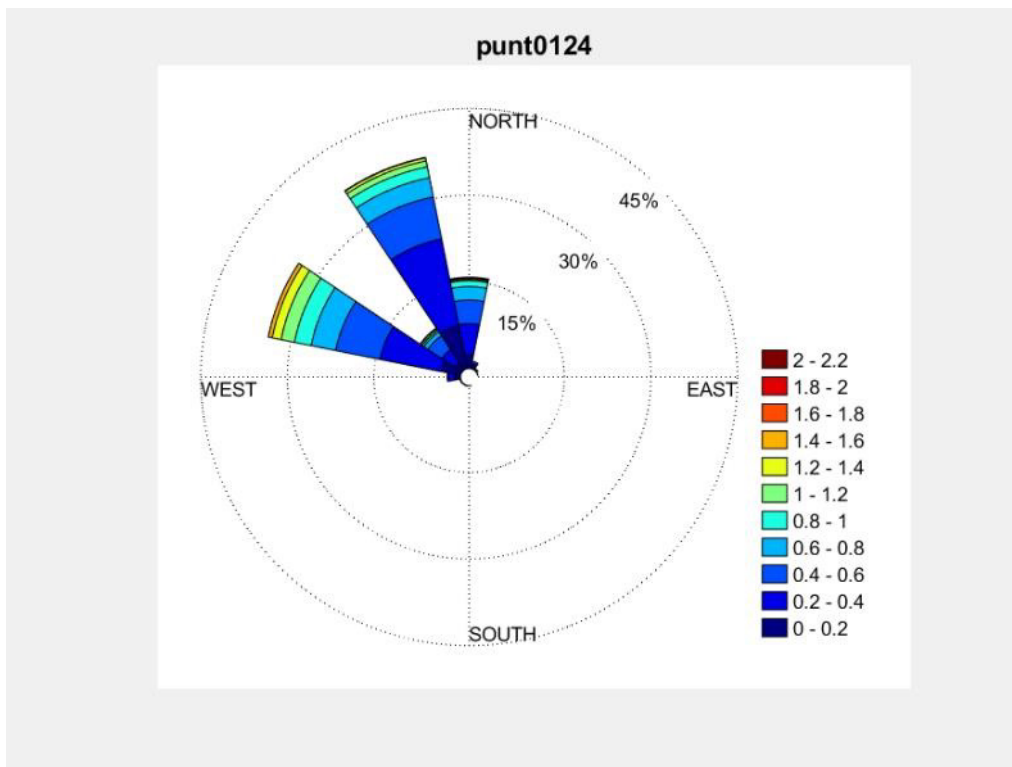


Figure 15. Wave rose Scaldis-Coast model.

In the time series waves with directions between  $90^\circ$  and  $250^\circ$  (coming from land) are replaced by  $H_m0=0.01$  m and direction  $350^\circ$ , as these waves, which do not contribute to sediment transport, cause model instability.

## 4.2 Tidal velocities

### 4.2.1 Introduction

ShorelineS has been extended with modules to incorporate tide, including tidal velocities (Roelvink and Huisman, 2023). In these modules the tidal velocity is calculated based on observed tidal velocities at a discrete number of points (in this case generated by a Delft3D model) and the local water depth (used for interpolation between observation points). For each location where the input of the tide is given, a table with the necessary coefficients (e.g. amplitude of M2 and M4, phase differences, longshore slope) are given. The table is obtained with a 2D model (e.g. Delft3D, Scaldis-Coast, ...). The are used to calculated the velocities in the cross shore profile (using a relation depending on the local water depth). For other cross shore profiles, interpolation is used. The points are selected on the cross shore profile (distance between 2 points is 10 m). The output are water levels and tidal velocities (in 24 phases) along the cross shore profile. Also the wave driven current in the same points is calculated. With these velocities and wave parameters the sediment transport is calculated using the formulation of Soulsby-Van Rijn.

It is remarkable that the cross shore variation of tidal velocity is approximately equal at LW compared to HW and approximately equal at maximum flood compared to maximum ebb (cf. Figure 16). This is the effect that, in very shallow water, the tidal velocity is in phase with the gradient of the water level, and it is maximal around MSL (Mean Sea Level), so at high tide it is approximately equal to that at low tide, and thus not very different; the net flow above MSL is then also on the order of mm/s in the case of tide only (pers. comm. with D. Roelvink). An example of the variation of the tidal velocity during a tidal cycle is given in Figure 17.

A minimum velocity of 0.1 m/s is used for dry parts (not affecting sediment transport rates).

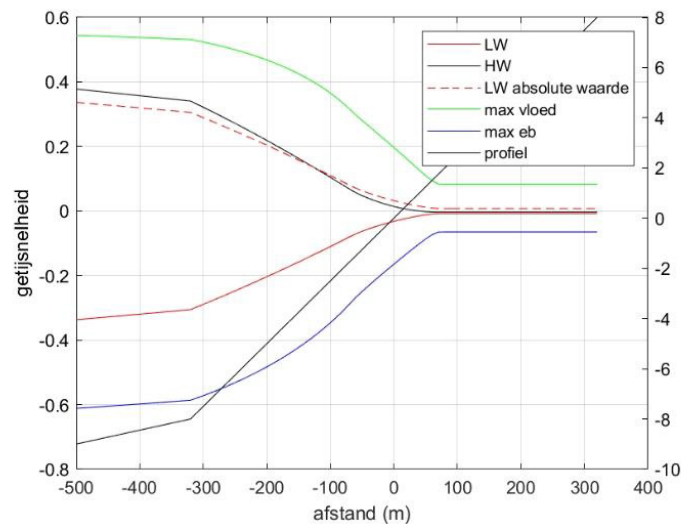


Figure 16. Cross shore distribution of the tidal velocity (right axis: elevation, in m MSL).

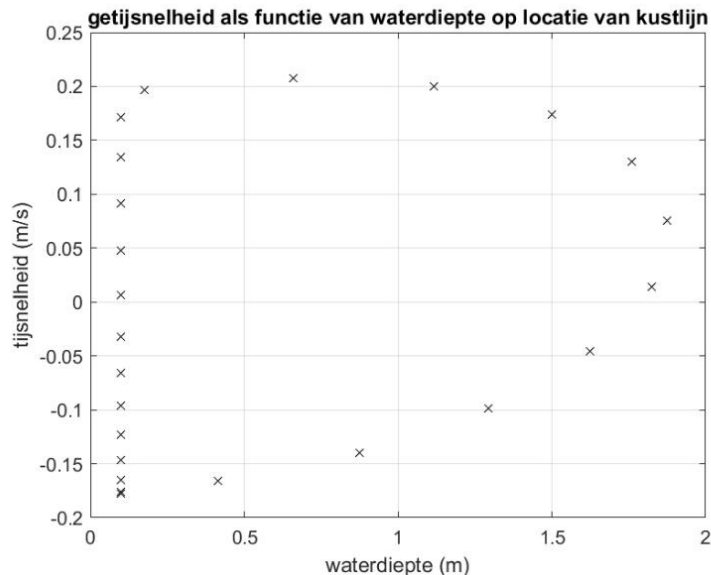


Figure 17. Tidal velocity as function of the water depth during a tidal cycle at MSL.

#### 4.2.2 Effect on longshore sediment transport

In this paragraph the effect of the tidal velocities on the net sediment transport is calculated for the Knokke case (using the version of ShorelineS spring 2023 (e.g. Chezy roughness instead of Manning for wave generated currents)). Figure 18 shows that the tide causes a reduction of the longshore transport calculated to the depth contour of 8 m below MSL. However, between 74k and 78k, the difference in longshore transport (=net erosion) is larger with tide. The variation of the tidal velocities has been shown in Figure 19. Over the project area the velocities are rather symmetric, with almost no net current. Figure 20 shows that including tide gives a wider cross shore distribution of the transport (mainly due to the varying water levels). This corresponds to the results of the Scaldis-Coast model when considering the Bijker sediment transport formula results (Dujardin *et al.*, 2024). Using Soulsby-Van Rijn (as in the ShorelineS model!) the sediment transport in the deeper area is even higher than in the breaking zone (Figure 21).

(A test was done to check the effect of depth of closure: a variation from 8 to 20 m below MSL does not show an effect on the sediment transport.)

Scaldis-Coast model results show that the effect of the tide would be much more important for locations west of Zeebrugge harbor.

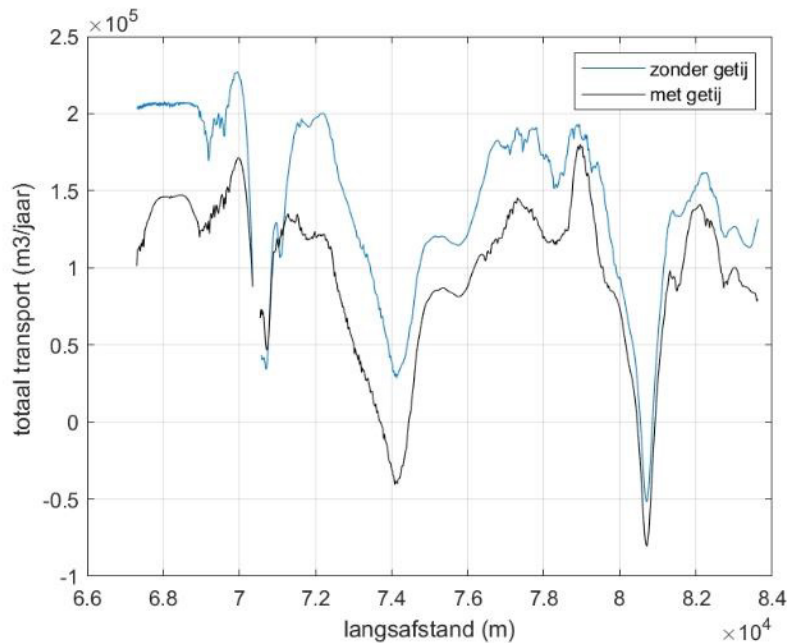


Figure 18. Effect of tide on the annual sediment transport.

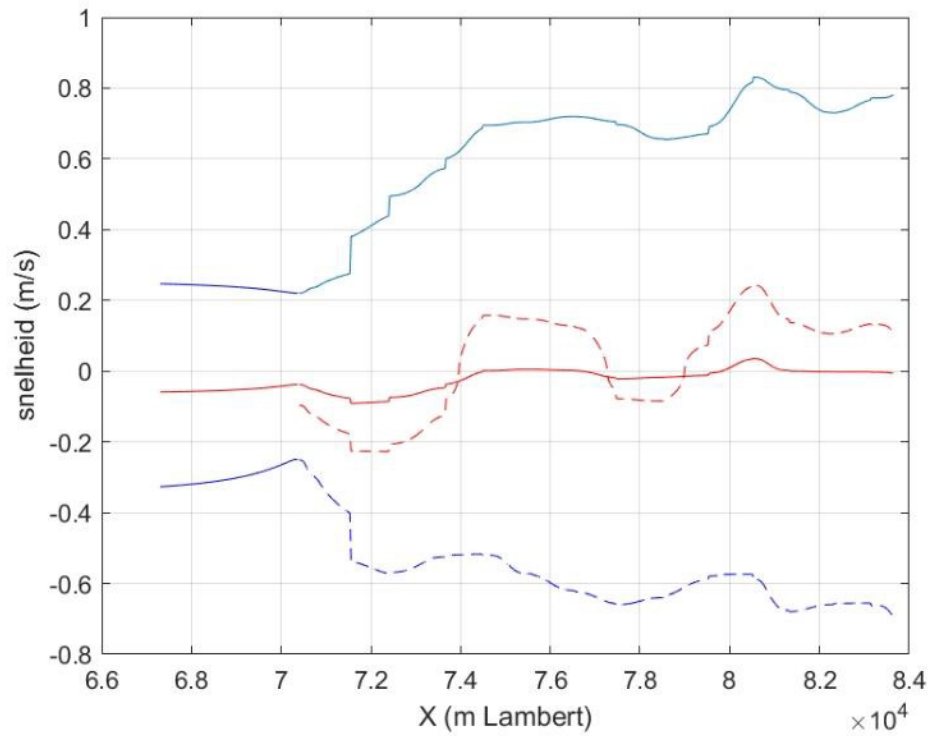


Figure 19. Variation of tidal velocities (blue: max/min; red: mean and stand. Dev).

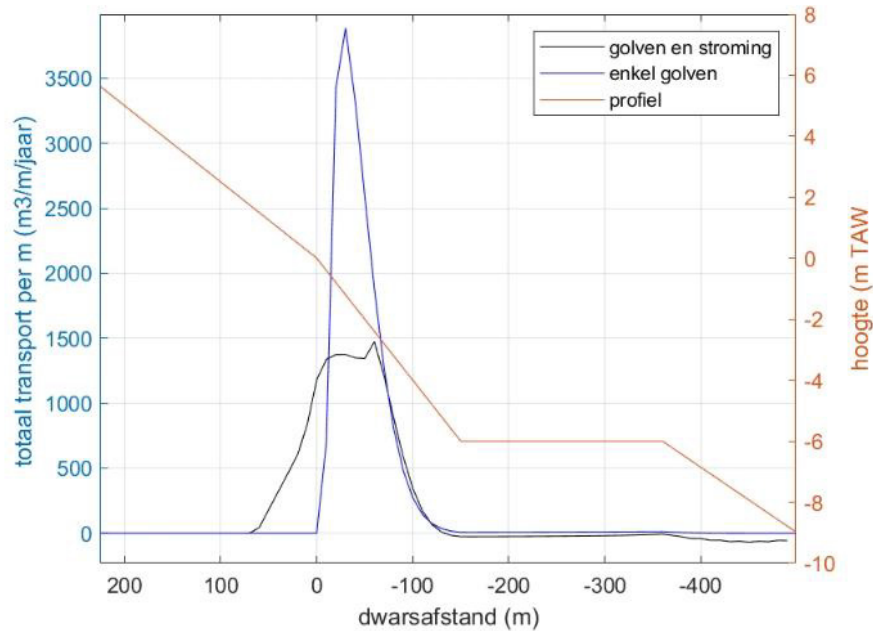


Figure 20. Effect of tide on the cross shore distribution of longshore sediment transport.

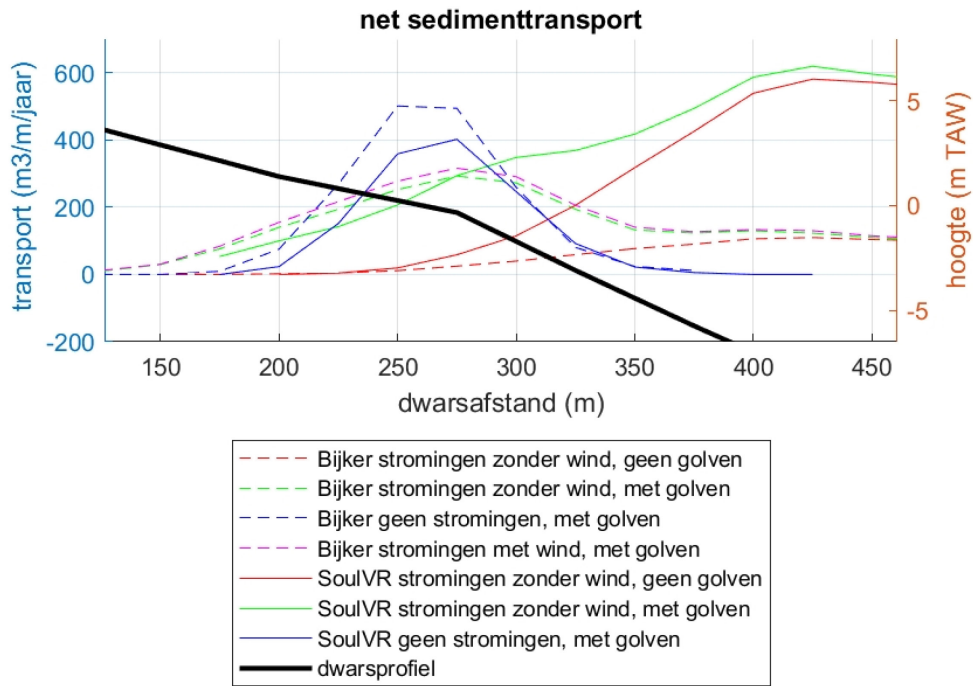


Figure 21. Effect of tide on the cross shore distribution of longshore sediment transport (Scaldis-Coast model). Simulations MO6\_004, MO6\_003, MO6\_005, MO6\_009, MO6\_011, MO6\_014, MO6\_012 respectively.

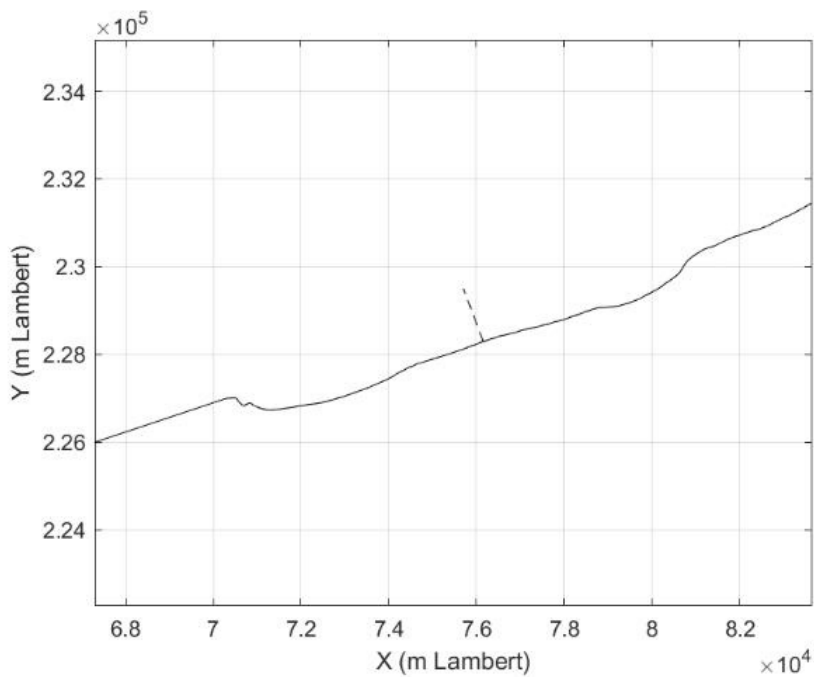


Figure 22. Coastline and location of the studied profile.

In the ShorelineS Knokke model, sediment transport across a profile at X=76150 m Lambert was studied in detail. The coastline is shown in Figure 22. The orientation of this profile is  $-18^{\circ}\text{N}$ .

Modeling of an annual climate indicated that the addition of the tide leads to lower transports. Cf. Figure 23, which shows that especially for waves generating a current towards Zeebrugge, the tide has an influence. (Used cross-profile 1/41 to MSL and below that 1/20 up to the flat bed, cf. Figure 20) In this figure, there may be an influence from varying coastline orientation and from the slope-change in the cross-profile. This is further detailed in this report.

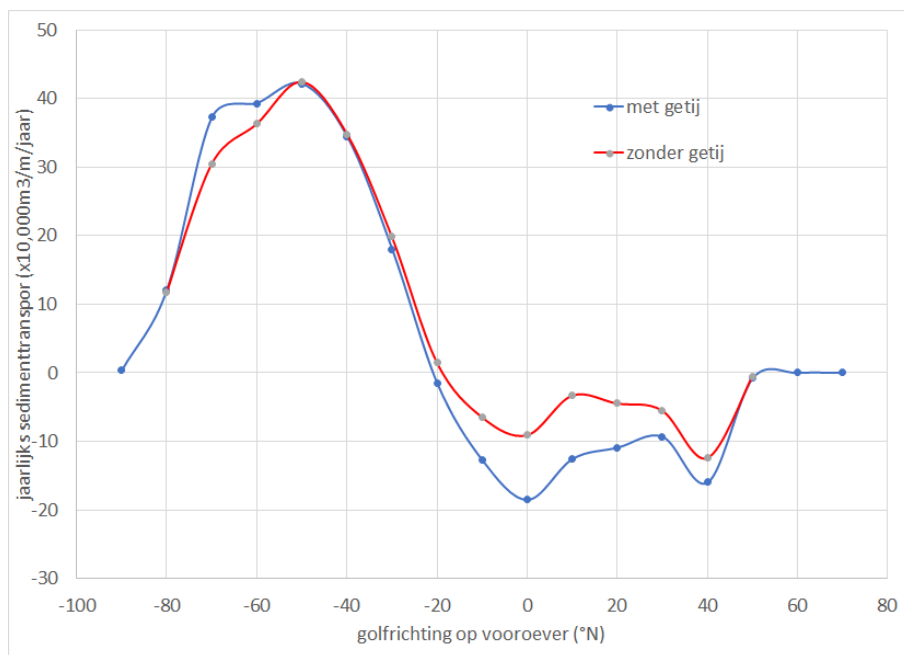


Figure 23. Annual sediment transport at location X=76150 m with the ShorelineS Knokke model with and without the tide.

To avoid the influence of varying slopes of the profile, a linear profile with a constant slope of 1/45 to a depth of 8m below MSL was initially used.

With this model, the transport across the profile was calculated for a series of wave heights: 0; 0.5; 1; ... 2.5 m and wave directions ( $-80$ ;  $-70$ ; ...  $70^{\circ}$  relative to N), both with and without the tide. Figure 24 and Figure 25 show the dependence of sediment transport on wave direction (on the foreshore) for waves of 1 m and 2 m respectively. It should be noted that the peak of positive transports is slightly lower than the peak of negative transports.

These figures show that for positive transports, the influence of the tide is small, while for negative transports, the tide has a reducing effect on the net littoral drift. Thus, the net effect of the tide on the net littoral drift is a reducing influence when calculating the annual climate.

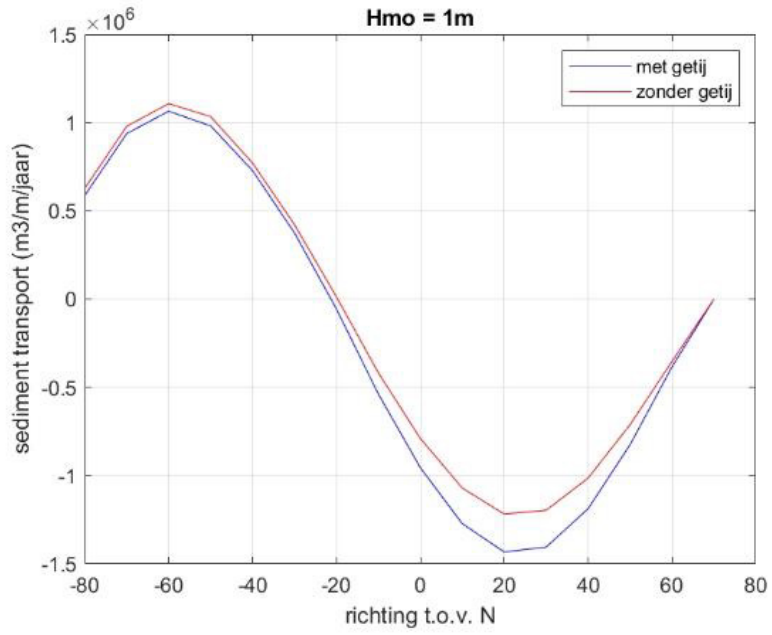


Figure 24. Annual sediment transport per direction for  $H_{m0} = 1\text{ m}$  on the foreshore.

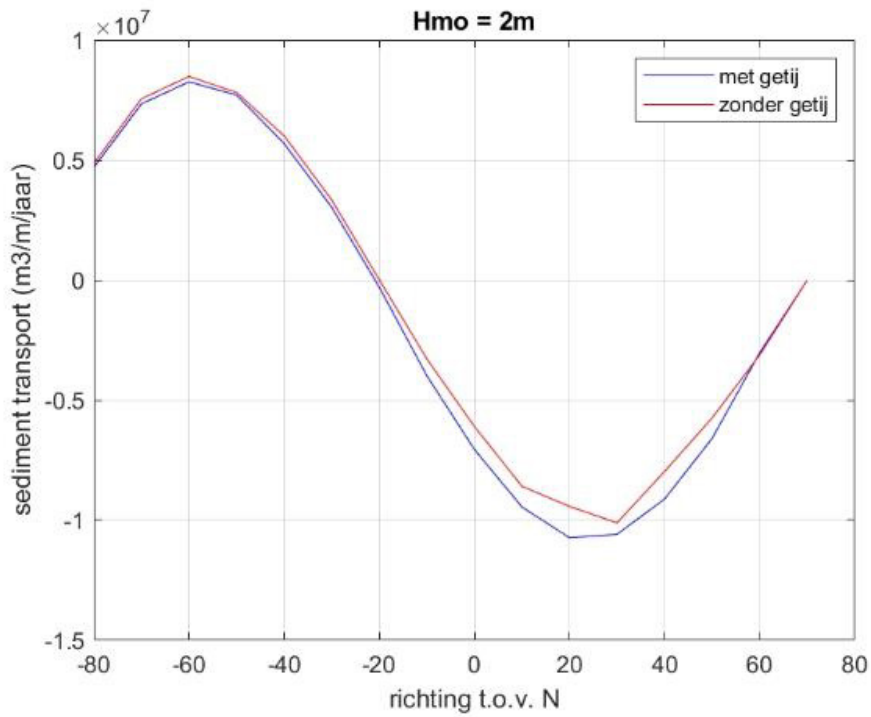


Figure 25. Annual sediment transport per direction for  $H_{m0} = 2\text{ m}$  on the foreshore.

For two directions ( $300^\circ$  and  $13^\circ$ ) that produce equal longshore currents without the tide (but in opposite direction), the results were examined in more detail. The wave height on the foreshore is  $H_{m0}=1$  m. Figure 26 shows the absolute value of the tide-driven and wave-driven velocities for the two directions at the moment when the maximum velocity at the point of wave breaking (location with maximum sediment transport) is reached. For the direction  $13^\circ$ , these are negative velocities (towards Zeebrugge).

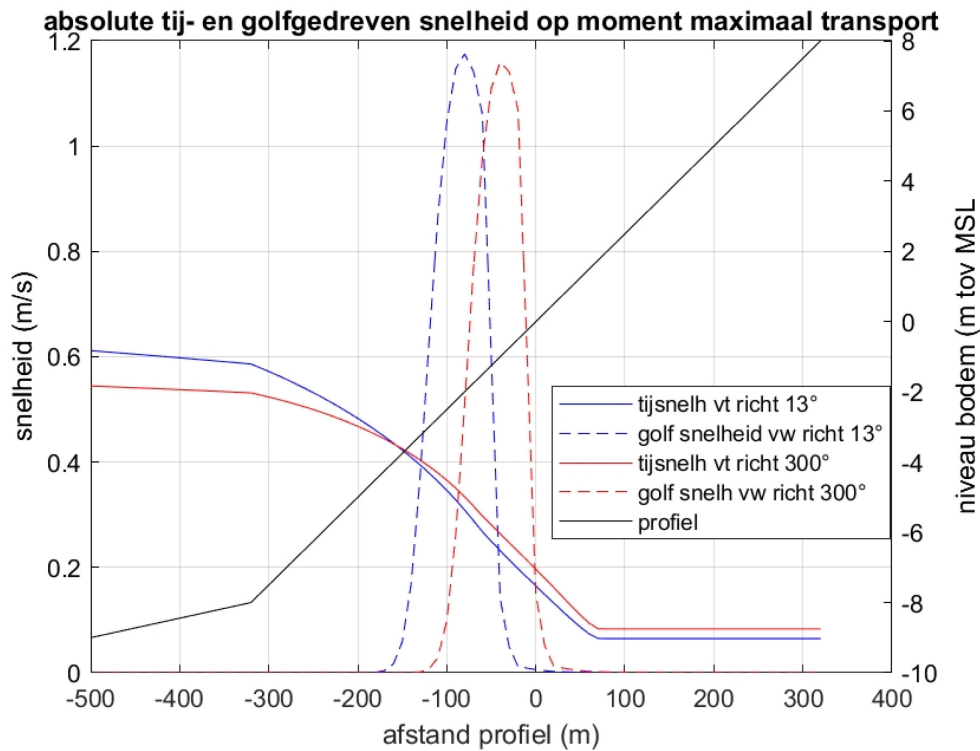


Figure 26. Velocities across the cross-profile.

For each tidal phase (in ShorelineS, the tide is divided into 24 phases), the location on the profile where sediment transport is maximal is determined. At this location, the tide-driven and wave-driven transports are then analyzed. In Figure 27, the tidal velocity in deep water (green) is shown; additionally, at the points of maximum transport, the tide-driven velocity is given. This is independent of the wave direction (blue line and red crosses). The maximum negative velocity is 0.30 m/s and the maximum positive velocity is 0.26 m/s. In deep water, however, the maximum positive velocity is greater (0.70 m/s) than the maximum negative (0.60 m/s). The maximum negative occurs at almost the same time as the maximum negative tidal velocity in deep water. For the maximum positive, there is a shift of 1.5 h. The net tide-driven velocity is -0.03 m/s (in deep water, this is only +0.03 m/s).

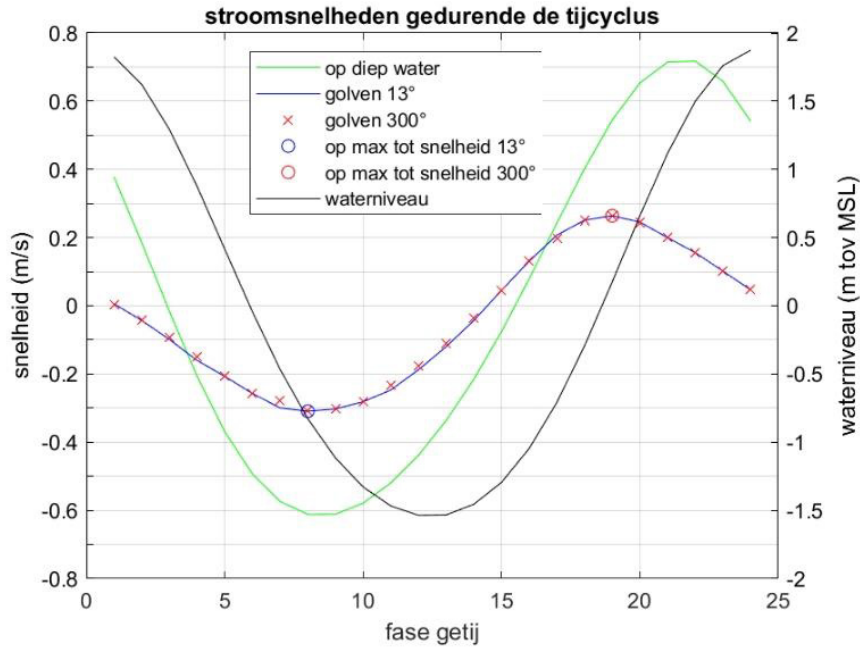


Figure 27. Tidal velocities during the tide.

Figure 28 shows the velocity profiles in the cross-profile (absolute values) at these three moments and it indicates the location where the sediment transport is maximal at that time. It can be seen that at maximum flood (green), the velocity in deep water is the highest, but the tidal velocity quickly decreases across the profile. At the location of maximum transport, the velocity is still very small (15 cm/s).

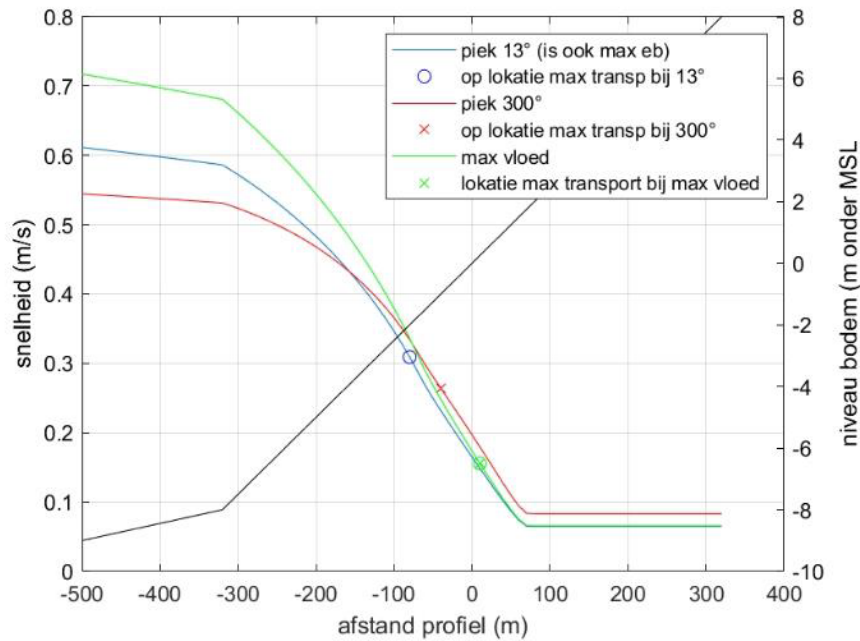


Figure 28. Velocity profiles.

Figure 29 shows the absolute value of the wave-driven transport. Here, a small influence of the tide is noticeable but the reason is not clear. The differences, apart from the direction, are not significant between the two wave directions. Figure 30 shows the water depth at the location of maximum transport as a function of the tide. A small difference is noticeable between the two directions.

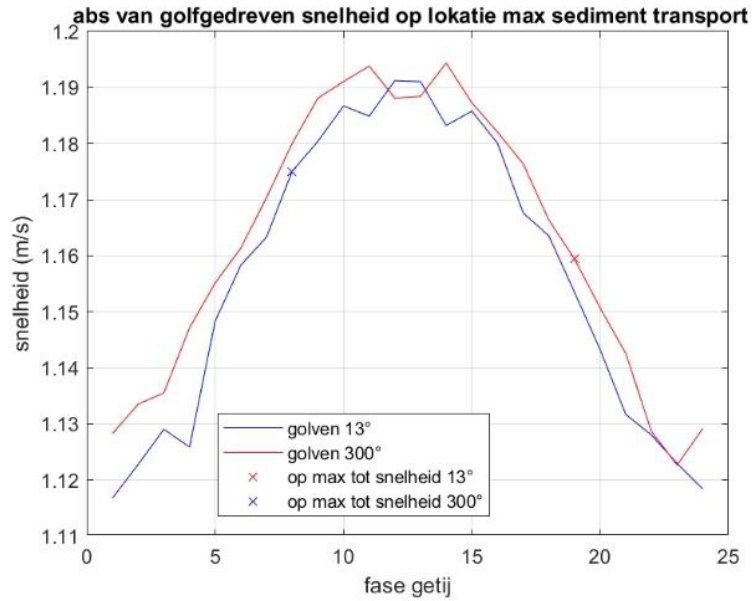


Figure 29. Wave-driven velocity at the location of maximum transport (absolute values; location of max transport).

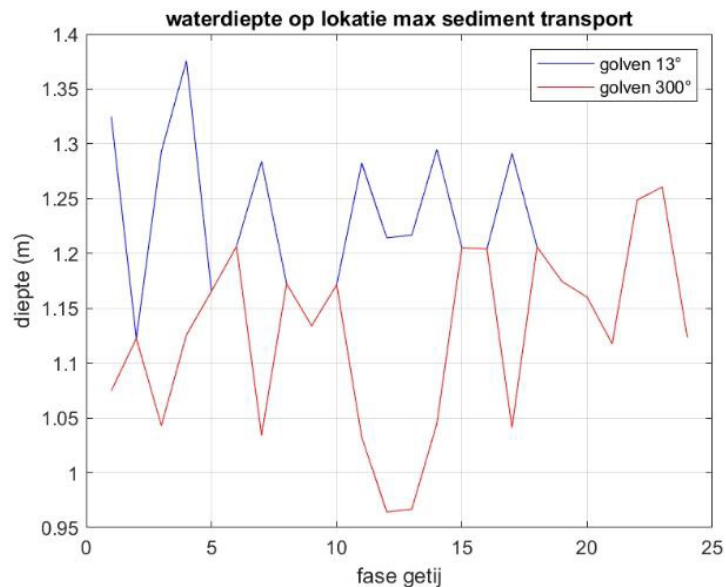


Figure 30. Water depth at the location of maximum transport.

Figure 31 shows the sediment transport for the simulation with the tide, with the sediment transport from the simulation without the tide subtracted. The absolute values of the velocity are also given. It can be seen that during the tide, for the wave direction 13°, the tide systematically results in lower values (more negative contribution) than for 300°.

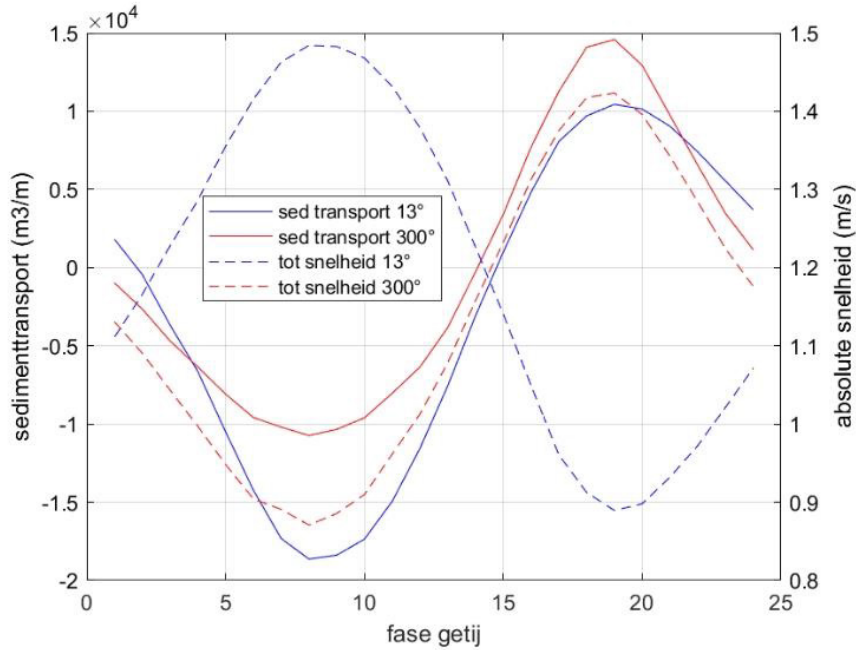


Figure 31. Extra sediment transport due to the tide.

Summing both velocities gives the value at the wave breaking location and the sediment transports at the same location (parameter Slong in ShorelineS at locations of breaking and averaged over the tide):

Table 1. Output parameters for different directions with and without tide.

	Average speed (m/s)	Maximum speed (m/s)	Net transport (x1000 m <sup>3</sup> /m)	Net transport over profile (x10 <sup>6</sup> m <sup>3</sup> /year)
300° without tide	1.155	1.155	26.9	1.11
300° with tide	1.127	1.42	26.6	1.06
13° without tide	-1.155	-1.155	-28	-1.12
13° with tide	-1.19	-1.48	-31.1	-1.33

For a non-uniform profile, the differences in sediment transport between without tide and with tide become even bigger. In Figure 32, it is visible that at high tide (with higher water levels) the differences are not noticeable. The steeper part of the profile is not directly influenced by the waves. At maximum low tide, this is strongly the case.

This also influences the transport as a function of direction (Figure 33 and Figure 34). The influence is rather small for directions with positive transport, but for directions with negative transport, the effect of the profile is quite noticeable. For waves of 2 m height which break more offshore, the influence of the tide increases for directions with positive transport.

Table 2 gives the values for net transport for  $H_{m0}=1$  m.

Table 2. Influence of profile shape on longshore transport.

	Net transport over uniform profile ( $\times 10^6 \text{m}^3/\text{year}$ )	Net transport over real profile ( $\times 10^6 \text{m}^3/\text{year}$ )
300° without tide	1.11	1.13
300° with tide	1.06	1.13
13° without tide	-1.12	-1.15
13° with tide	-1.33	-1.42

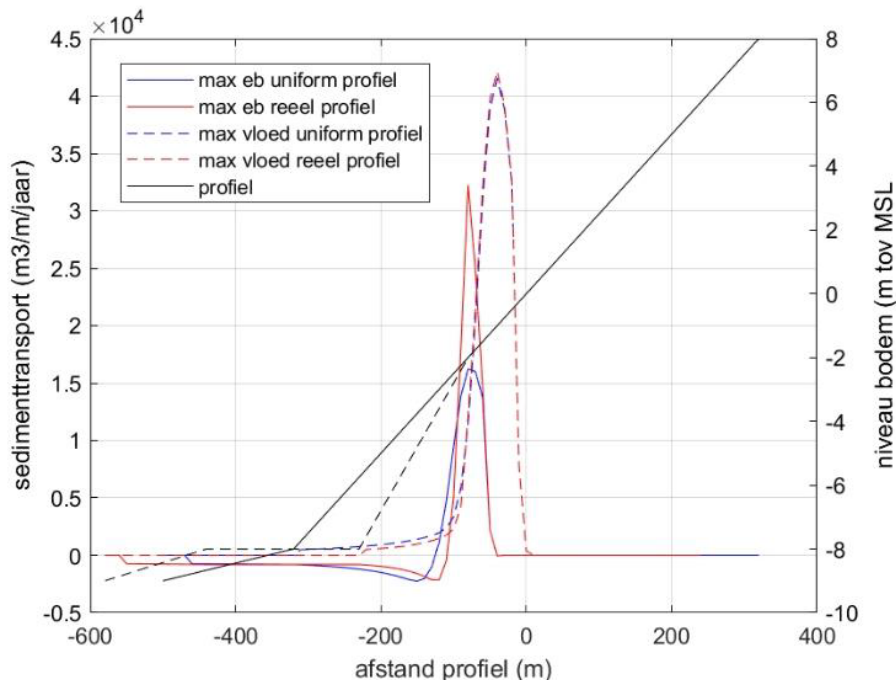


Figure 32. Longshore transport over the profile for  $H_{m0}=1$  m, direction 300° at maximum low tide and maximum high tide (at the point of maximum transport).

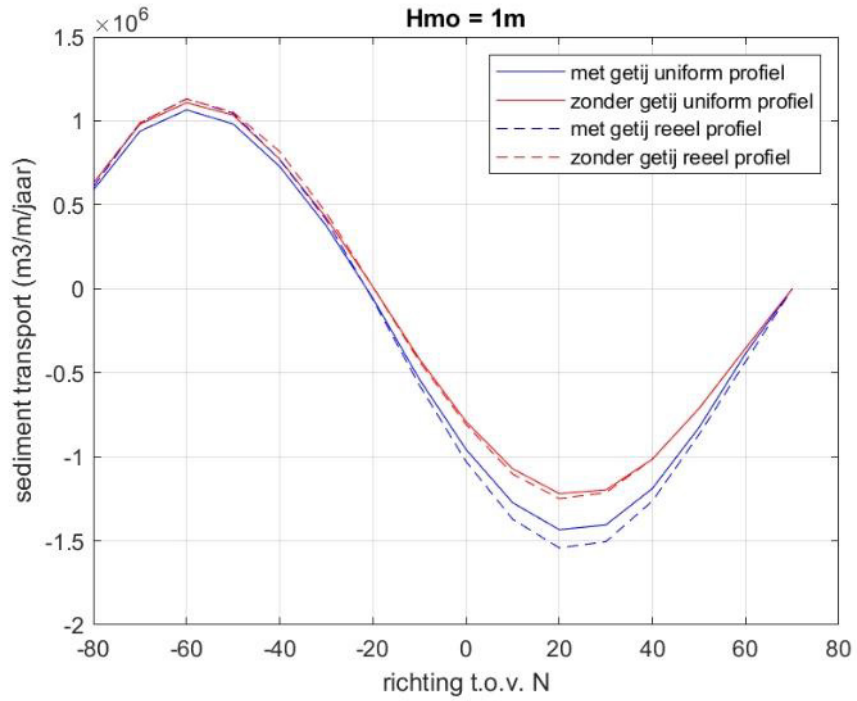


Figure 33. Net transport (per year) for Hm0=1 m for different directions.

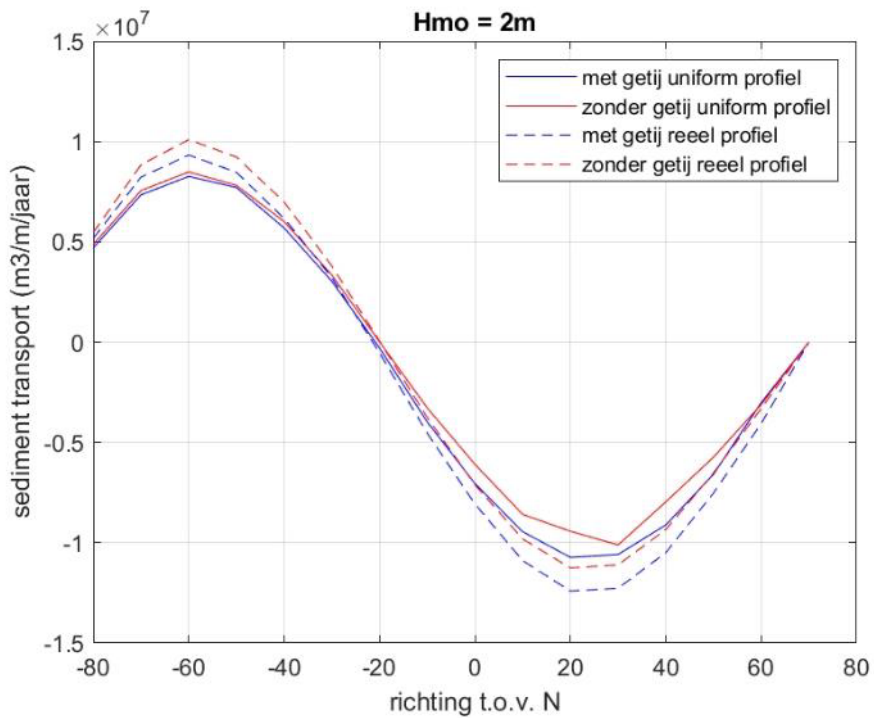


Figure 34. Net transport (per year) for Hm0=2 m for different directions.

## Conclusion

The main parameter that matters for the influence of the tide is the tide-driven velocity at the location where the waves break. The higher the water level, the higher in the beach profile this occurs. It appears that the higher in the profile, the lower the tide-driven velocity at this location. The positive tide velocities (in deep water) occur at an average water level that is 1.5 m higher than the negative velocities. Thus, the tide mainly enhances negative transports and therefore has a reducing effect if the net transport is positive (which is the case for Knokke).

### 4.2.3 Comparison with Scaldis-Coast

The comparison with the Scaldis-Coast model (run MO6\_009; Dujardin *et al.*, 2024) is not obvious since the model works with a morphological tide, which is different from the M2/M4 tidal components used in ShorelineS. So the comparison is rather qualitative.

Figure 35 compares the ebb and flood velocities. The black curves represent maximum flood, the red curves represent maximum ebb. The dots are from the original input file for tidal parameters in ShorelineS (based on Deltares, Roelvink *et al.*, 2023). From Scaldis-Coast run MO6\_009 three input files were derived (see appendix 3): the circles and x's result from 2 simulations with the tide 1 input file (the difference with and without nodal-correction is small), and the diamonds are from the tide 2 file. The output positions from the tide 1 file are located more offshore than those of the tide 2 file. It is surprising that maximum flood is smaller than maximum ebb here!. The full black and red lines are from ShorelineS simulations, using Manning roughness (0.02) instead of Chezy roughness (0.0023). The differences are rather small, although using Manning gives generally a higher roughness in shallow areas.

Next, also the relationship from the Scaldis-Coast tidal velocity output (from VEL\_crs30.fig; cross-section 30, run MO6\_009) was extracted. Those are the green (ebb) and blue(flood) points. It is noticeable that these tidal velocities are much smaller than those from ShorelineS, more than what can be expected due to the different approach to schematize the tide (morphological representative tidal cycle vs. M2 and M4 components only).

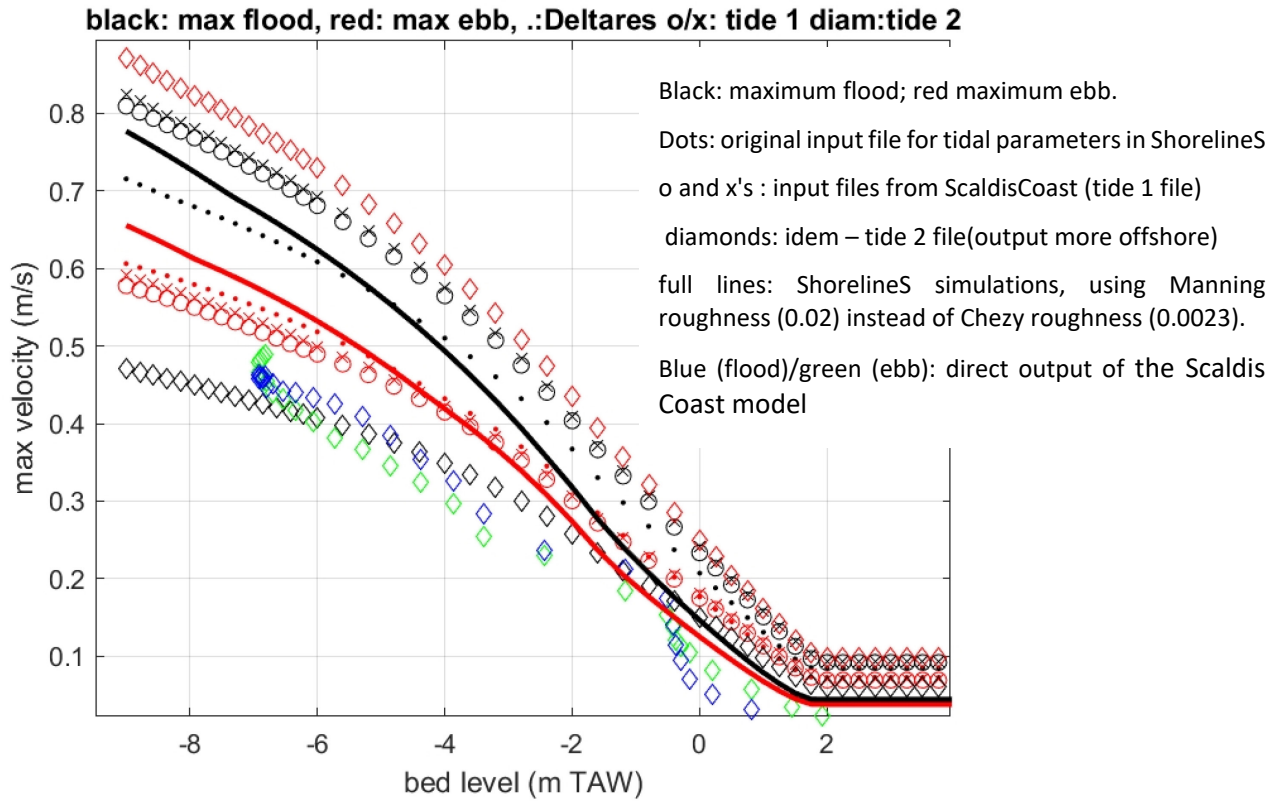


Figure 35. Comparison between longshore velocity Scaldis-Coast model vs ShorelineS model.

## 5 Adaptations to the ShorelineS modules

Following changes have been made (per routine)

### 5.1 Run\_shorelineS.m

Extra input parameters:

- S.Acal: for calibration of the Soulsby Van Rijn formule
- S.groinelev= elevation of the groyne (with reference level the mean water level)
- S.submerged (=1 is groynes are submerged, 0 otherwise)
- S.n : Manning coefficient for wave induced current. (default = 100: if n>1:Chezy instead of Manning will be used)

[S,0,H]=ShorelineS(S); extra output parameter H.

H includes (per calculated time step):

transg1: transport over the groyne in both directions  
 QS: longshore sediment transport per (in time variable grid cell)  
 dt: time step (variable)  
 Hs: offshore wave height (per time step, per grid point-  
 PHI: offshore wave direction (per time step, per grid point-  
 coastx: x position of the coastline (variable per time step)  
 coasty: y position of the coastline (variable per time step)

### 5.2 ShorelineS.m

In phase 1

[GROYNE]=transport\_bypass(TRANSP,WAVE,COAST,STRUC,GROYNE,TIDE.x,TIDE.zb,tel); in red: extra parameters, needed in the transport\_bypass script.

Variables TRANSP COAST GROYNE WAVE TIME are saved every 500 time steps. (in order to allow hotstart after a crash or for investigation.

In phase 2:

Write parameters to H

The east to west transport over the groyne is added to the west to east transport over the groyne. The sum of both is written to both sides (GROYNE.QS(ii,a): for a both 1 and 2

### 5.3 Transport.m

When using WAVETIDEPROF

Extra input parameters for the script tide\_wave\_transport: TRANSP.Acal,TRANSP.n

In case of submerged groynes: calculation of DLT, zs and QS for each of the 24 phases of the tide. With some adaptations in case the transport is tide dominated without much influence of waves: in that case DLT is less relevant, but a value is needed in order to continue the calculations.

Some code to allow the output (current velocities, transport) at a requested cross shore profile (standard disabled)

## 5.4 Tide\_wave\_transport.m

Introduction of parameters Acal (used in soulsy\_van\_rijn.m) and n (in wave\_current.m)

## 5.5 Wave\_current.m

Use of Manning coefficient if  $S.n < 1$ . (Manning is converted to depth dependent Cf value).

## 5.6 soulsy\_van\_rijn.m

Correction of  $Asb = 0.005 * h * (D50./h/delta/g/D50).^1.2$ ; (instead of 0.05 in the original code)

Scaling of the transport with the parameter Acal

## 5.7 transport\_bypass

In this module a new approach is implemented (cf. Trouw, 2024))

For each of the 24 phases of the tide:

- $D_s$ ,  $D_{sa}$  and  $D_{lt}$  are calculated using the water level corresponding to the tidal phase. For  $D_s$  also the cross shore profile is used (from the TIDE-variable) instead of assuming a Dean profile
- The transport rate  $Q_{st}$  as calculated in transport.m (phase depended) is used
- The bypass factor is calculated, taking into account a reduction due to limited elevation of the groyne, using the formule derived in Appendix 2)

Important:  $Q_{sgroin}$  has to be reset for both sides, so inside “for side=1:2”

The script might not work correctly if  $maxbypass > 1$  !

## 5.8 Prepare\_transport.m

In the original version the input value of  $A_w$  is overruled in case a time series is used as input for the waves. This is removed.

Transfer of values  $S.n$   $S.Acal$  and  $S.submerged$  to the TRANSP – struct-variable.

## 5.9 Prepare\_structures.m

```
STRUC.groinelev=S.groinelev;
```

## 5.10 Initialize\_defaultvalues.m

```
S.n=100;  
S.Acal=1;  
S.submerged=0;  
S.groinelev=[];
```

## 5.11 get\_timesteps

```
if isnan(max(abs(TRANSP.QSmax)))  
    adt=dsmin^2*h0min / (4*max(abs(TRANSP.QS)));  
end
```

otherwise, if  $Hm_0=0.01$ ,  $QS_{max}$  is NaN and the minimum time step is obtained, although wave transport is zero. If  $QS_{max}=NaN$ ,  $QS$  is used.

## 6 Run\_shorelineS -parameters

Below is the script to start up ShorelineS. In red comments are added, based on experience with the Knokke-case (not always detailed in this report).

```
%%%%%%%%%%%%%%%%%%%%%%%%%%%%%%%%%%%%%%%%%%%%%%%%%%%%%%%%%%
addpath(genpath('C:\shorelines\functies_basis'));
%%%%%%%%%%%%%%%%%%%%%%%%%%%%%%%%%%%%%%%%%%%%%%%%%%%%%%%%%%
```

This path contains the new functions as described in chapter 5 (and the standard ones)

```
%%%%%%%%%%%%%%%%%%%%%%%%%%%%%%%%%%%%%%%%%%%%%%%%%%%%%%%%%%
%% MODEL INPUT PARAMETERS
%%%%%%%%%%%%%%%%%%%%%%%%%%%%%%%%%%%%%%%%%%%%%%%%%%%%%%%%%%
```

```
S=struct;
S.LDBcoastline='kustlijn1999.txt';           % LDB with initial coastline shape
[Nx2] <- leave empty to use interactive mode!
The initial coastline. It is assumed to be at the MWL. Some smoothing is recommended.
```

```
S.WVCfile='golfklimaat_19992005.wvt';
This file contains the names and coordinates of 5 time series at 5 different locations.
In the earlier versions of ShorelineS, using a wave climate instead of a time series
resulted in very large time steps, so that the weight of storms was too small ! To be
checked if this is still the case in the most recent version.
```

```
S.n=0.02;
Manning coefficient for wave induced currents
S.Cf=0.0023;
Cheze coefficient for tide induced currents
S.ks=0.05;
Roughness height used for Soulsby-Van Rijn transport formulation (not for the
calculations of currents.
S.d50=300e-6;
S.d90=400e-6;
Grain sizes used for Soulsby-Van Rijn transport formulation (not for the calculations
of currents.
```

```
S.ddeep=9; %diepte op de plaats waar je het golfklimaat ingeeft
The used wave climate is the result of SWAN calculations with output at -5 à -7m TAW.
Adding the mean water level of 2.3 gives a value of about 9m. The result is sensitive
to this value, since the deeper, the more refraction occurs (giving a reduced
transport) (cf. Figure 36)
```

```
S.d=12;           % active profile height [m]
A depth of closure of -6m TAW is used, together with 6m (slightly higher than HW level
of 4.5m TAW). Value can be used to further calibration.
```

```
S.trform='WAVETIDEPROF';
S.tidefile='tidalforcingFE_Lambert.txt';
S.dx=10;
Use of the tidal module, with a cross shore grid size of 10m (finer does not make
sense).
```

```
S.profile='profileknokke99.txt';
The cross shore profile as described in this report
```

```
S.reftime='1999-10-01';           % Reference time <- leave empty to use t=0
S.endofsimulation='2004-04-04';   % End time of simulation
```

```
S.tc=0.6;
Time step is reduced with this factor
```

```

S.smoothfac=0.01;
Smoothing factor applied to the coastline after each time step. Effect is not really
visible. One simulation done with recommended factor 0 after 1 month it crashed.
Generally, little to no influence could be seen. Only at a very sharp bend in the
coastline, instabilities occurred.
S.ds0=25; % initial space step [m]
Given the complex coastline a smaller value as recommended is used. It is understood
that ShorelineS adapts this when necessary. Too small initial values (0(10m) would lead
to possible instabilities
S.ns=100; % number of ...?
S.twopoints=1;
% upwind treatment involving two points (1) or 1 point (0) not further investigated

Following parameters are in the default input file, but not used here (no nourishments
tested)
S.growth=0;
S.nourish=0; % switch (0/1) for nourishments
S.LDBnourish=''; % LDB with nourishment locations
[Nx2] (i.e. polygon around relevant grid cells) <- leave empty to use interactive mode!
S.nourrate=100;
S.nourstart=0;
S.spit_width=50; % width of tip of spit (used for overwash)

load('x_hardnieuw');
load('y_hardnieuw');
S.x_hard=x_hard;
S.y_hard=y_hard;
Contour of the groynes. Between 2 groynes a NaN value is given

S.struct=1; % switch for using hard structures
load('zgroin');
S.groinelev=zgroin-2.3;
Zgroin gives the elevation of the offshore tip in m TAW. -2.3 to have MSL as reference
level
S.submerged=1;
Set at 1 for submerged groynes, otherwise no calculations of zs, Qs, ... during the tidal
cycle is gathered and used in the transport_bypass script.
S.spread = 30;
S.spread is only used in case of 1 wave height (S.Hm0 e.g.), not for the time series.
So in the final runs, no spreading is taken into account. The spreading is a variation
of the wave direction around a mean value and not really directional spreading (which
is zero !)
S.Aw = 1.27; reference is made to appendix 2: only relevant for emerged groyne
setting, otherwise Aw is not used.
S.diffraction = 0; %in hun voorbeeld nemen ze 0 en 1
S.dirspr=10; in case of diffraction
Diffraction is tested and seems to reduce transport, but crashed after 10 days. To be
examined further.
S.Acal=0.5;
Calibration factor for Soulsby Van Rijn transport formule
S.outputdir='output'; % output directory for plots and animation
S.fignyear=192;
%%%%%%%%%%%%%%%%%%%%%%%%%%%%%%%%%%%%%%%%%%%%%%%%%%%%%%%%%%%%%%%%%%%%%%%%
%% RUN SHORELINES MODEL
%%%%%%%%%%%%%%%%%%%%%%%%%%%%%%%%%%%%%%%%%%%%%%%%%%%%%%%%%%%%%%%%%%%%%%%%
S0=S;
[S,O,H]=ShorelineS(S);
save('output\Results.mat','S','O');

```

Another parameter is S.hclosure. This is the depth at which the longshore transport is cut off. The default value of 8 (m) is used.

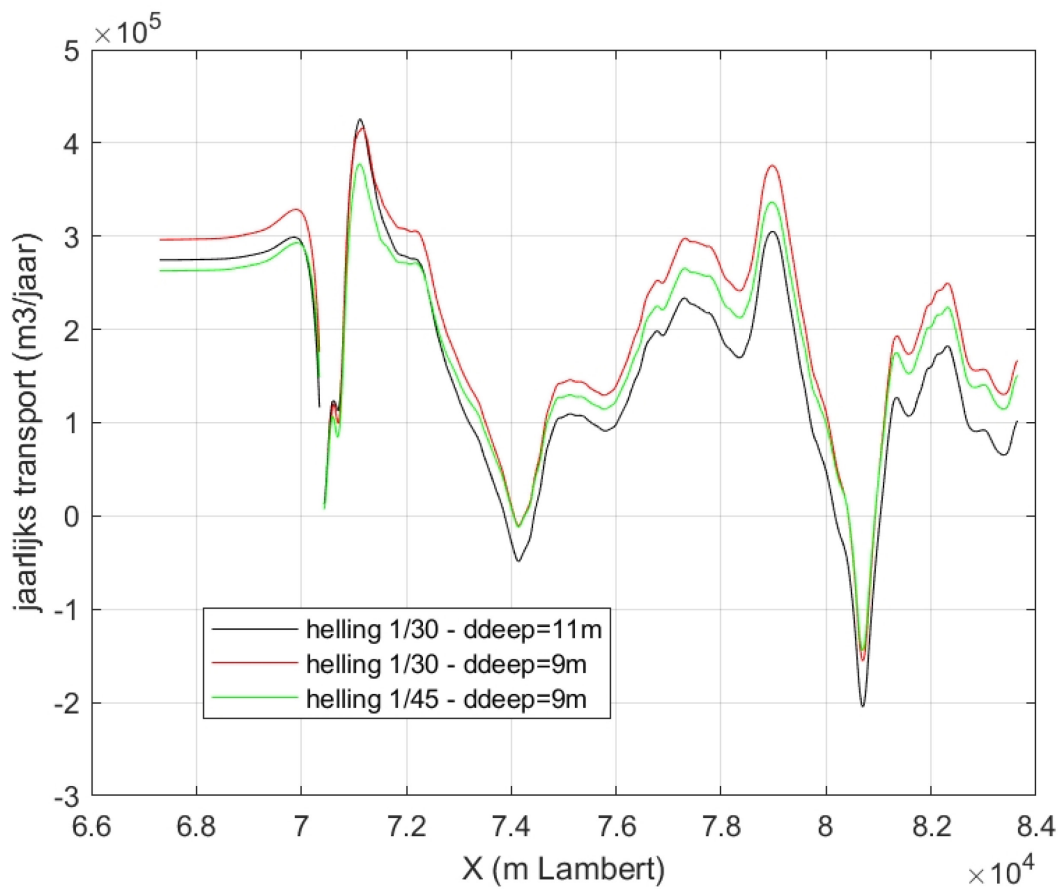


Figure 36. Effect of ddeep and beach slope.

## 7 Final simulations

### 7.1 Introduction

Using the scripts as developed in chapter 5 and 6 simulations have been done for the period 1999-2004 for the coastline between the harbour of Zeebrugge and just east of the Zwin inlet entrance. Tidal currents influence is included in these simulations. In this period, no significant nourishments were carried out. Three cases have been modelled: without groynes (except Zeebrugge harbour), with emerged groynes and with real, low-crested groynes (described in chapter 3).

The zone is divided in 5 coastal stretches (excluding Baai van Heist, just east of the harbour dam, which is not suitable to be modelled with a 1-line model). The modelled differences in longshore transport over these zones (=erosion or sedimentation) are compared with observed volume changes in this period.

### 7.2 Observed volume changes

Volume changes per year have been compiled by Houthuys et al. (2022) for different coastal stretches. Each stretch consist of 2 to 10 sections. These sections are shown in Figure 37. This was done for the zone above LW (above +1.39 m TAW), for the shoreface (down to -4.11 m TAW), and the seabed (from -4.11 m TAW to the end of the section, 1500 m offshore). From these series, data between the end of 1999 and 2004 were selected (for the shoreface, data were included until 2007 due to uncertainty about some data in the 2003/2004 period). Trend lines were then determined through these points. These are shown in Figure 38 to Figure 42).

For Duinbergen (Figure 38) the 2007 point for the shoreface might look like an outlier. However, looking to the longer term evolution, 2003 should be identified as outlier (too low value). The seabed is outside the section boundaries, so there is no evolution.

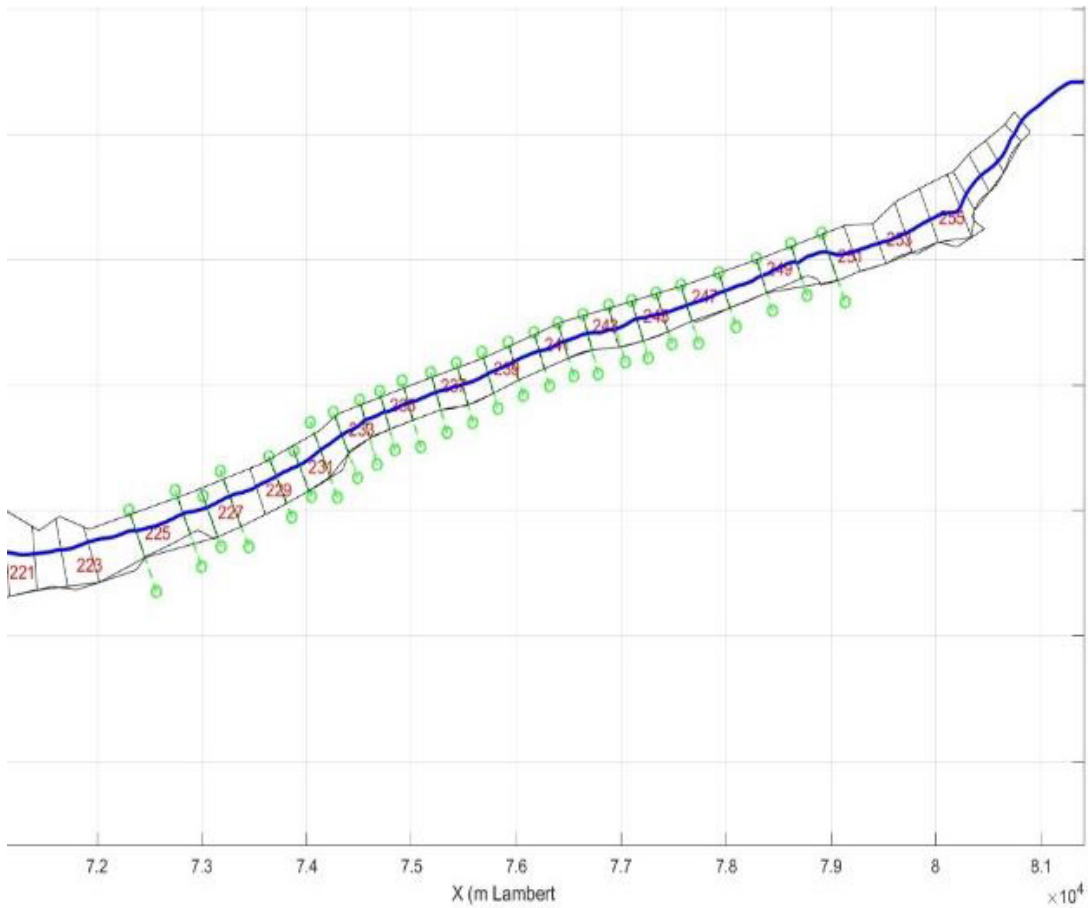


Figure 37. Sections (red numbering), coastline (blue line) and groynes (green).

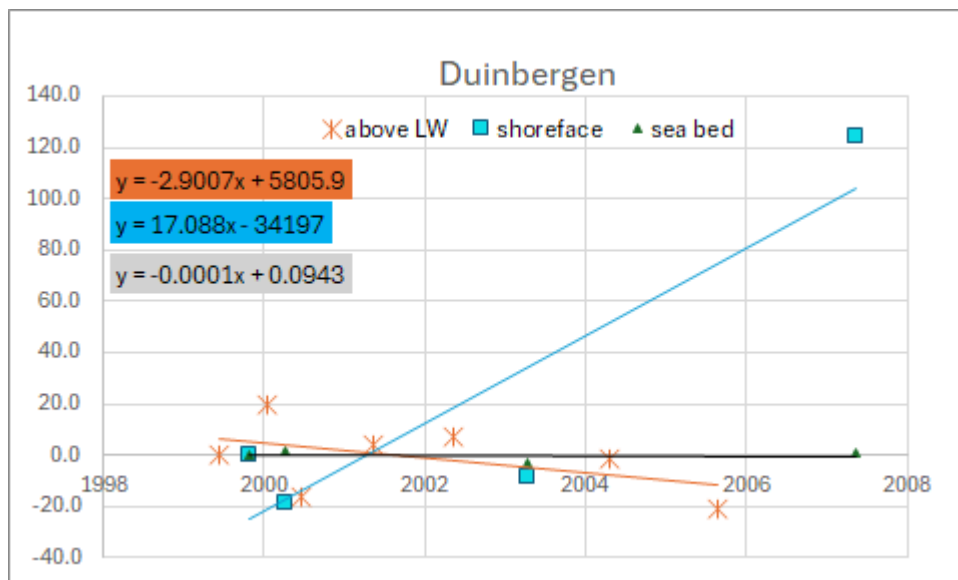


Figure 38. Observed volumes (m<sup>3</sup>/m) for Duinbergen (sections 225-226).

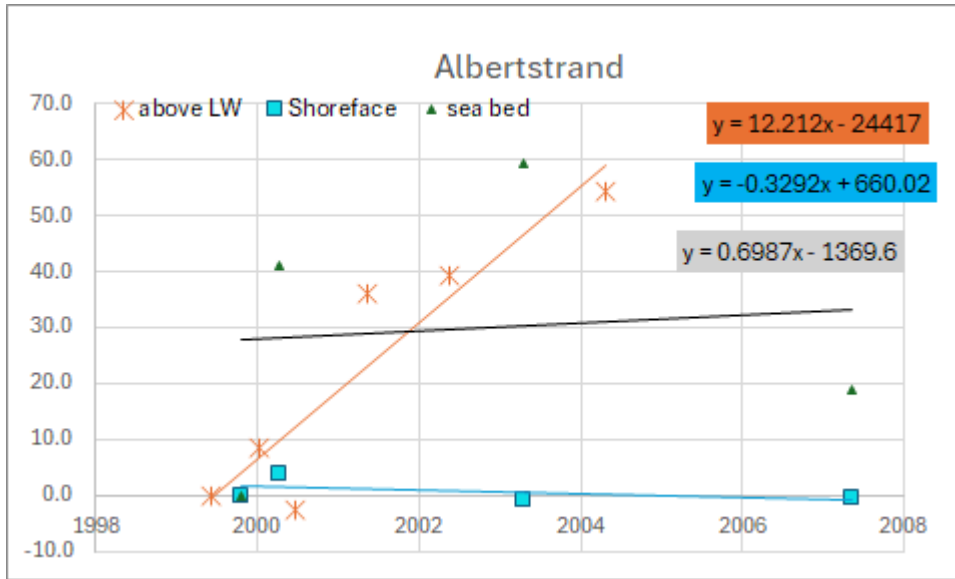


Figure 39. Observed volumes (m³/m) for Albertstrand (sections 227-232).

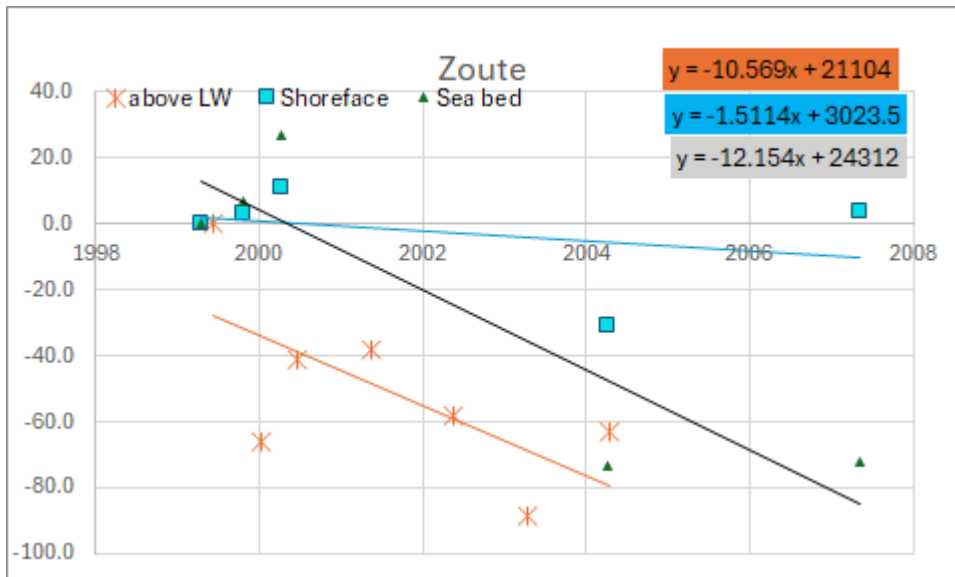


Figure 40. Observed volumes (m³/m) for Knokke-Zoute (sections 233-241).

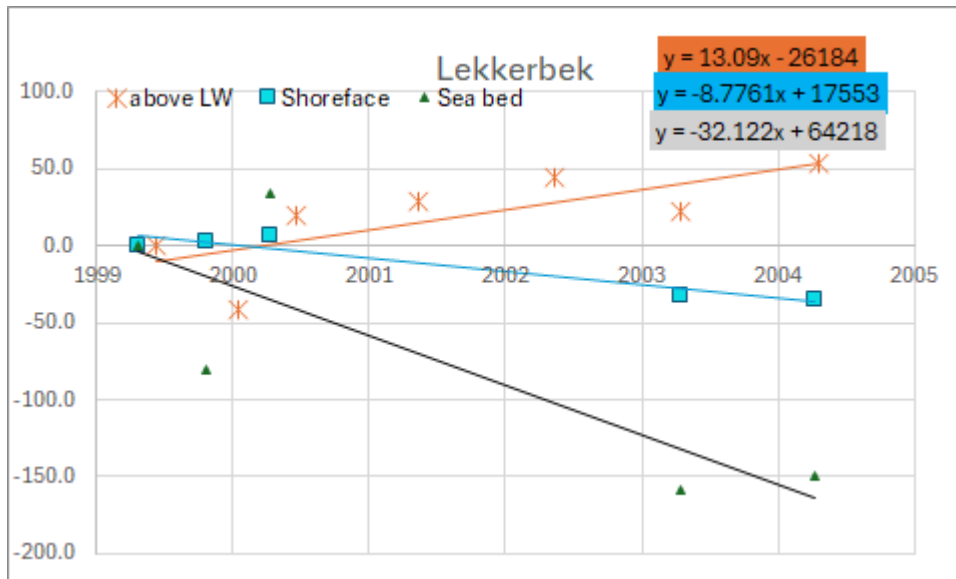


Figure 41. Observed volumes (m³/m) for Knokke-Lekkerbek (sections 242-249).

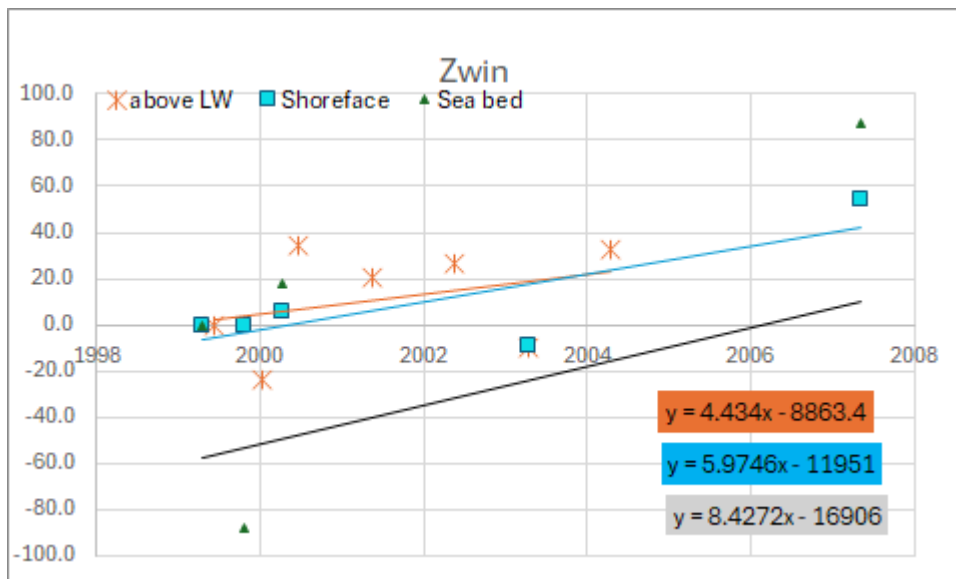


Figure 42. Observed volumes (m³/m) for Zwin (sections 250-255) (the seabed data point for 2003 is -190 m³/m).

The observed trends are summarized in Table 3. The sea bed (below -4.11 m TAW up to 1500m offshore) includes the Appelzak gully. The -4.11 m TAW contour and the toe of the profile are only at a small distance. So, taking into account the complete sea bed evolution does not make sense to describe the beach volume evolution. For this reason, also the total volume above LW+ shoreface has been given, without the sea bed volume evolution.

### 7.3 Modelled volume changes

In Table 4 the volumes as modelled with ShorelineS are given. These are calculated as the difference in longshore sediment transport (over the groyne when a groyne is present) over the boundary of the coastal stretches. Figure 43 shows the longshore transport in the project area as an average over de 4 year modelling period (end 1999 – begin 2024). The groynes have a significant influence in the groyne field, but the effect disappears over a short distance east of the last groyne. The longshore transport seems to reach zero a few times, but this is an artificial effect of how the shadow zone of the groyne is modelled in ShorelineS (illustrated in §7.4). Figure 44 shows the result as obtained in the Mozes project (Dujardin et al, 2024). The small transport just east of Zeebrugge and, after 3 to 4 km the strong increase in longshore transport is comparable. The coastline evolution is shown in Figure 45. The important effect of the most eastward groyne is illustrated in Figure 46. In Table 5 the result for the scenario with real groynes is divided per year, showing a large temporal variation. The volume changes are also compared in Figure 47. In this figure the modelled volume changes have been scaled in such way that for the stretch Zoute the same result is obtained as observed. This is equivalent to scaling the longshore transport rates (with  $A_{cal}$  in the formule of Soulsby-Van Rijn) such that the volumes correspond at Knokke-Zoute. It can be seen that the results with emerged groynes significantly differs from the other results. The observed sedimentation rate in stretch 5 (Zwin) is a complex mix between erosion just east of the last groyne and more sedimentation towards the mouth of the Zwin. For Lekkerbek (stretch 4) the erosion of the sea bed is very large and adding a small part of this erosion to the profile/beach erosion would result in an observed erosion in this stretch instead of sedimentation). Also the large temporal variations (modelled) should be examined in more detail. Figure 48 shows that the outflux in year 4 is much larger than for other years, while the influx is rather constant. This is partly due to a reorientation of the coastline, as shown in Figure 51 and less due to variations in undisturbed sediment transport (calculated as the sum of  $H_{m0}^2 \cos \alpha \sin \alpha$ , with  $H_{m0}$  the input value and  $\alpha$  the wave direction relative to the coastline normal (results shown in Figure 50). For reference, also the longshore transport per year in case no groynes are present is shown (Figure 49).

It is also noted that the results depend much on the initial coastline. This is visible in Table 5 where the coastline obtained after the first year is used as a starting coastline for which the wave climate of the first year is repeated again. The effect on the erosion/sedimentation volumes is significant (in the first year the erosion was almost equal in Lekkerbek and Zwin (resp. -21 and -30m<sup>3</sup>/m/y), while in the repeated year it is all concentrated in Lekkerbek (-51m<sup>3</sup>/m/year).

The used coastline is the one at MWL. Other coastlines show more effect of the groyne. For example the jump in the coastline at the most eastward groyne (cf. Figure 46) is smoothed out in the initial coastline. This could be studied in more detail.

Table 3. Observed erosion/sedimentation trends (in m<sup>3</sup>/m/y) in the period 1999-2004/2007)  
(based on data of Houthuys et al, 2022).

	Duinbergen (225-226)	Albertstrand (227-232)	Zoute (233-241)	Lekkerbek (242-249)	Zwin (250-255)
Length of coastal stretch (m)	700	1410	2237	2310	1590
above LW	-3	12	-11	13	4
shoreface	17	0	-2	-9	6
sea bed	0	1	-12	-32	8
above LW+shoreface	14	12	-12	4	10
all	14	13	-24	-28	19

Table 4. Modelled erosion/sedimentation rates (m<sup>3</sup>/m/year) for a period of 3 years starting from 1<sup>st</sup> of October 1999.

	Duinbergen (225-226)	Albertstrand (227-232)	Zoute (233-241)	Lekkerbek (242-249)	Zwin (250-255)
emerged groynes	-5	13	-3	-4	-51
without groynes	21	27	-37	-14	37
real groynes	33	21	-17	-18	-12

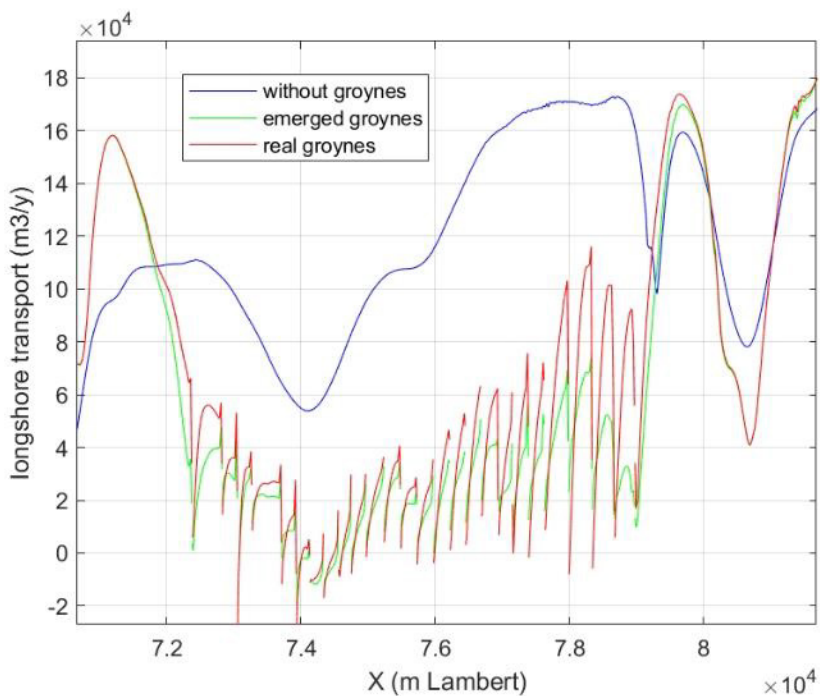


Figure 43. Modelled longshore transport.

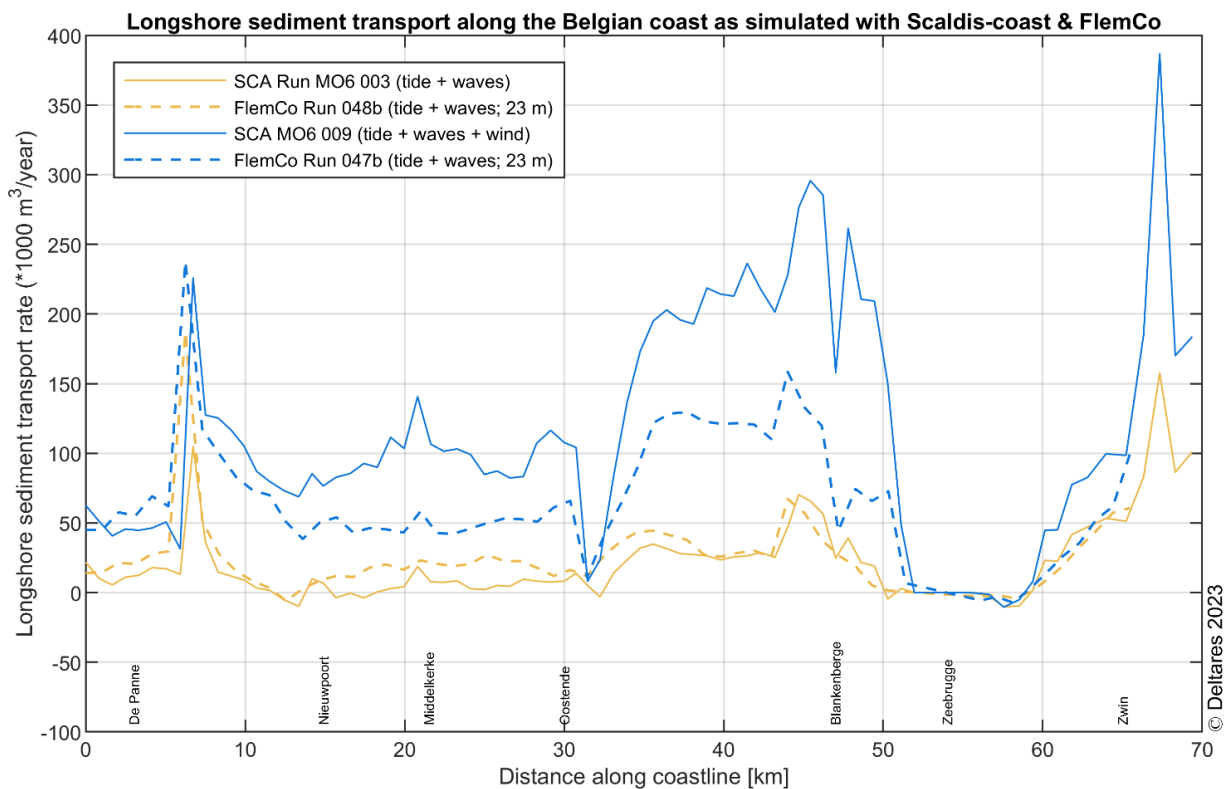


Figure 44. Modelled longshore transport with Scaldis-Coast (full lines) and Flemco (dotted). Orange:without wind, blue with wind.

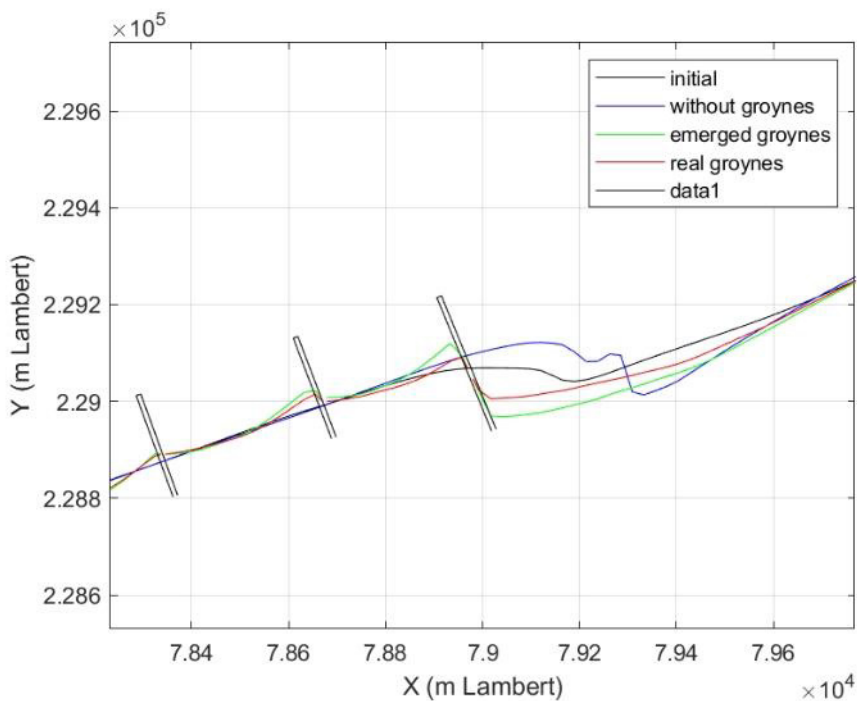


Figure 45. Coastline after 3 years for the 3 different scenarios.



Figure 46. Google Earth image of the effect of the most eastward groyne.

Table 5. Modelled erosion/sedimentation per year (scenario with real groynes)

	Duinbergen (225-226)	Albertstrand(227- 232)	Zoute (233-241)	Lekkerbek(242- 249)	Zwin (250- 255)
year 1	14	22	-22	-21	-30
year 2	67	38	-25	-25	2
year 3	27	6	-5	-10	-4
year 4	83	31	-18	-62	8
year 1 repeated after year 1	36	26	-20	-55	-1

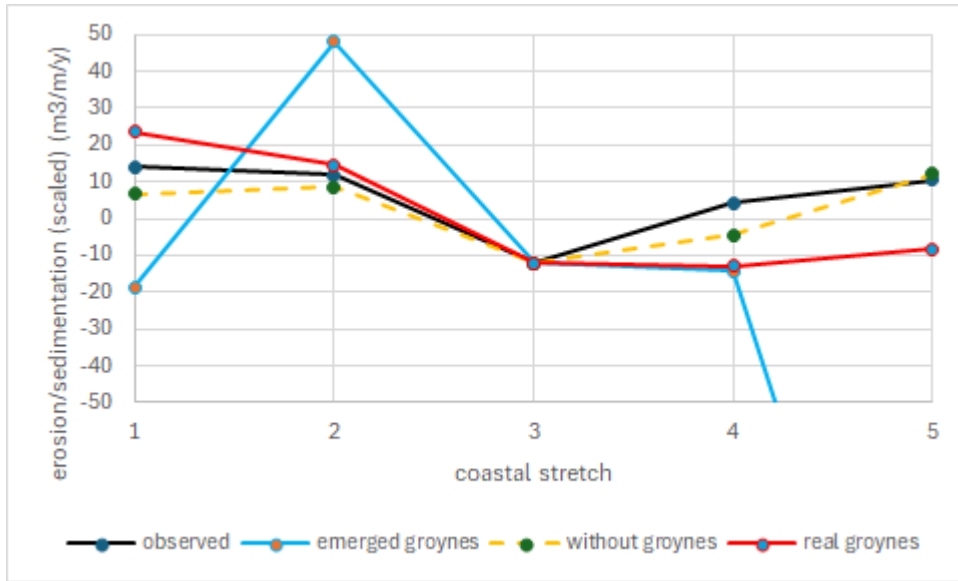


Figure 47. Comparison between observed erosion/sedimentation rates and modelled (scaled).

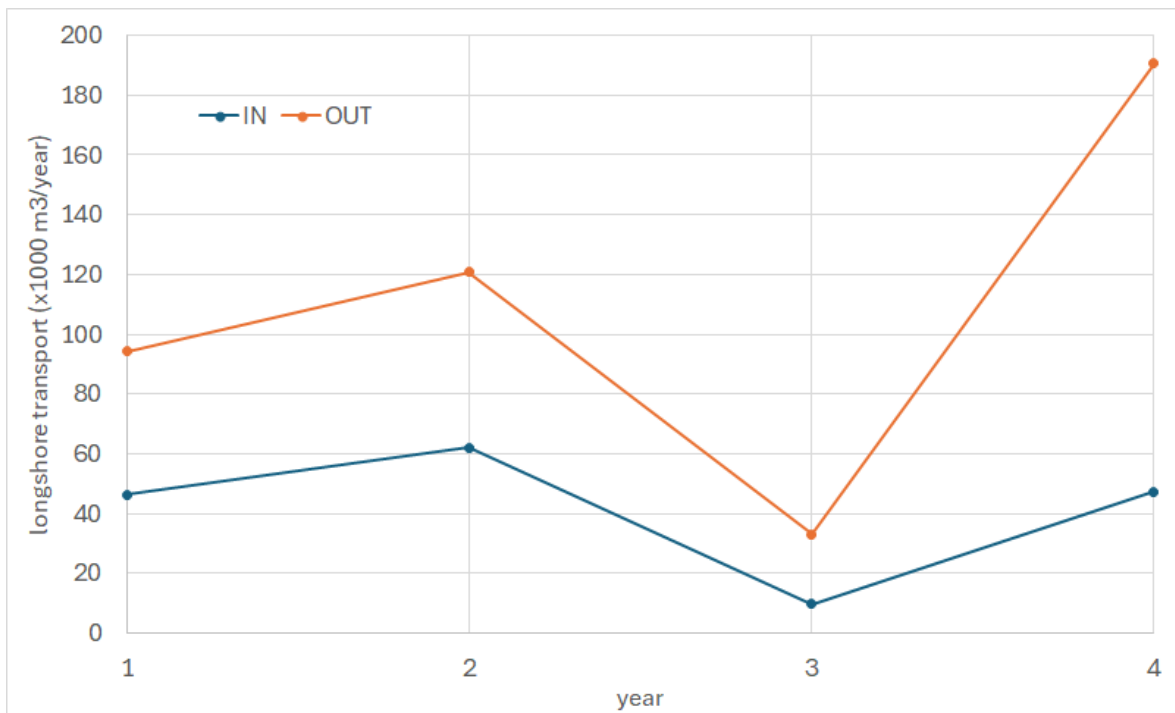


Figure 48. Temporal variation of in and out flux of stretch 4 (Lekkerbek).

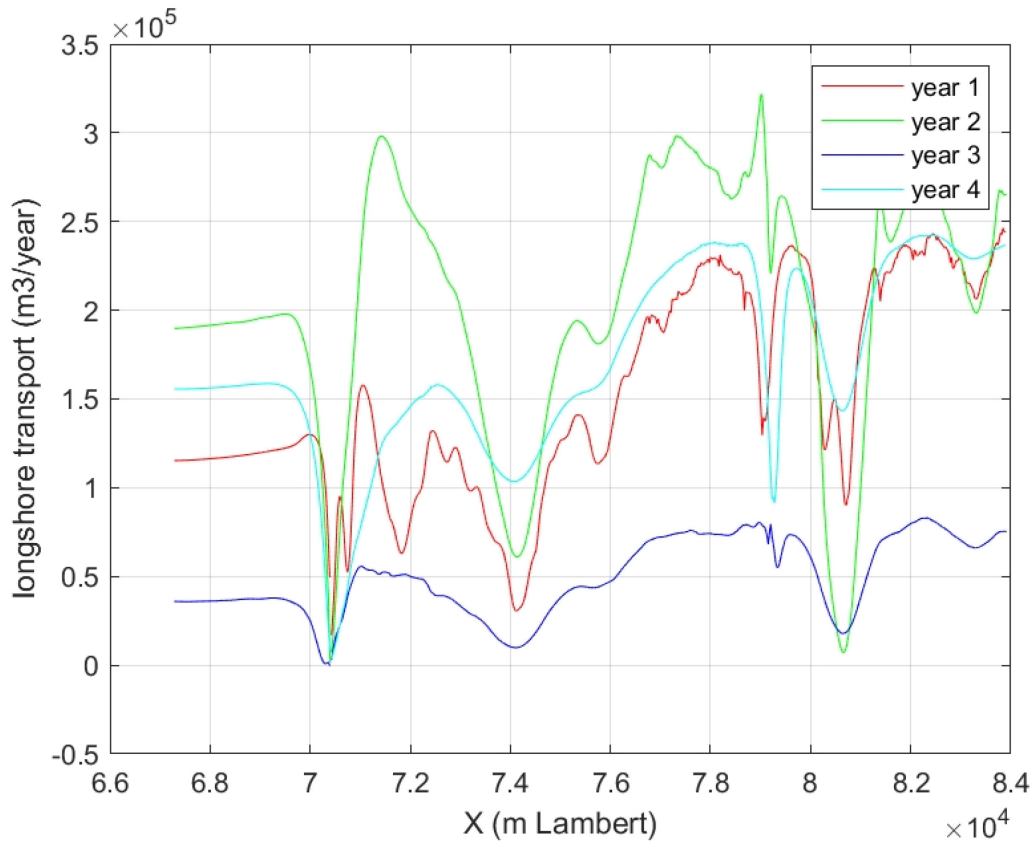


Figure 49. Longshore transport per year (case without groynes).

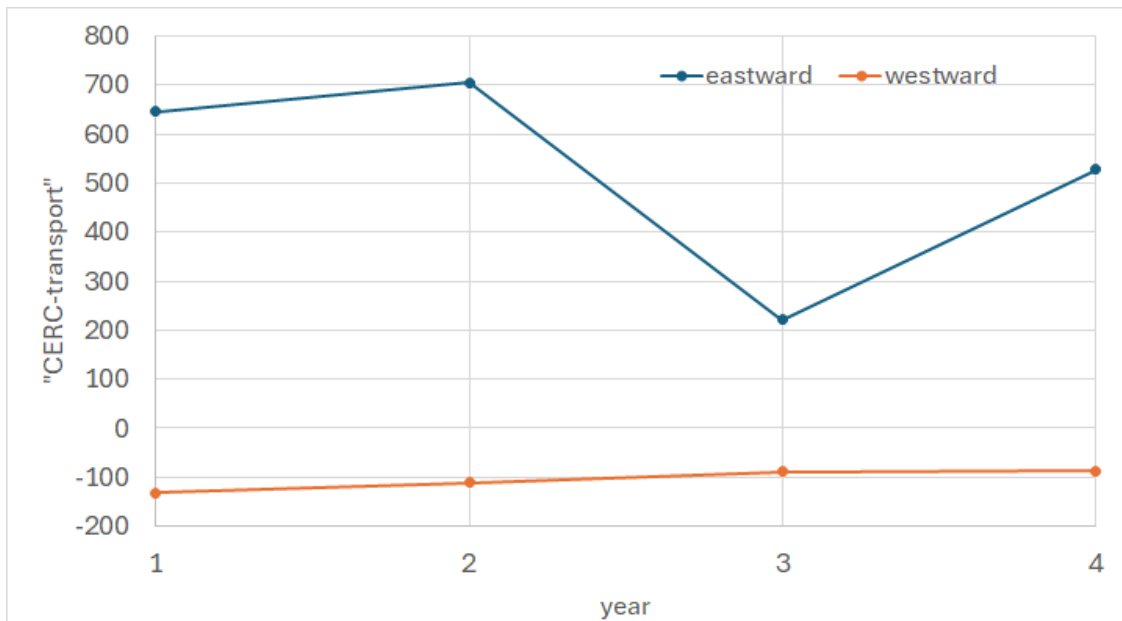


Figure 50. Temporal variation of  $Hm0^{\cos(\alpha)}\sin(\alpha)$ .

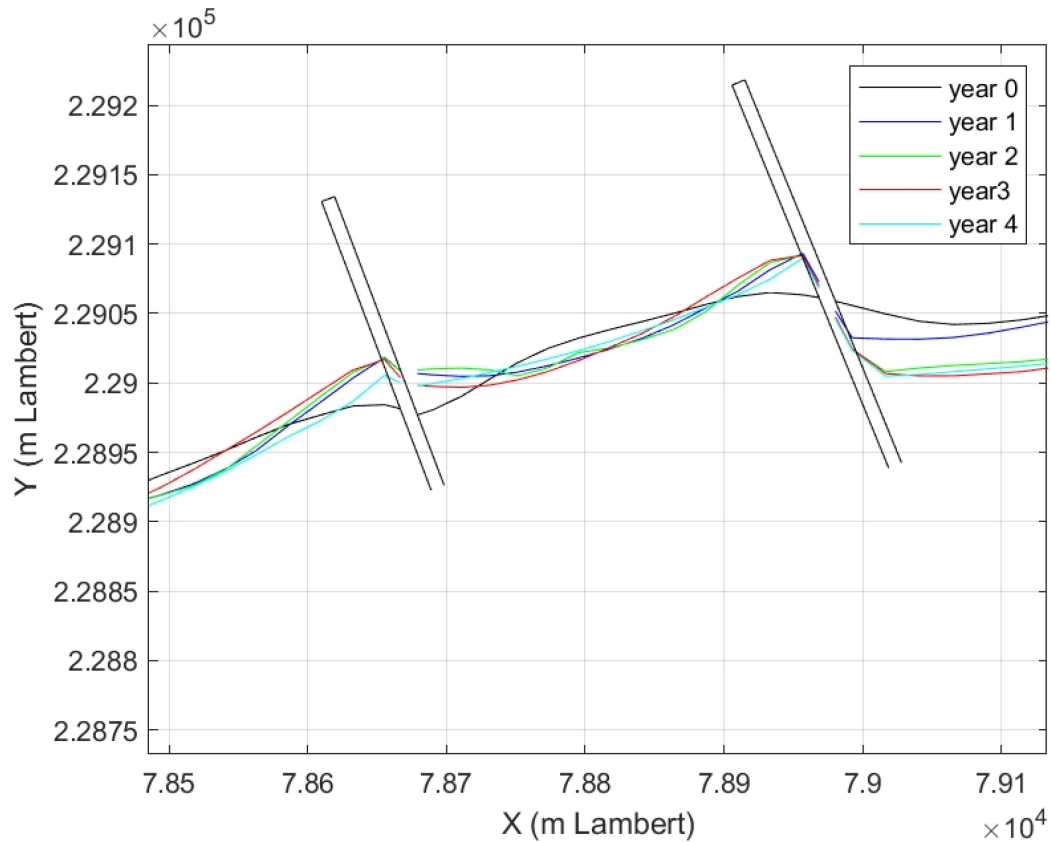


Figure 51. Time evolution of the coastline near the eastward boundary of stretch Lekkerbek.

## 7.4 Other observations

The groyne blocks all the waves creating a shadow area. In this area, the longshore sediment transport (TRANSP.QS) is zero and just outside this zone it jumps to undisturbed values (cf. Figure 52 for oblique waves or Figure 53 where the transport is shown as function of the offshore wave direction for a location in the middle between 2 groynes). However, the model redistributes the transport passing the groynes in this zone.

Using diffraction might (partly) result in a more smooth transition. A simulation with diffraction crashed after 10 days. During these 10 days, the coastline change was much less than the one obtained with a simulation over the same period but without diffraction. This should be examined further.

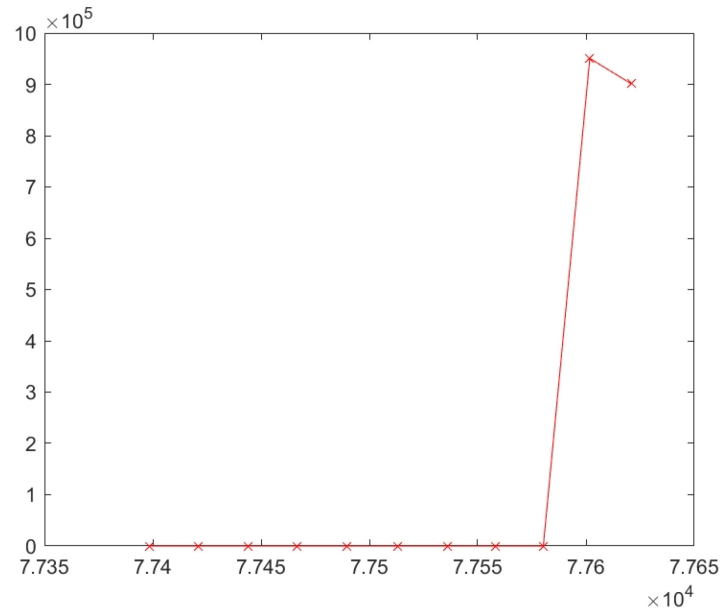


Figure 52. Longshore transport between 2 groynes for 1 time step with oblique waves.

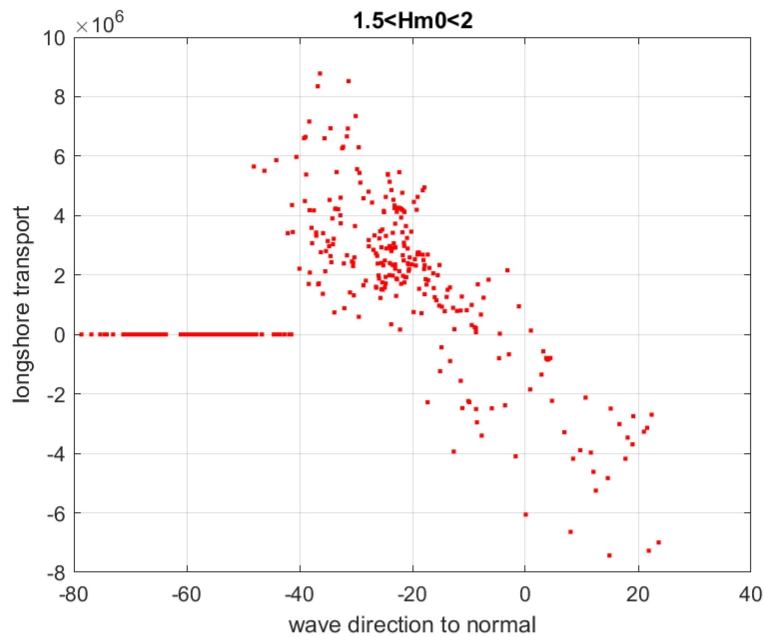


Figure 53. Longshore transport for a location in between 2 groynes.

During each time step, the transports over the groynes are calculated for a tidal cycle. This means that possibly, transport occurs in both directions. If the sum of all transport (over all time steps and tidal phases) in eastward direction is added up and the same for the westward, the ratio of both can be calculated. This is shown in Figure 54. For the second most eastward groyne, this ratio is 6 (number 26), but for all other groynes, the westward transport is quasi neglectable.

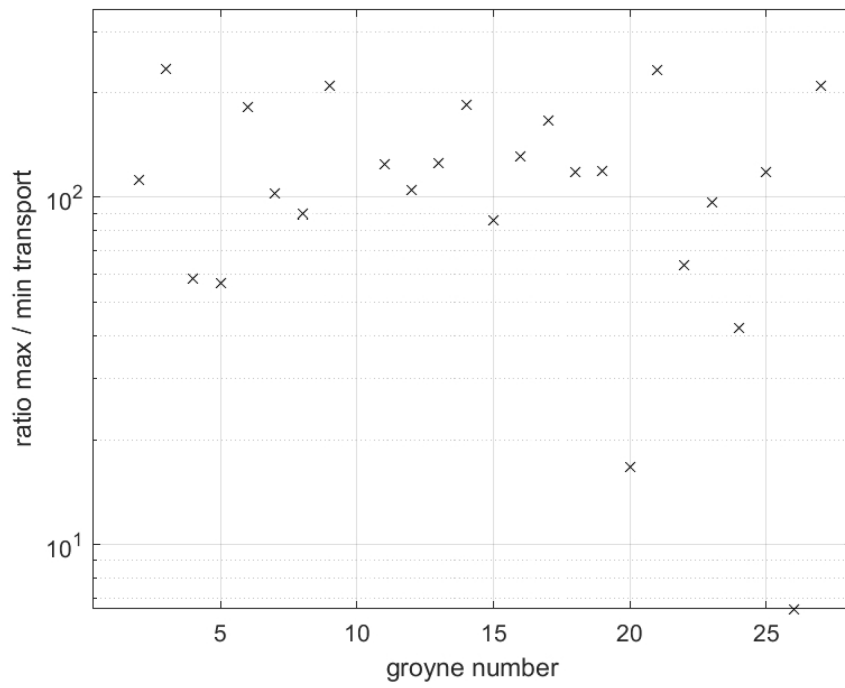


Figure 54. Ratio of maximum transport during tidal cycle (westward) over minimum transport (eastward) (absolute values).

## 8 Recommendations

Based on the finding in the present study a series of recommendations can be proposed:

- Analyze in more detail to the observed morphological changes in the period 1999-2004. For this reason, it is regrettable that no bathymetrical data (only partial Lidar) is available for 2003-2004. Implementing the sand nourishments carried out in 2004, 2006, 2007 and continue up to 2007 might be a solution. It should be looked up in detail how much erosion occurs between the toe of the cross shore profile and -4 m TAW, since this part is missing if only “shoreface changes” is used, without “sea bed changes”
- Work with wave climate instead of time series. Now e.g. “year 1” is year 1 added up with part of year 2 to fill up the gaps. Probably the new version of ShorelineS can handle this. Gaps in the wave climates could also be filled up (e.g. to avoid that storm conditions are underestimated). It is advised to use the existing time series to find a relation between wind speed and wave height at the given location for different wind directions. And use this relationship to fill up gaps.
- Test the use of extra locations for the wave climate, especially just east of Baai van Heist
- The depth of the locations of the wave climate influences the refraction and thus the wave obliqueness at the breaking point. Since this is important for the longshore transport, this should be taken into account during further validation/sensitivity studies
- Use other contour lines, e.g. contour lines where the effect of the groynes is more visible. And use less smoothing around the groynes, in order to start the modelling with a more realistic coastline.
- Update the implementation of the groynes to their actual length
- Look for the reasons of the important temporal variations of the erosion/sedimentation rates
- Use other modelling periods, together with the use of nourishments in the model
- Look in more detail to parameters that are not yet examined (e.g. diffraction around groyne, transmission of waves over the groyne, ks-value, grain size, ...)
- In the Scaldis-Coast project, it was found that the wind generated current has an important impact on the longshore transport (Wang *et al.*, 2024). It could be examined how this can be incorporated into ShorelineS.
- Develop scripts in order to have variable cross shore profiles along the coast.
- 

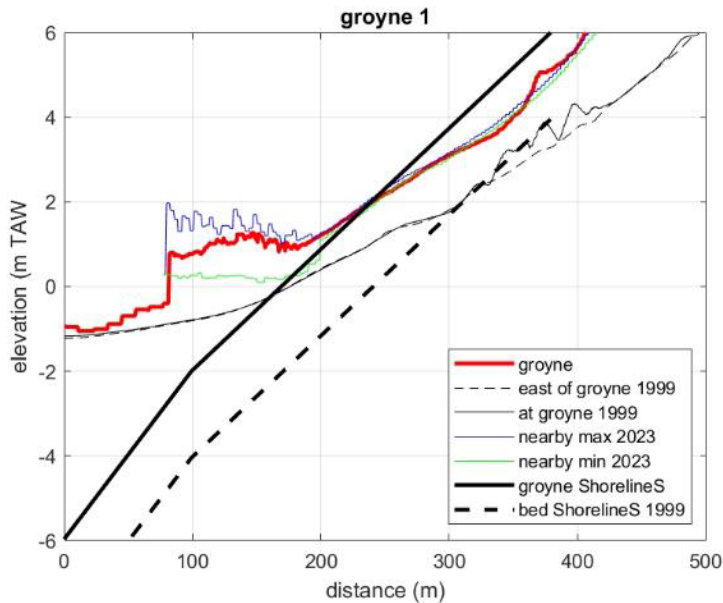
In Verwaest (2022; 2023) resp. the long and short time evolution of the coastline is inventoried, described and explained. This is a basis to validate ShorelineS for other periods.

## 9 References

- Dujardin, A.; Houthuys, R.; Nnafie, A.; Röbbke, B.; van der Werf, J.; de Swart, H.E.; Biernaux, V.; De Maerschallck, B.; Dan, S.; Verwaest, T.** (2024). MOZES – Research on the Morphological Interaction between the Sea bottom and the Belgian Coastline: Working year 2. Version 4.0. FHR Reports, 20\_079\_2. Flanders Hydraulics Research: Antwerp
- Houthuys, R.; Verwaest, T.; Dan, S.** (2022). Morfologische trends aan de Belgische Kust: Evolutie van de Vlaamse kust tot 2019. Versie 3.0. WL Rapporten, 18\_142\_1. Waterbouwkundig Laboratorium: Antwerpen.
- International Marine and Dredging Consultants.** (2009). Afstemming Vlaamse en Nederlandse voorspelling golfklimaat op ondiep water: deelrapport 5. Rapportage jaargemiddelde golfklimaat. Waterbouwkundig Laboratorium: Antwerpen.
- Monbaliu, J.; Mertens, T.; Bolle, A.; Verwaest, T.; Rauwoens, P.; Toorman, E.; Troch, P.; Gruwez, V.** (eds.). CREST Final scientific report: Take home messages and project results. VLIZ Special Publication, 85. 145 pp. Flanders Marine Institute (VLIZ): Oostende, 2020. ISBN 978-94-920439-0-0.
- Roelvink, D., van Thiel de Vries, J. S. M., & Huismans, Y.** (2020). ShorelineS: A new simple model for coastline evolution. *Coastal Engineering*, 157, 103628. doi:10.1016/j.coastaleng.2020.103628.
- Roelvink, D., Huisman, B.** (2023) Tides, mean current and wave ShorelineS (internal ?) memo
- VERWAEST, T.** (2022). Kustlijnveranderingen te Knokke-Heist in de afgelopen 50 jaar. Versie 4.0. WL Memo's, 21\_091\_1. Waterbouwkundig Laboratorium: Antwerpen.
- VERWAEST, T.** (2023). Kustlijnveranderingen te Knokke-Heist in de afgelopen 50 jaar. WL Memo's, 21\_091\_3. Waterbouwkundig Laboratorium: Antwerpen.
- Wang, L.; Kolokythas, G.; Breughem, A.; De Maerschallck, B.** (2024). Morphodynamic modelling of the Belgian Coastal zone: Sub report 2 – Release notes Scaldis-Coast 2024. Version 0.1. FHR Reports, 21\_104\_2. Flanders Hydraulics Research: Antwerp
- Trouw, K.** (2024) Calibration of a groin in Shorelines using XBeach (internal report)

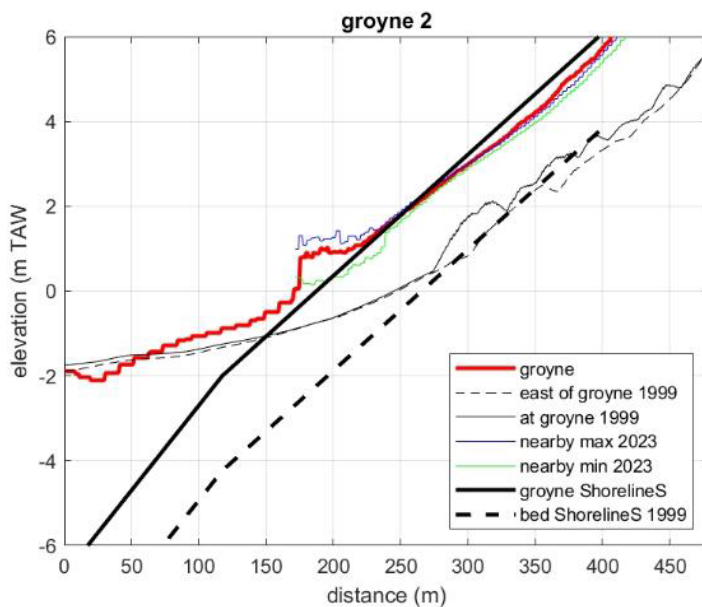
## Appendix 1 Groynes Knokke-Heist

Figures below show the groynes as incorporated in the ShorelineS model. Each time the distance at which the offshore tip of the groyne is supposed to be is mentioned. This is not always at the real tip. **The inventarisation of the groynes is still going on, so in the near future an update will be required.**



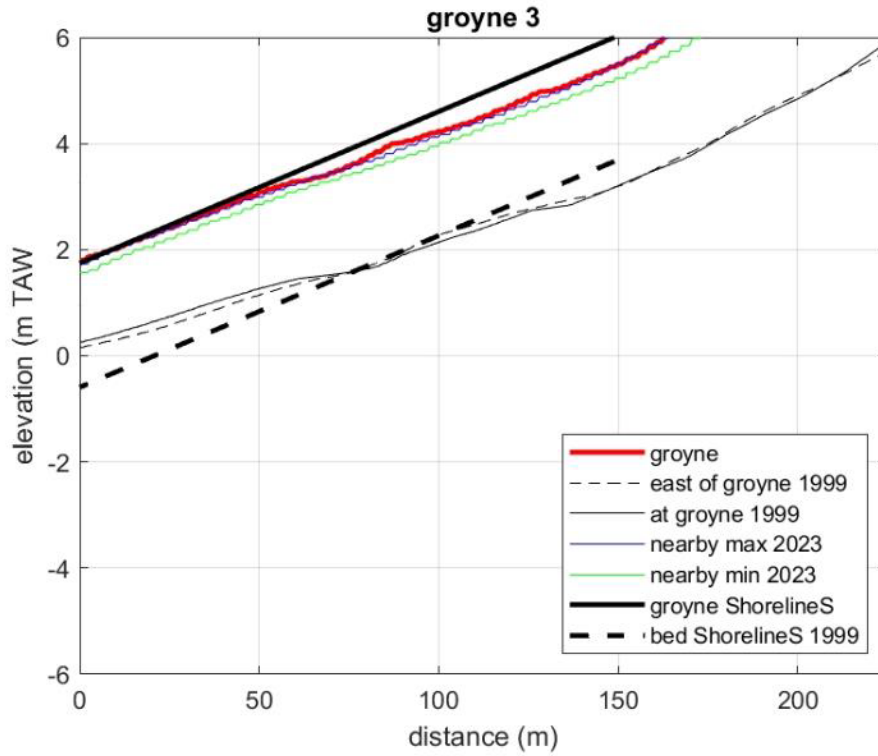
ShorelineS cross shore profile is much too steep, but the relative groin height (2 m in 1999) is represented in the crucial zone. It can be noticed a remarkable jump in the real groin profile at 80 m.

Limit groin up to real depth of groin at -1 m TAW, thus offshore tip at distance 150 m.

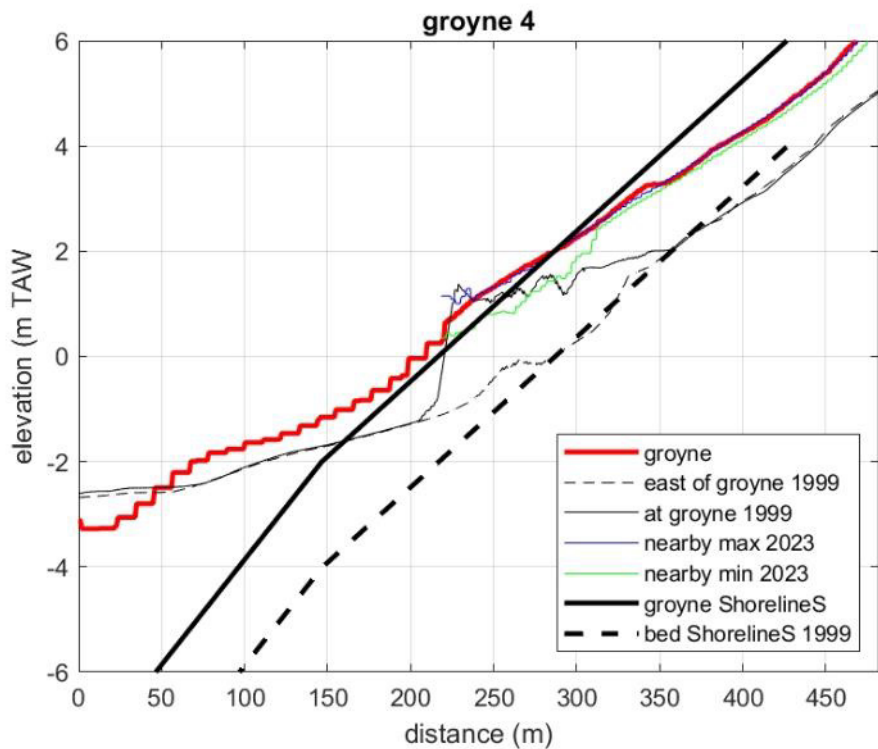


Remarkable jump in the real groin profile at 160 m.

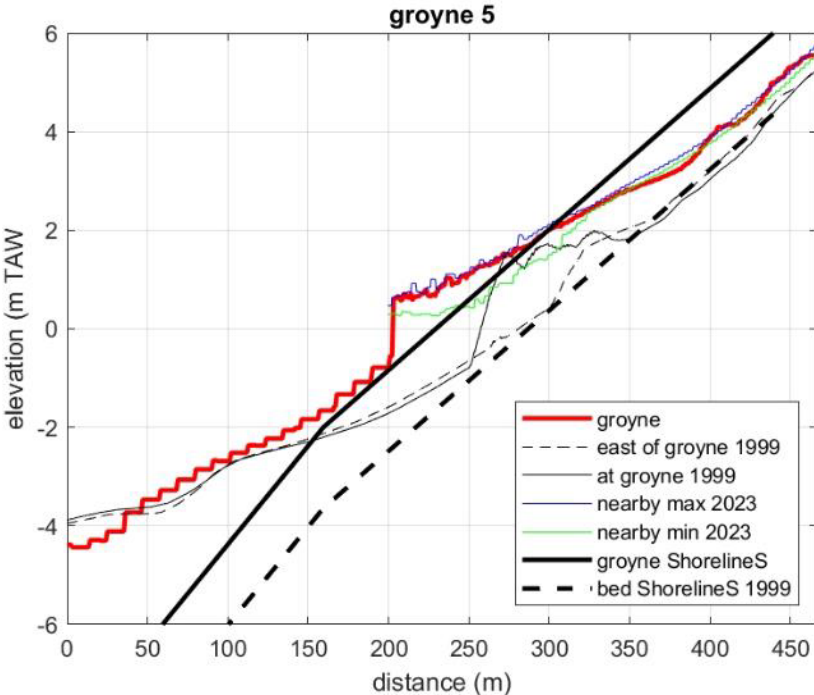
Limit groin up to real depth of groin (at -1 m TAW, thus offshore tip at distance 150 m).



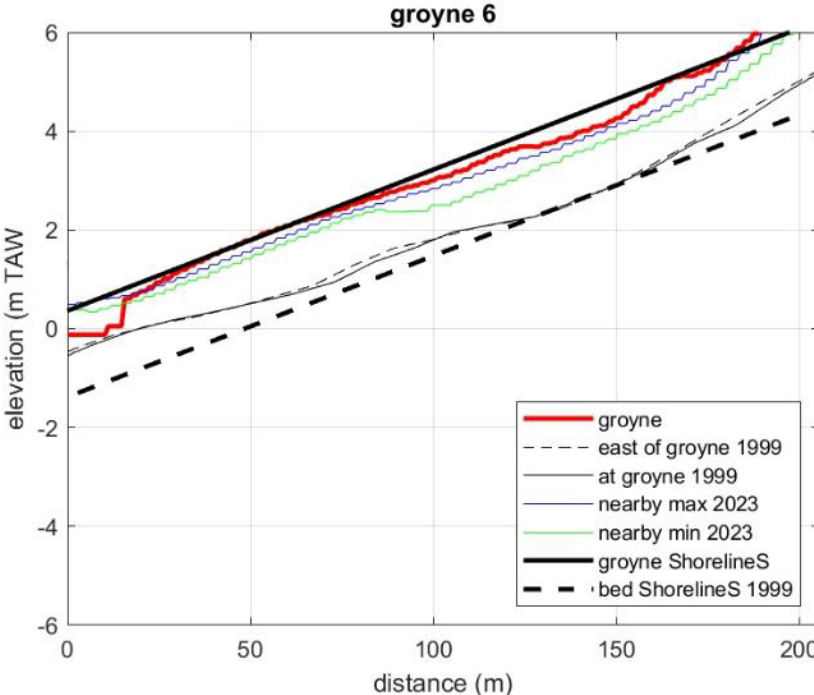
Groyne well represented, offshore tip at distance 0



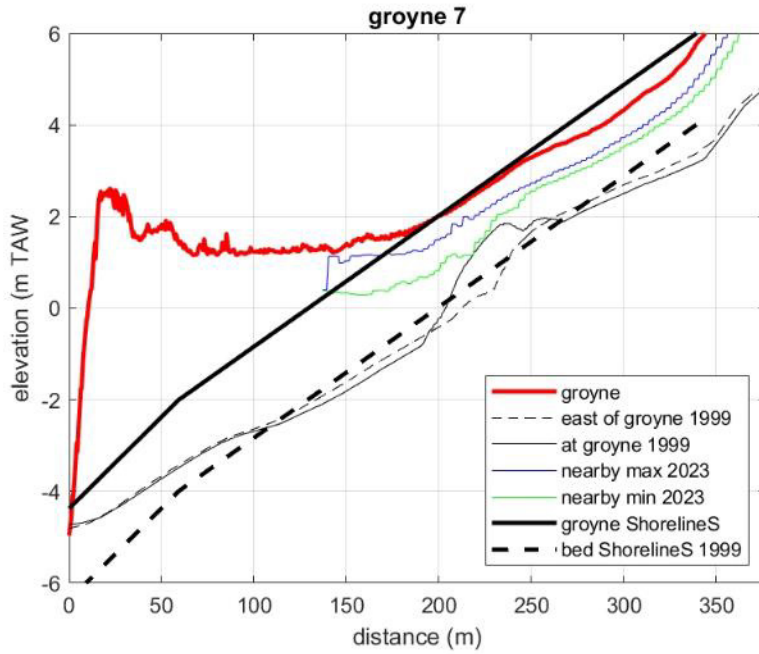
Groyne well represented, offshore tip at distance 150.



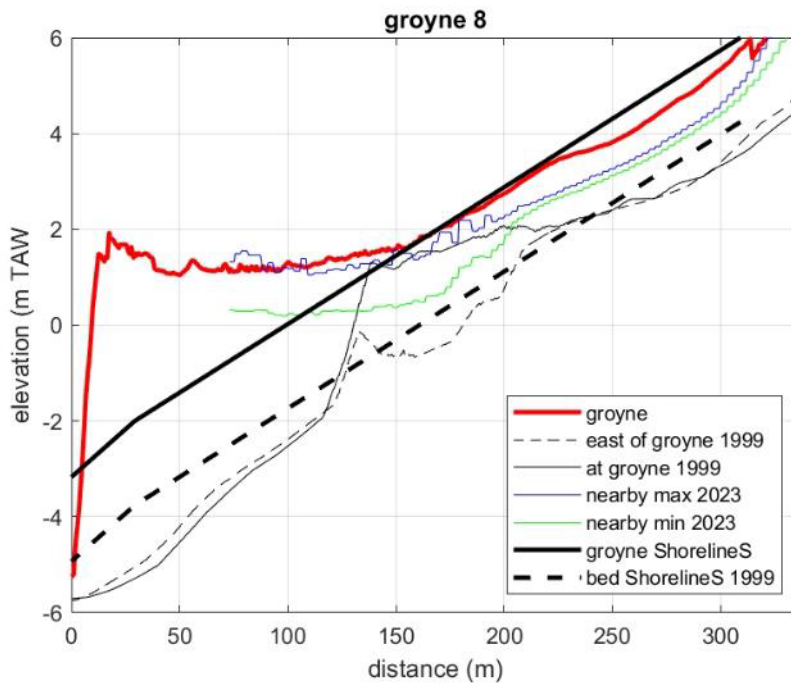
groyne well represented, offshore tip at, distance 180 (limit of tested range)



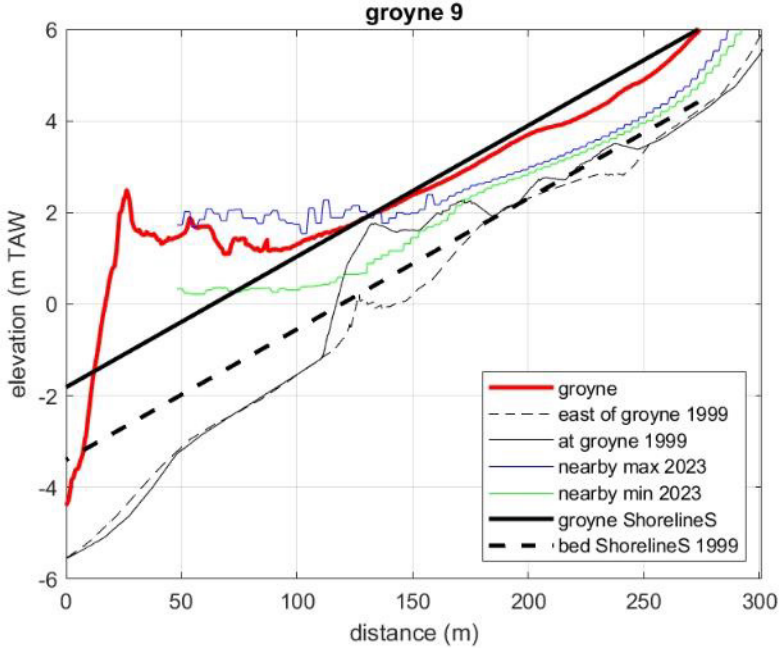
groyne well represented, offshore tip at distance 0 This is probably groyne of piles.



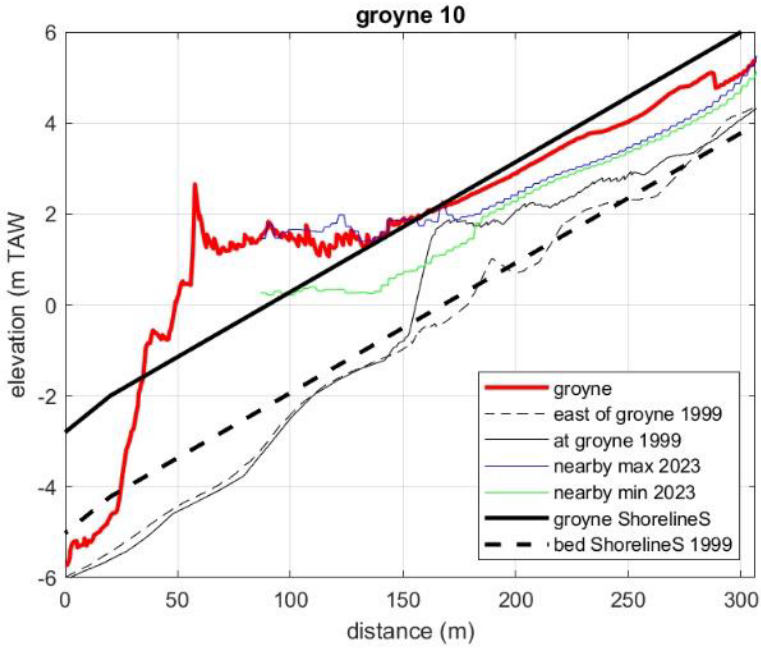
It is remarkable that the maximum observed elevation in 2023 is significantly lower than the groyne elevation.  
Distance 50 m



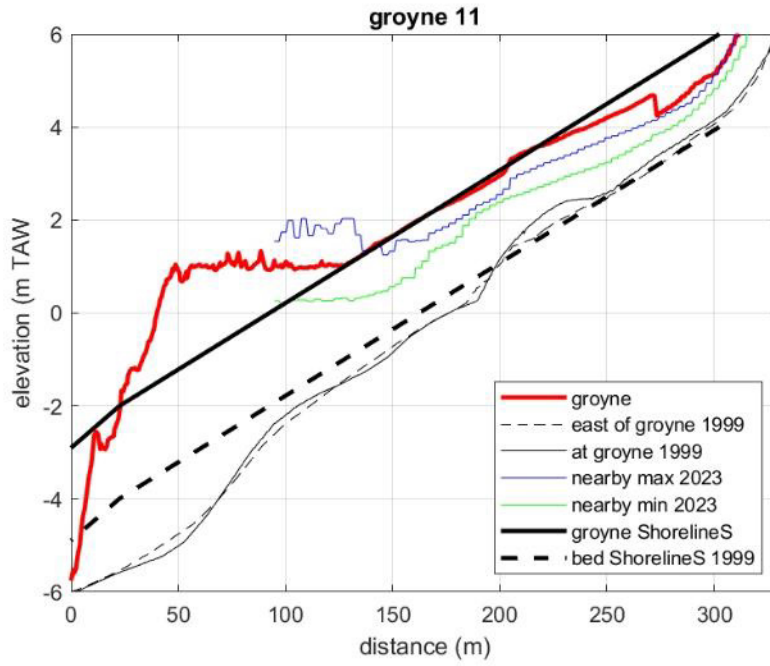
It is remarkable that the maximum observed elevation in 2023 is significantly lower than the groyne elevation.  
Distance 50 m



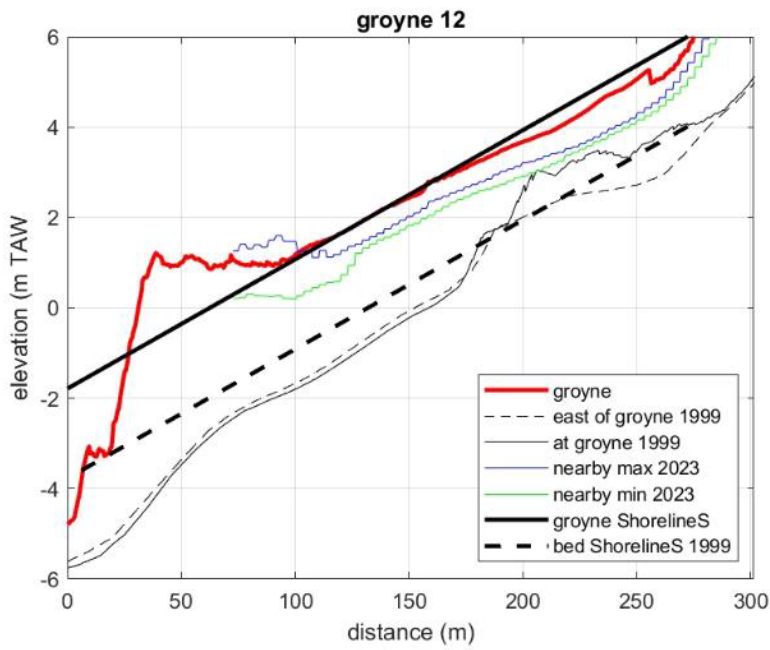
It is remarkable that the maximum observed elevation in 2023 is significantly lower than the groyne elevation. A large difference between max 2023 and groyne elevation (distance 30: end of horizontal part) is observed. .



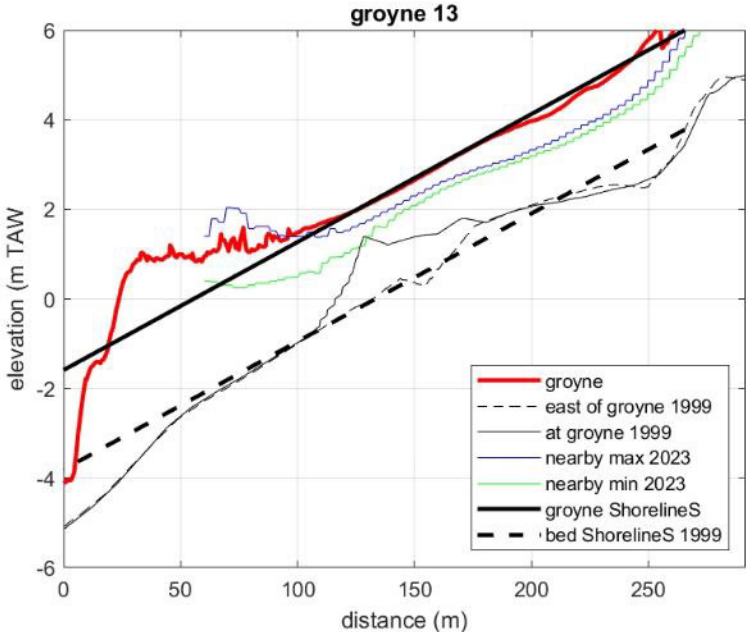
Idem; (distance 60: end of horizontal part)



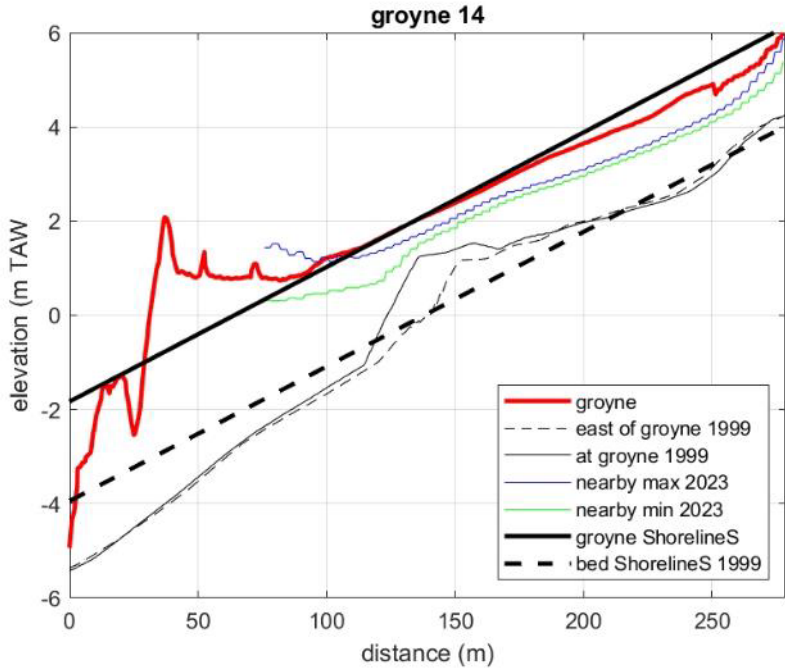
Distance 50 m



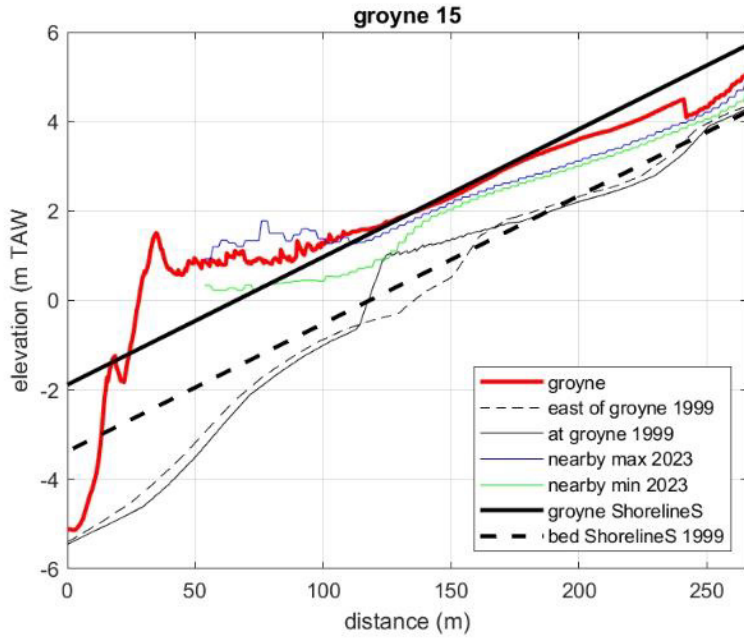
Distance 50 m



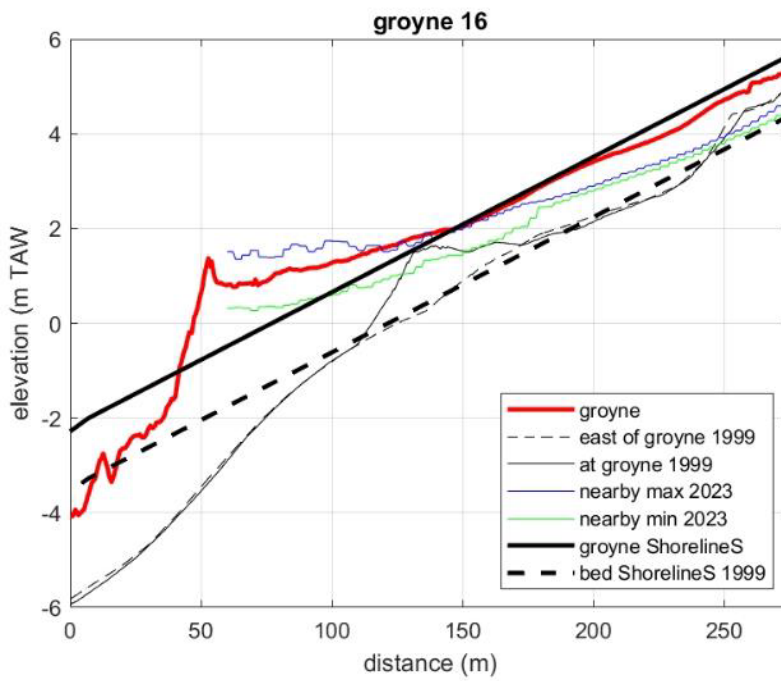
Distance 40



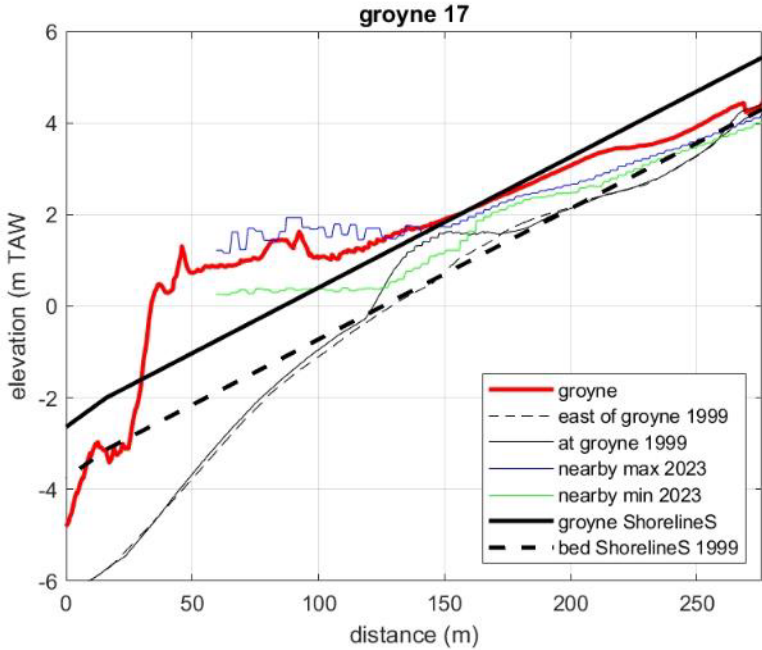
Distance 40



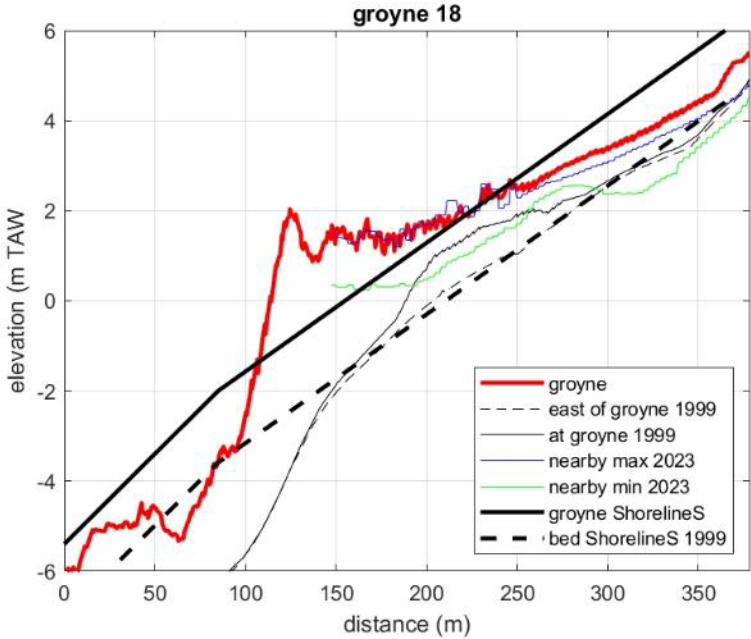
Distance 40



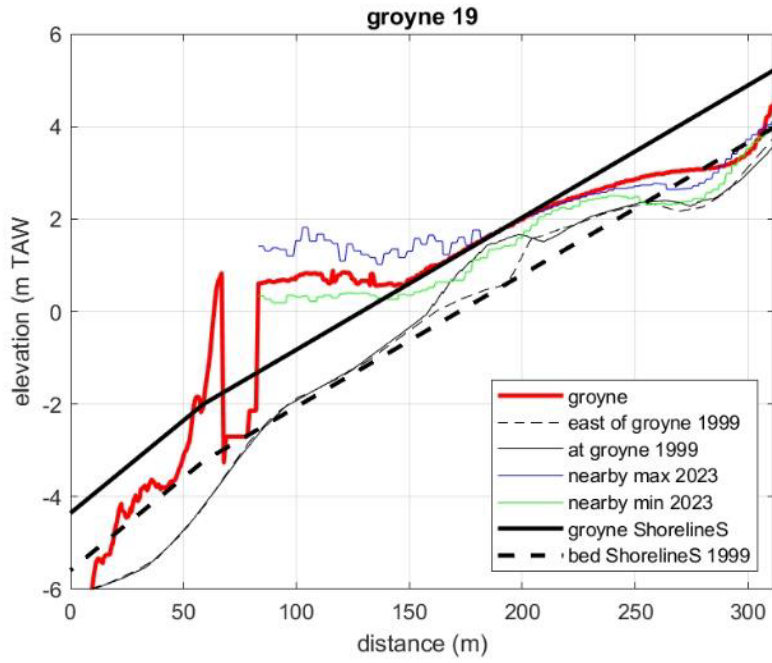
Distance 50



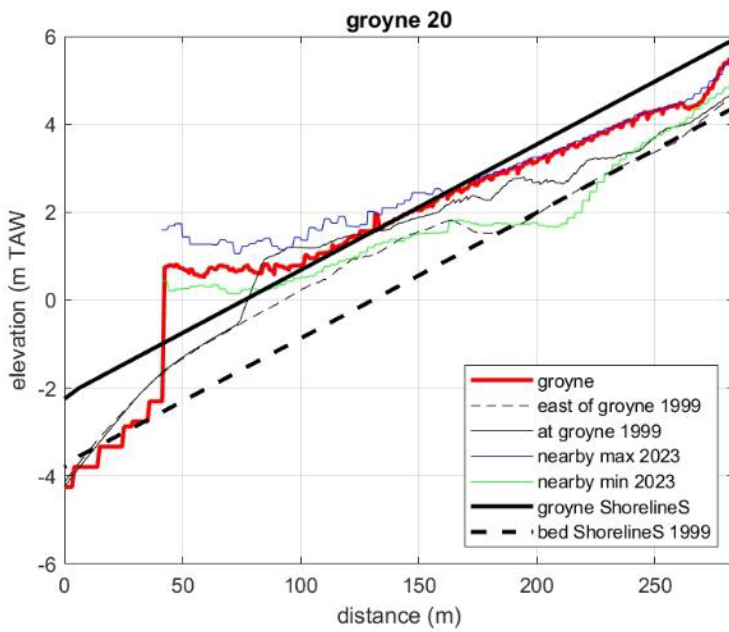
Distance 50 m



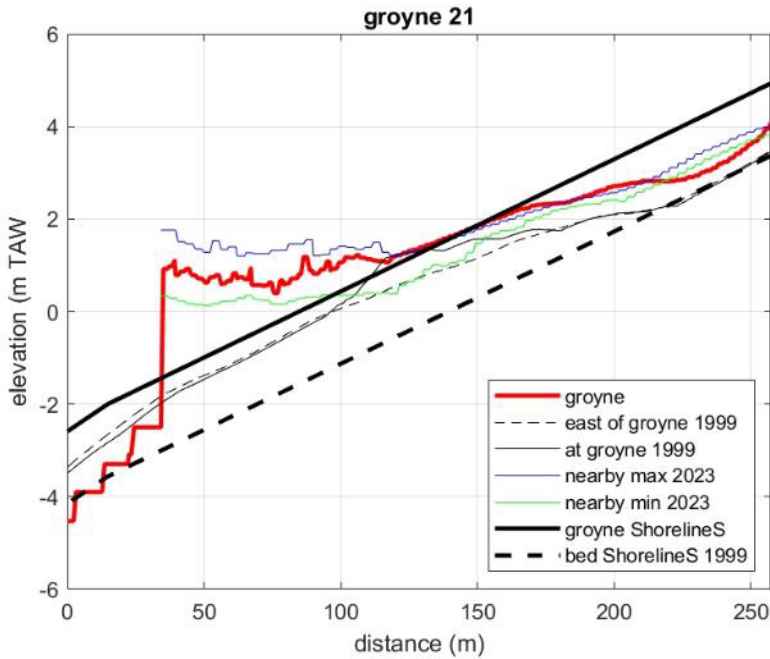
Distance 130 m



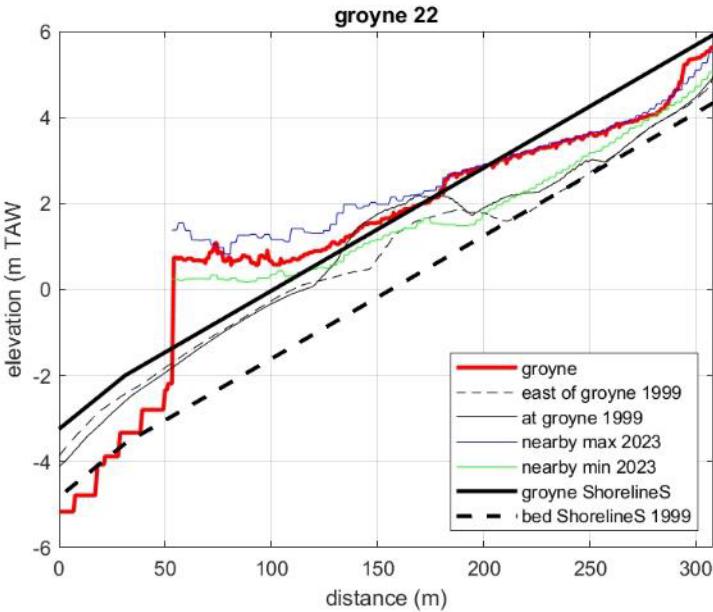
Distance 70 m



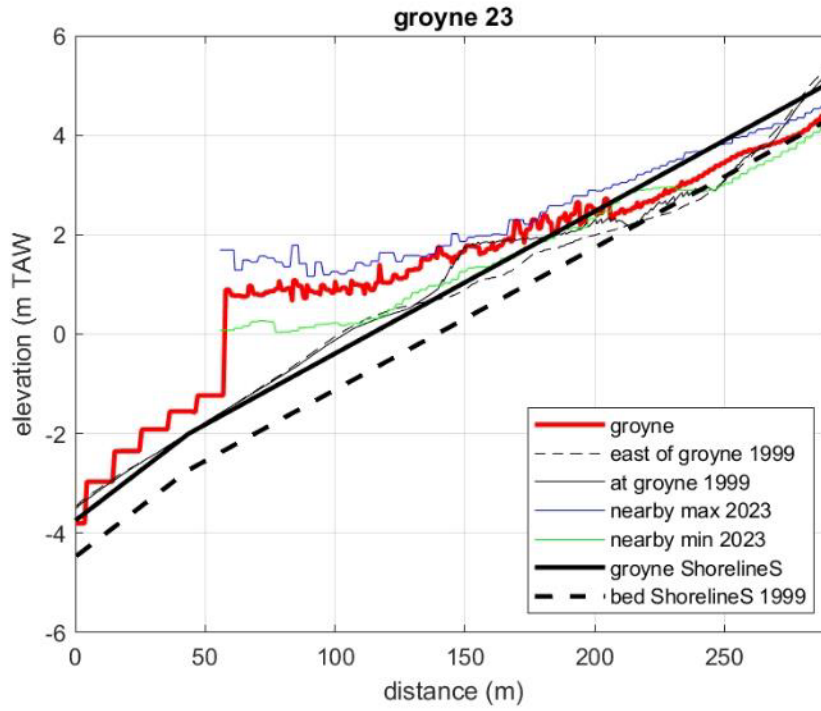
Distance 40 m



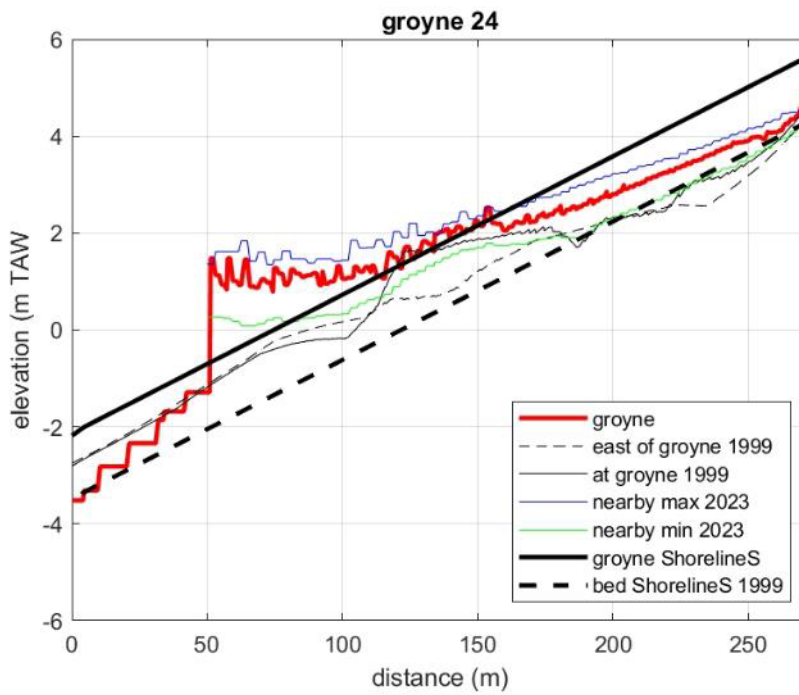
Distance 40 m



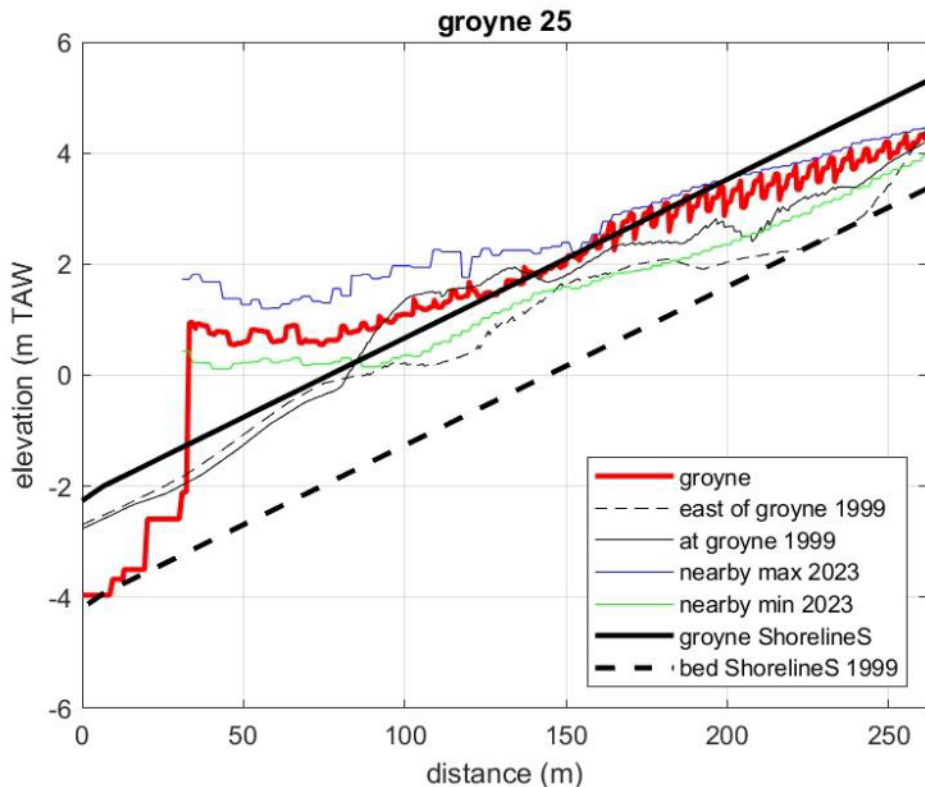
Distance 60 m



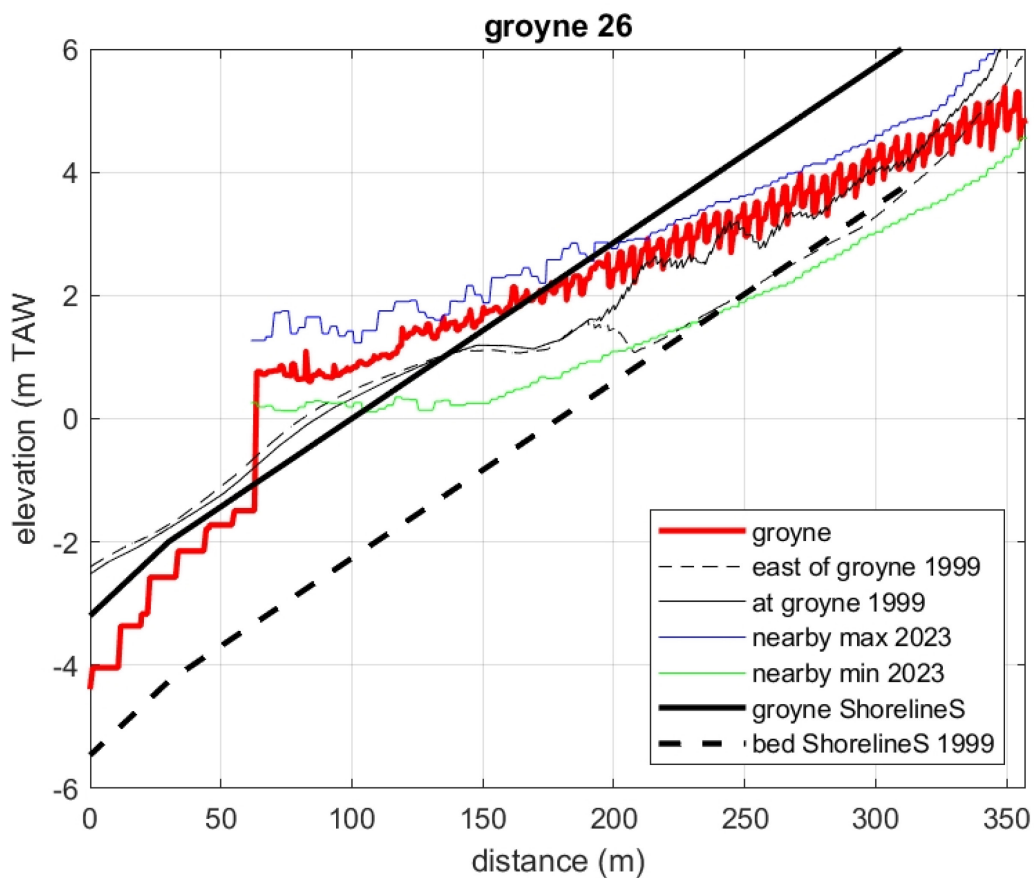
Distance 60 m



Distance 50 m



Distance 40 m



Distance 60 m

## Appendix 2 Bypass over low crested, sloping groynes in ShorelineS - Memo

In this memo Xbeach is used to develop a methodology to incorporate submerged groins in ShorelineS. At this moment ShorelineS supposes emerged groins. In XBeach a submerged groin can be modelled using a hard layer.

In chapter 2 simulations with both XBeach and ShorelineS have been done and compared. The main conclusion is that if equal settings (using Manning roughness in ShorelineS and Soulsby Van Rijn transport formulation in XBeach) the correspondence is very good, both for longshore velocities as longshore transport.

In chapter 3 a first exploration of the mechanism of blocking in ShorelineS and XBeach has been described. The relation between  $D_s/D_{lt}$  and the blocking in both XBeach and ShorelineS is shown, indicating that ShorelineS gives somewhat more blocking compared to XBeach. In XBeach some preliminary simulations are done for submerged groins. 2D plots of the sediment transport are shown. These illustrate that the main reason of the sediment blocking is due a decreased velocity near the groin. A first attempt (without success) is made to estimate the blocking of a submerged groin based on the blocking of a emerged groin and geometrical parameters.

In chapter 4 final XBeach calculations are done for emerged groins for a longer period. With the aim of doing also longer term simulations, the profile development due to cross shore transport is examined. A strong development influences the cross shore distribution of the longshore transport and thus also the blocking. Using the WTI settings gave a rather stable profile.

In chapter 5 final XBeach simulations have been done for both emerged and submerged groins. Based on these simulations a relation is derived to estimate the blocking due to a submerged groin based on the blocking of an emerged groin and the parameters  $D_s'/D_s$  and  $D_s/D_{lt}$  (water depth at tip of groin ( $D_s'$ ) over water depth at the nearby bed ( $D_s$ ) and  $D_s$  over water depth of the offshore limit of the sediment transport ( $D_{lt}$ ). The relation predicts blocking within an accuracy of 0.05 (standard deviation of the obtained blocking relative to the modelled blocking).

Based on these results, modifications on ShorelineS have been made (chapter 6). The results of the modified model are compared with the XBeach model results.

In chapter 7 a long term simulation is done.

## 1. Comparison XBeach – ShorelineS without a groin

For the coast of Knokke Heist a 3km long stretch is selected. The coastline is straightened. A profile 1/45 is used up to -8m. This profile is extended offshore to -20m TAW (slope 1/30) to avoid the formation of spurious long waves in XBeach. This profile is also used for ShorelineS, in order to have a 1:1 comparison.  $D_{50}=0.2\text{mm}; d_{90}=0.3\text{mm}$ .

Relevant parameters in Xbeach are based on the WTI-settings.(cf Annex). In XBeach Van Thiel Van Rijn and ShorelineS is used for sediment transport

In ShorelineS the tidal model with Soulsby Van Rijn is used with standard parameters, except the coefficients in the Soulsby Van Rijn Formulation. (coefficient for  $A_{sb}$  is set at 0.005 instead of 0.05 conform value in literature)

### *Tide only calculations*

ShorelineS calculates the water level at the eastern and western boundary of the model. These values (at the offshore locations) are used as input water level time series for the XBeach model. A Manning coefficient of 0.02 (corresponds with the bed friction coefficient in Shorelines of 0.0023) is used in XBeach. The tide type is hybrid. The longshore velocities are compared in Figure 2-1 at -5m TAW (-7m MSL). At -1m TAW, the comparison is still good, ShorelineS gives slightly higher velocities especially at flood.

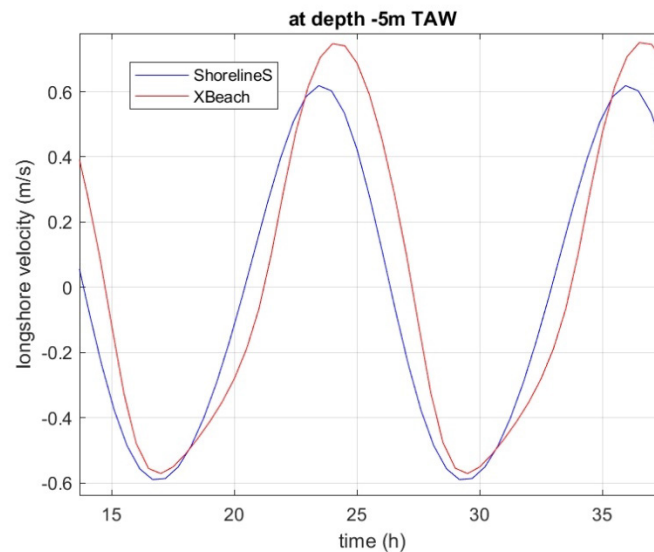
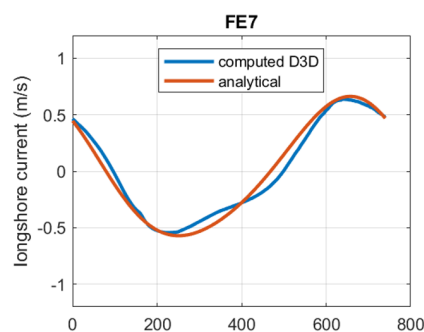


Figure A2.1 Comparison of longshore velocity at deep water (-5m TAW).



Time between max ebb and max flood is almost the same. Peak velocities at FE7 are 0.66m/s and 0.56m/s, while in the simulation with the straight coastline, this is resp. 0.62m/s and 0.58m/s (but the location of the output point is also slightly different).

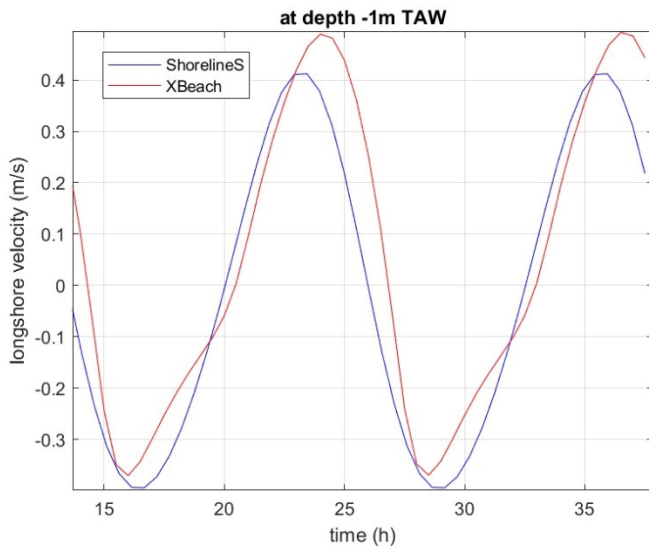


Figure A2.2 Comparison of longshore velocity at -1m TAW.

Figure A2.3 shows the maximum flood and ebb velocities variations over the profile (given by the bed elevation). In Shorelines the maximum ebb and maximum flood velocities are rather equal to each other. For the XBeach simulations the ebb velocities are comparable with the ShorelineS velocities, but the flood velocities are higher in XBeach.

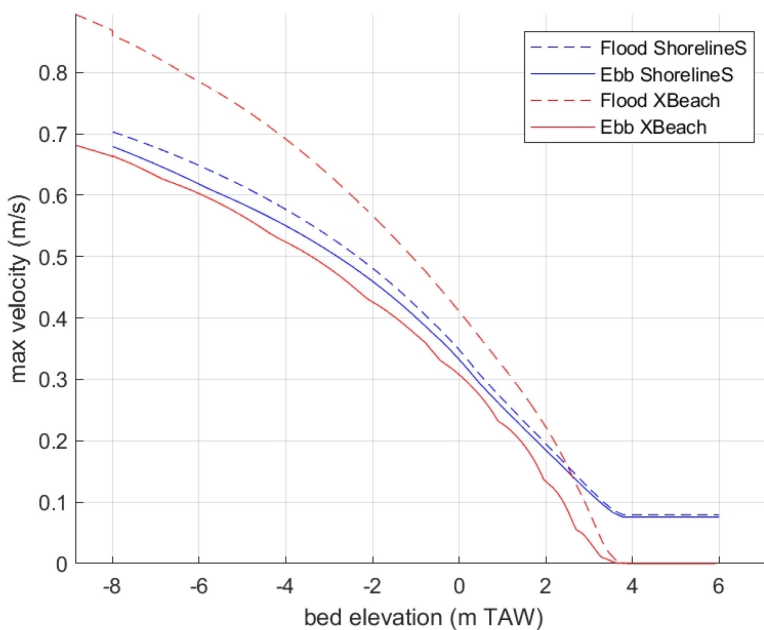


Figure A2.3 Max ebb velocities (full lines) and max flood velocities (dotted).

**Waves only**

Waves with  $H_{m0}=1$  and 2m, with  $T_p$  resp 7s and 8s and a direction of  $30^\circ$  to the normal are used for comparison between XBeach and ShorelineS. The water level is constant at +2m TAW (+/- MSL).

Since in XBeach Manning (=0.02) is used, simulations are done in ShorelineS using a Chezy roughness  $C_f$  of 0.0023, but also using a Manning coefficient (the routine `wave_cur_1D` is adapted).

Using a Manning coefficient gives for small water depths (where wave breaking occurs) larger Chezy Coefficients as the used one of 0.0023.

n/h	2	5	10
0.02	0.0031	0.0023	0.0018
0.03	0.0070	0.0052	0.0041

Chezy roughness for different water depths and Manning coefficients.

The effect of these larger roughness is illustrated in the tables below for the peak of the longshore velocity for the sediment transport. The effect is larger for smaller wave heights (as the breaking occurs at shallower water).

Hs	Chezy=0.0023	Manning =0.02
1m	0.79	0.58
2m	1.17	1.01

Peak longshore velocity (m/s)

Hs	Chezy=0.0023	Manning =0.02
1m	0.97	0.56
2m	3.4	2.5

Peak longshore sediment transport ( $10^{-3}$  m<sup>3</sup>/m/s)

Figures A2.4 and A2.5 compares the wave height along the profile. In both models the wave height reduces with 5 to 10% at the foot of the actual profile. For the 1m wave height, the reduction is equal in both models, for the 2m wave height the reduction is larger in ShorelineS and also the shoaling just before breaking is smaller.

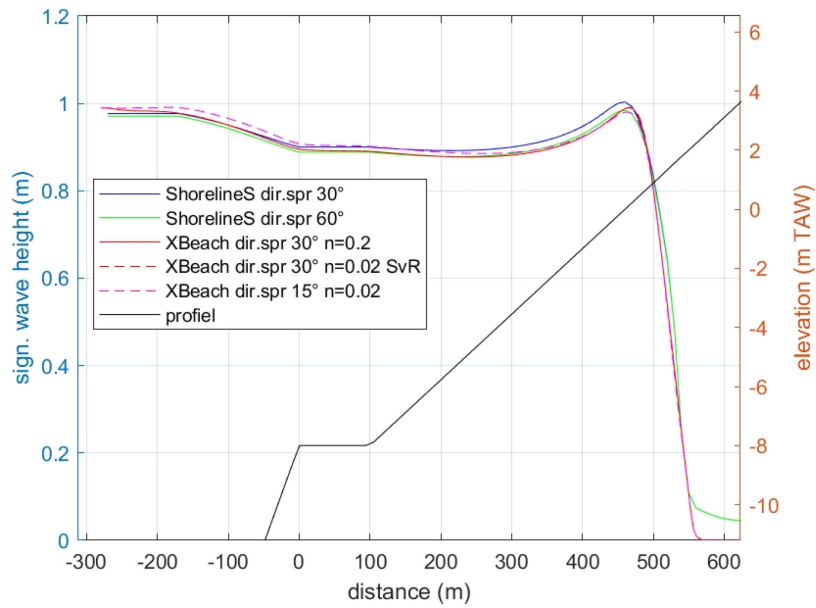


Figure A2.4 Comparison of the wave height along the profile ( $H_{m0}=1\text{m}$ )

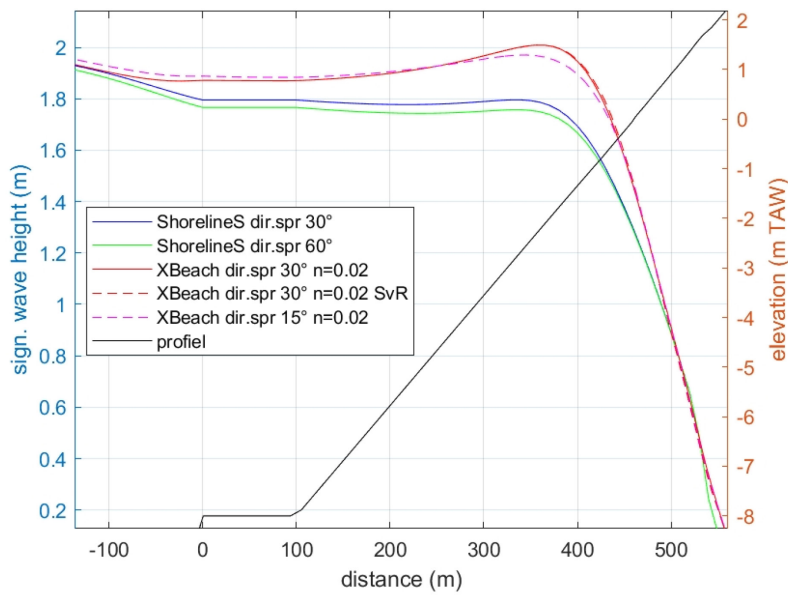


Figure A2.5 Comparison of the wave height along the profile ( $H_{m0}=2\text{m}$ ).

Figure A2.6 compares the longshore velocity for different roughness formulations and variation in wave direction (S.spread) ( $H_{m0}=1\text{m}$ , wave direction  $30^\circ$ ). It is clear that using a Manning coefficient instead of Chezy results in much smaller velocities. Larger values for S.spread give smaller velocities. In ShorelineS the parameter S.dirspr seems not to have effect on the longshore current/transport (due to the use of Snell (?)). For this reason, the wave direction is varied around the desired value, using S.spread (which gives a variation of the wave angle over different time steps). It is understood that the value in ShorelineS is 2-sided).

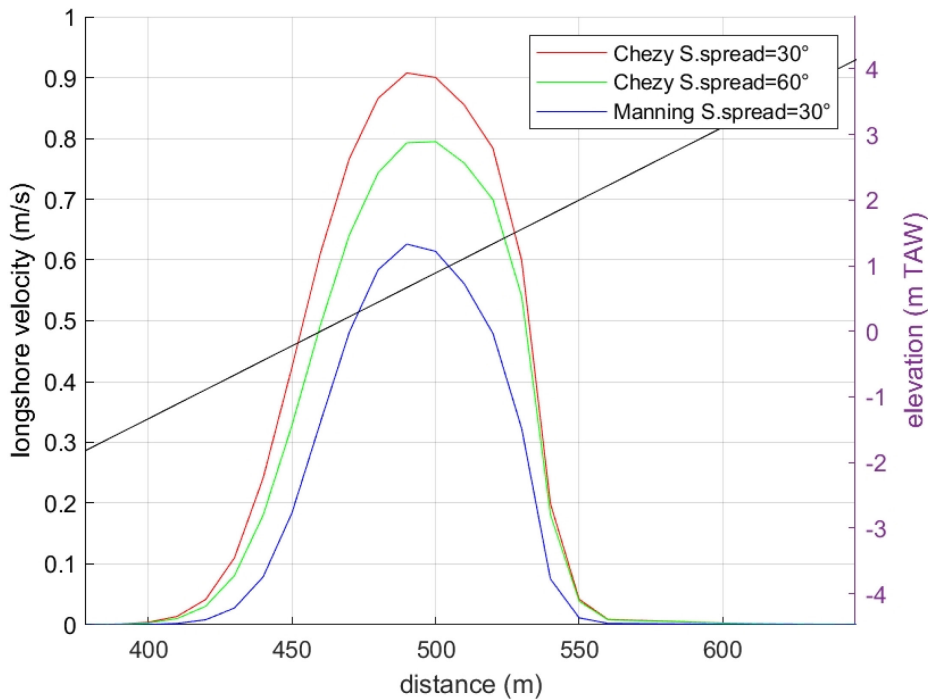


Figure A2.6 Comparison longshore velocity for waves only (1m, 30°) – different ShorelineS settings.

From now on ShorelineS is used with a Manning coefficient ( $=0.02$ ). (as the velocities correspond much better to the values of Xbeach).

In XBeach a variation of directional spreading values is tested. For the longshore velocity, using a small directional spreading gives the best correspondence with XBeach. For the longshore velocity, the correspondence is very good!

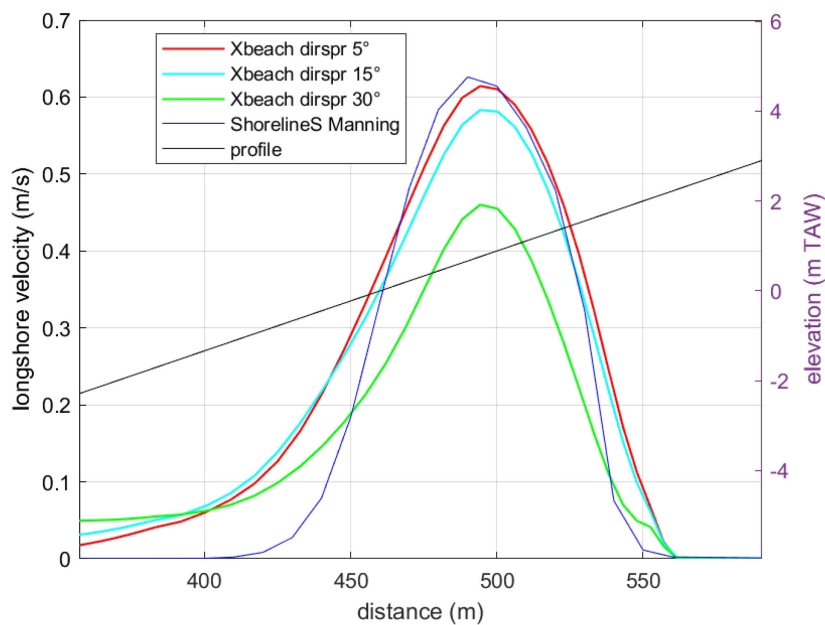


Figure A2.7 Comparison longshore velocity for waves only (1m, 30°).

The longshore sediment transport is compared in Figures A2.8 and A2.9. Using Soulsby-Van Rijn in XBeach gives a good agreement between ShorelineS and XBeach for the cases with a small directional spreading. The transport is smaller when using Van Thiel-Van Rijn in XBeach.

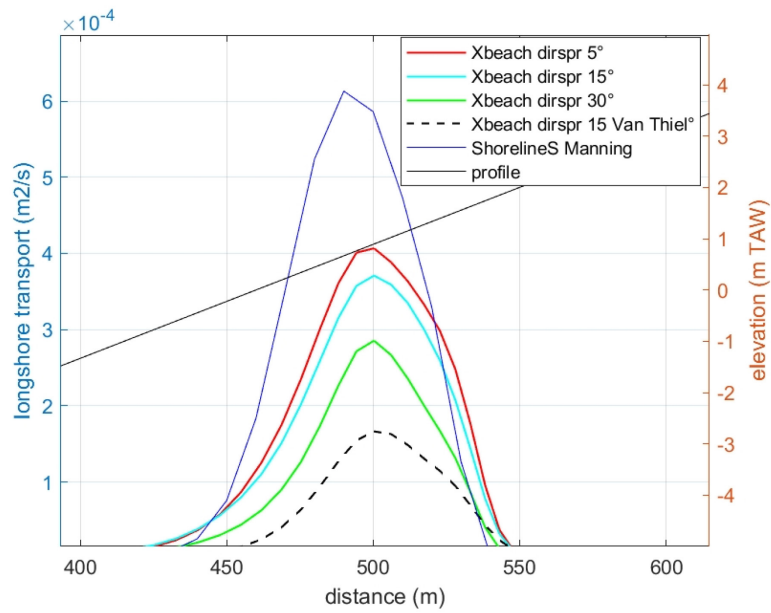


Figure A2.8 Comparison of longshore sediment transport (Hmo=1m).

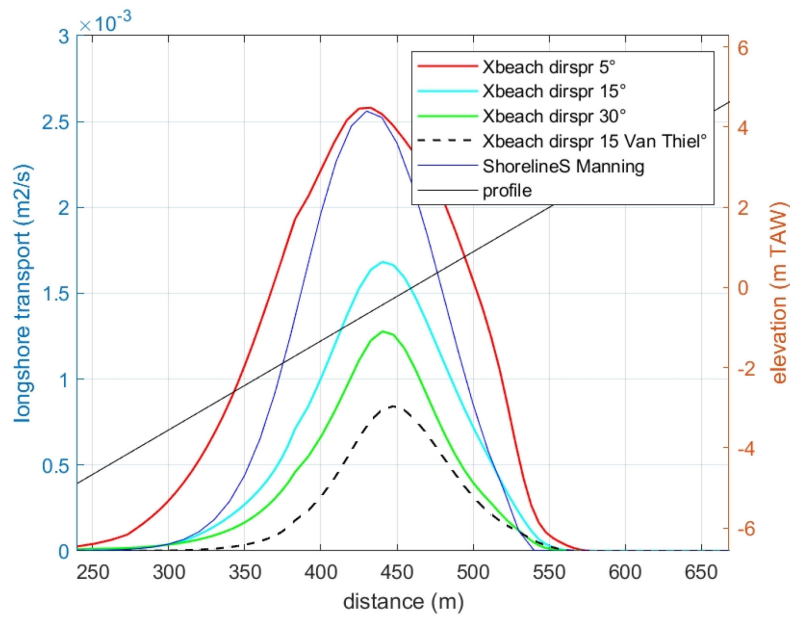


Figure A2.9 Comparison of longshore sediment transport (Hmo=2m).

In the table below comparison for the integrated longshore sediment transport values for the different settings and for 2 wave heights.

Hm0 (m)	transport (m <sup>2</sup> /s)				
	dir.spr. 30°	dir.spr. 15°	dir.spr. 5°	dir.spr. 15° with Van Thiel	ShorelineS
1	0.0157	0.0226	0.0251	0.0091	0.03
2	0.1339	0.1907	0.398	0.0791	0.38

## 2. Initial calculations with a groin

Results in this chapter are done with the original ShorelineS (with Chezy), but this might only change some numbers a little bit, without changing the conclusions. XBeach simulations have been done with the Van Thiel Van Rijn formulation, but as will be shown later, this has little influence on the blocking. This chapter is only indicative.

### **Methodology**

In ShorelineS 3 groins are considered, resp. stretching up to -1.5m TAW, 0m TAW and 1.5m TAW (with a water level of +2m TAW). In prepare.transport Aw is set at 5 in case a fixed wave condition is given. For this exercise this is disabled. Aw=1.27 is used.

In Xbeach these 3 groins are also used, with height above the seabed of 1, 2 and 8m (8m=above water level). The width is about 15m.

All simulations are done for 2 hours in XBeach (and the last 0.5 hours are used, when equilibrium is reached) and for 100 time steps in ShorelineS (enough to get a representative number of wave directions around the required main direction (using S.spread=30)).

Figure A2.10 gives an example of the output in XBeach and ShorelineS for Hm0=2m, direction 60° to the normal and a groin up to -3.5m below the water level. In both cases, the transport downstream the groin (x>2020m) is smaller than the transport over the groin.

In Xbeach the blocking is calculated with the ratio of the transport at the location of the groin over the transport at the same location in case no groin is present. (this ratio is quasi equal in case not the transport without groin is used, but the transport in the actual simulation, far enough upstream). The location of the groin is not in all cases the location of the minimal longshore transport (due to the formation of the eddy behind the groin). This is illustrated in Figure 3-1 for very oblique waves (60°) and a very long high groin.

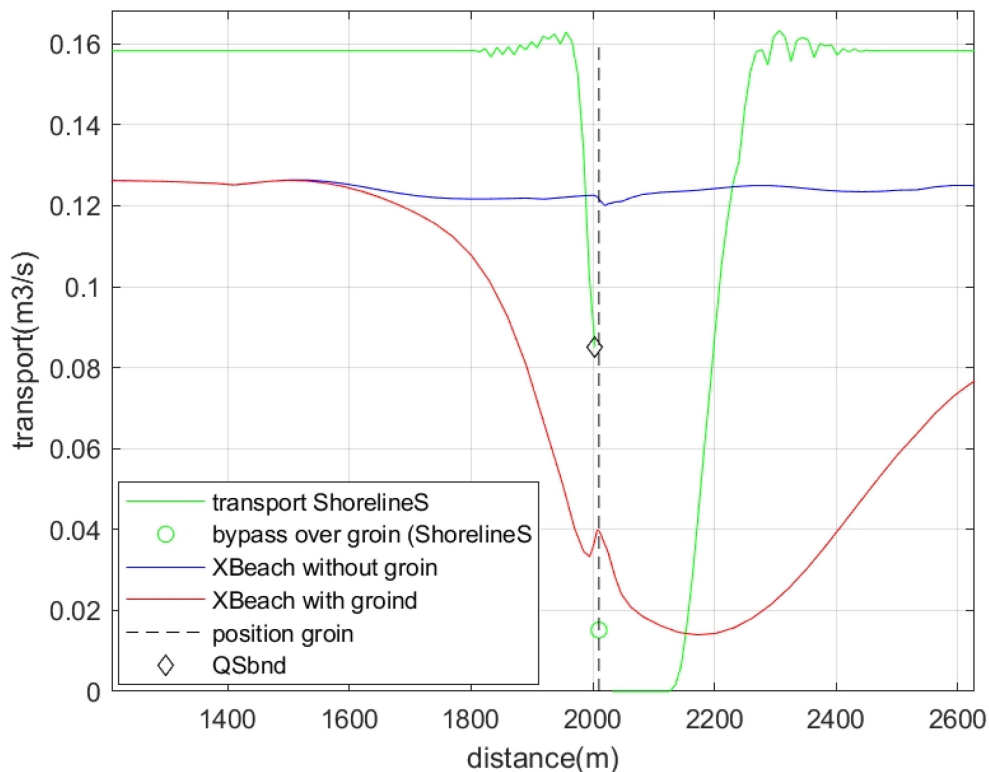


Figure A2.10 Longshore transport ( $H_{m0}=2\text{m}$ , direction  $60^\circ$ , groin up to  $-1.5\text{m TAW}$  ( $3.5\text{m}$  below water level), groin above water level (QSbnd: the longshore transport on which the blocking coefficient is applied).

In ShorelineS the parameter QS does not contain the transport over the groin (= non existing value), but the parameter GROYNE.QS (green circle in Figure A2.10 - red cross in Figure A2.11) is used and compared with TRANSP.QS 1km upstream the groin. It is remarkable that this blocking can differ about 10% from the blocking calculated by the ratio of the sand accumulation and the upstream transport. The sum of the sand accumulation upstream and erosion downstream is also not zero.

The blocking ratio due to the groin is not equal to  $(1-DF/Dlt)$ . (df: depth at the tip of the groin, dlt: depth of offshore limit of the longshore transport), as this parameter is applied to the longshore transport 1 cell upstream (QSbnd in Figure 3-1), which is already lower than the undisturbed transport.(e.g. in Figure 3-2 a blocking factor of 0.5 is calculated ( $Ds/Dlt$ ). This is applied to a longshore transport of  $0.012\text{m}^3/\text{s}$ . The total blocking is  $(0.0165-0.006)/0.0165=0.63$ . The reduced transport at the first upstream cell compared to 1km more upstream is due to the immediate re-orientation of the coastline due to the presence of the groin (although the simulation is only 1 day). Using the reduced transport 1 cell upstream in ShorelineS is a correct methodology, but makes comparing with XBeach more difficult as probably XBeach does not react that fast, since in reality (and thus in XBeach) the effect on the whole profile (and thus on the wave refraction) probably needs more time.

Three definitions are used:

- Blocking: the relative amount of longshore transport that is blocked by the groin (relative to the undisturbed longshore transport)
- blocking coefficient defined as  $Ds/Dlt$ .
- Blocking ratio: blocking coefficient  $\times A_w / \gamma$  (= the coefficient applied in ShorelineS on the longshore transport from the cell just upstream)

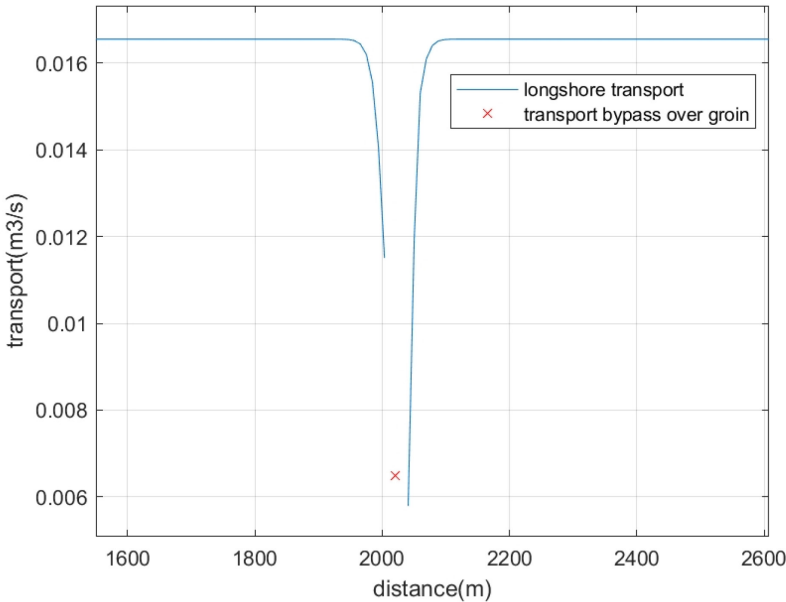


Figure A2.11 Longshore transport with groin at x=2000m (Hm0=1m, direction 30°, groin up to 0.5m below water level).

**Analysis velocity and sediment transport around groin in XBeach**

For 1 condition (Hm0=2m, direction 30°, groin offshore tip at depth (Ds) -3.5m, the results for the different groin heights are compared (velocities and sediment transport). Figure 3-3 shows the water depth for the configuration with a 2m high groin. Figure A2.12 shows the velocities and the sediment transport.

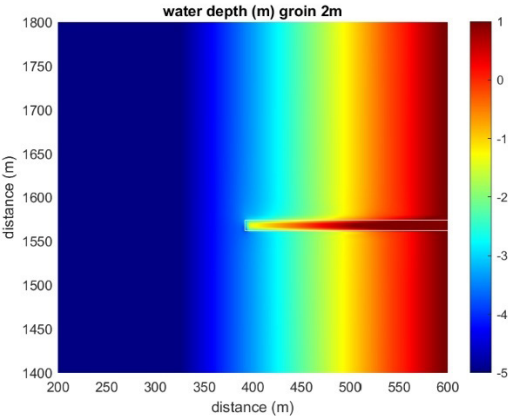


Figure A2.12 Water depth for a groin with crest height 2m.

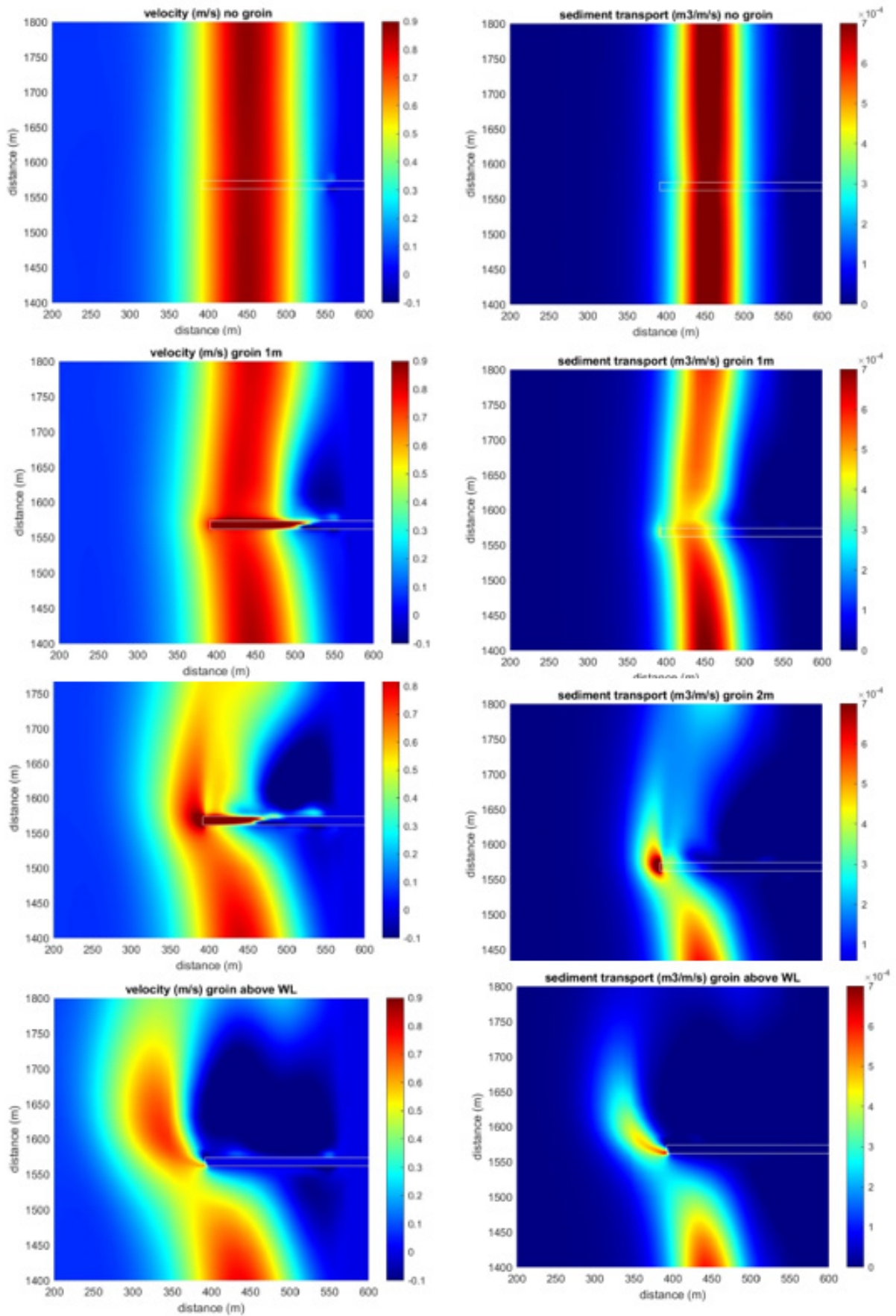


Figure A2.13 Velocities (left) and sediment transport (right) for 4 different groin heights (0,1,2m and above WL).

The figures show that the main reason why the submerged groins block sediment is the reduction of the velocity near the groin (at shallow water) and an increase more offshore (at deeper water). This is also illustrated in Figures A2.14 and A2.15. The blocking of the 4 groins is resp. 0 ; 0.3 ; 0.43 and 0.57, while ShorelineS gives for the high groin a blocking of more than 0.9 (as can be seen in Figure 3-6 in theory the groin blocks almost all longshore transport).

The erosion/sedimentation pattern (Figure A2.16) shows only little effect at the offshore tip of the 1m groin. Most water is passing over the groin, causing some more erosion downstream the groin.

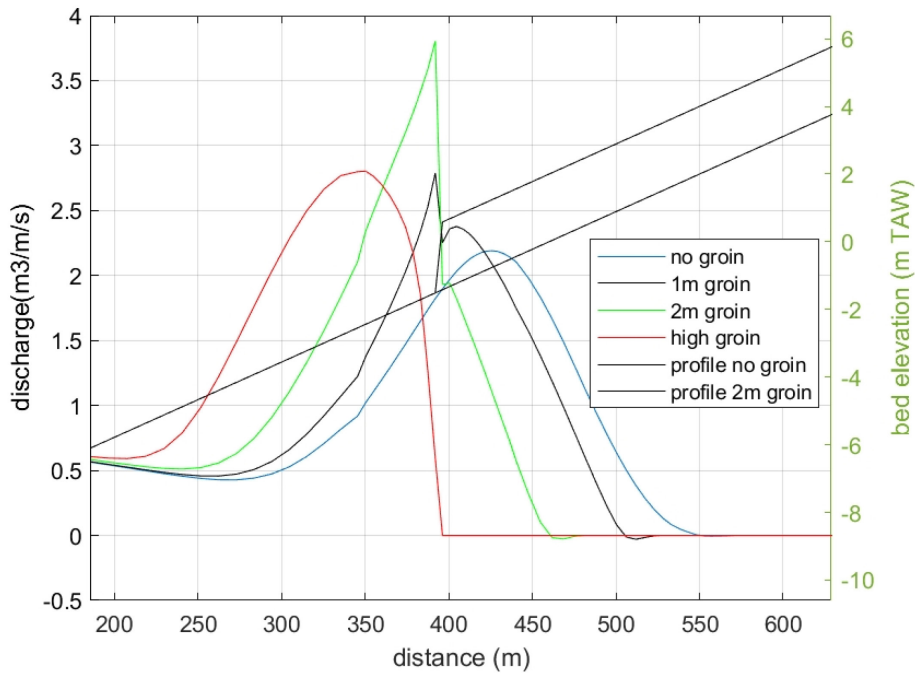


Figure A2.14 Discharge over groin (velocity x local water depth).

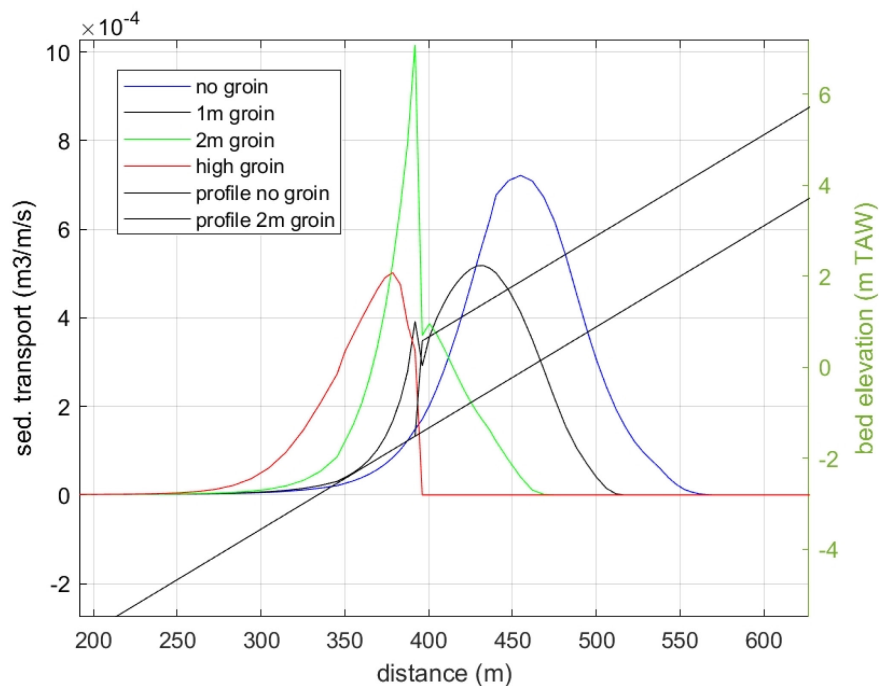


Figure A2.15 Sediment transport over groin.

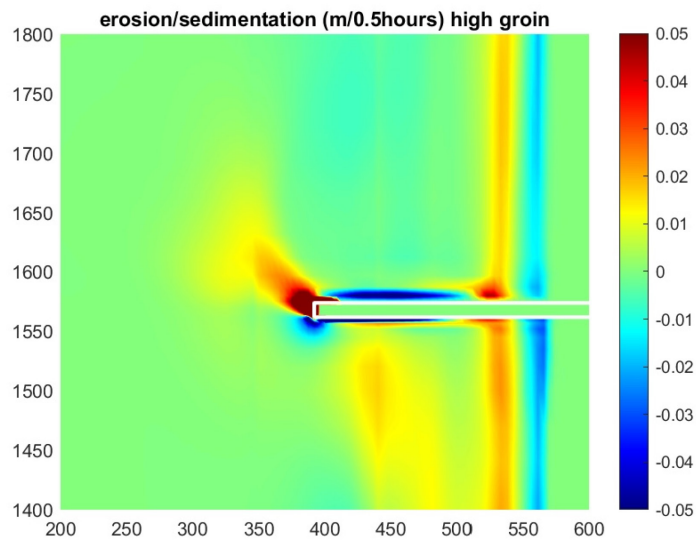
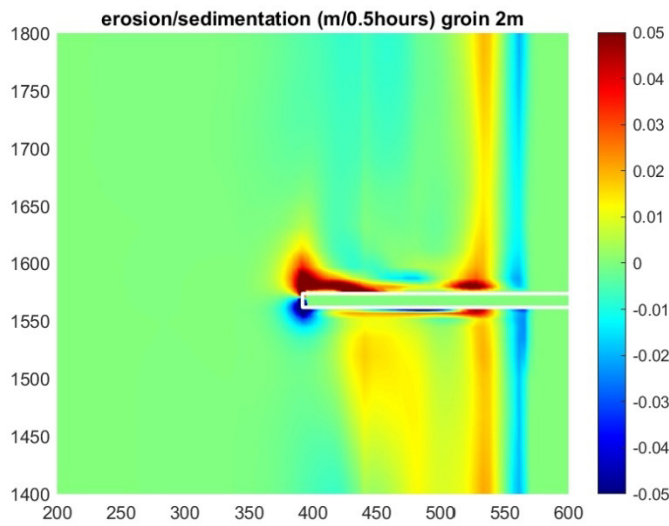
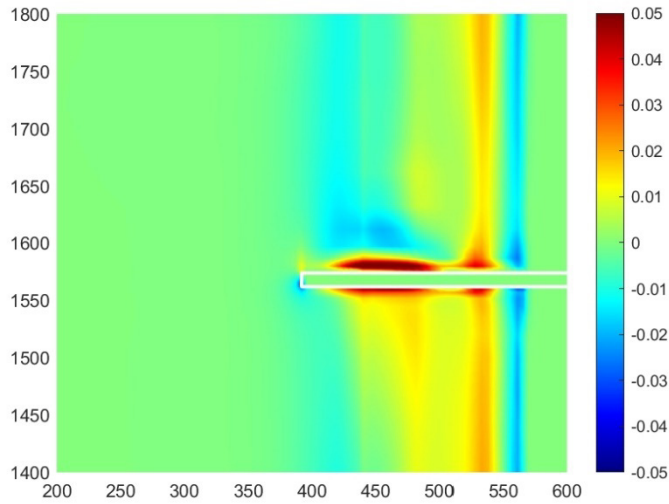


Figure A2.16 Erosion and sedimentation (m in half an hour) for resp. 1m ; 2m and emerged groyne.

**Results for emerged groins**

As an example results for the 2 cases in the previous figures are shown in the table below. In XBeach the real blocking is lower than  $D_s/D_{lt}$ . In ShorelineS it is higher (as far as no complete blocking occurs). In ShorelineS additional blocking occurs due to the reorientation of the shoreline (more perpendicular to the wave direction, so lowering the longshore transport), this occurs less fast in XBeach.

Hm0	1	2	
direction	30°	60°	
$D_s$	0.5	3.5	real depth at tip off groin
$D_{s\_dean}$	0.76	2.75	depth calculated with the Dean profile
$D_{lt\_theor}$	1.76	3.52	Theoretical offshore limit: $A_w H_{m0}/\gamma$
$D_{lt\_xbeach}$	1.8	3.22	offshore limit longshore transport in Xbeach
$D_{lt\_shorelines}$	2.44	4.22	offshore limit longshore transport in ShorelineS
$D_s/D_{lt\_theo}$	0.28	0.99	using the real depth ( $D_s$ )
$D_s/D_{lt\_xbeach}$	0.28	1.09	using the real depth ( $D_s$ )
$D_s/D_{lt\_shorelines}$	0.20	0.83	using the real depth ( $D_s$ )
blocking Xbeach	0	0.68	
blocking ShorelineS_Dean	0.63	0.91	default calculation using the Dean profile
blocking ShorelineS	0.46	0.99	using the real depth ( $D_s$ )

In this memo from now on, in ShorelineS the real  $D_s$  will be used instead of the one derived from the Dean profile. Figure A2.17 shows the relationship between the theoretical blocking coefficient and the observed blocking in XBeach and ShorelineS. The theoretical blocking coefficient does not depend on the used model, as both  $D_s$  and  $D_{lt}$  can be calculated using the geometry and the wave height. Thus, the comparison gives direct info about the relation between blocking in XBeach vs ShorelineS for equal input parameters. The blocking in ShorelineS is for all conditions significantly higher than in XBeach. The curve fitting in the figures is done for all conditions with  $D_s/D_{lt} < 1.2$ . Using the  $D_{lt}$  as calculated with XBeach (based on the cross shore distribution of the longshore transport) gives for XBeach a smaller scatter, but not for ShorelineS (Figure A2.18). Using  $D_{lt}$  from ShorelineS does not really reduce the scatter (Figure A2.19).

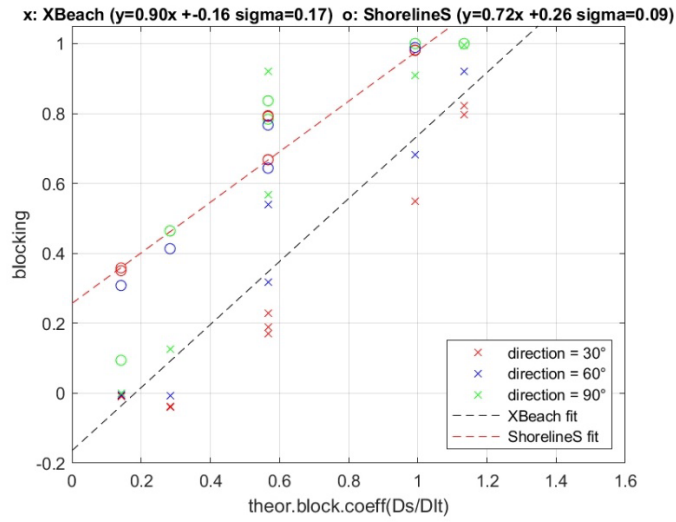


Figure A2.17 Blocking ratio in function of the theoretical blocking coefficient.

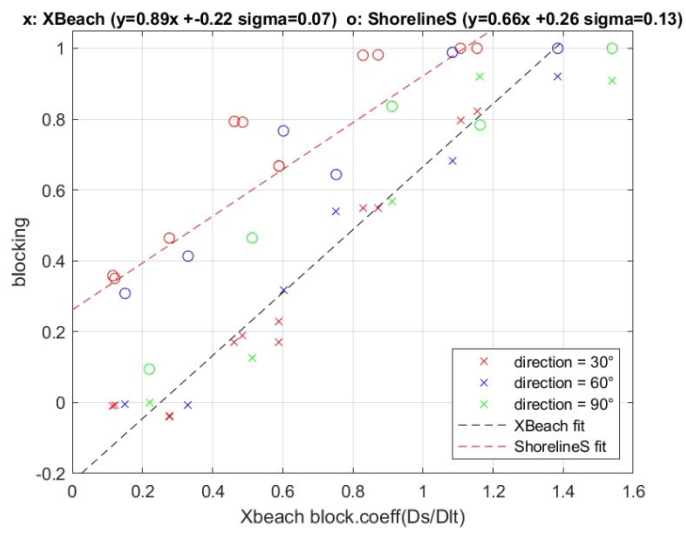


Figure A2.18 Blocking ratio in function of the blocking coefficient obtained by XBeach.

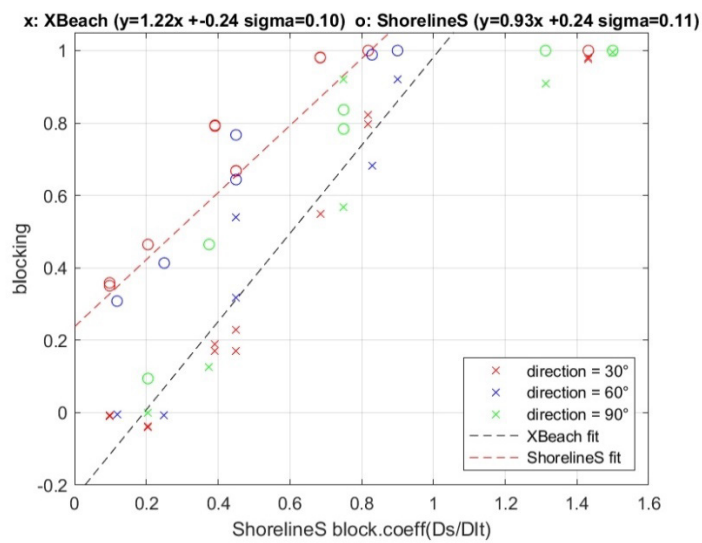


Figure A2.19 Blocking ratio in function of the blocking coefficient obtained by ShorelineS.

An alternative simulation is done with ShorelineS where the bypass is not based on the transport of the first upstream cell, but 1000m more upstream. The results are shown in Figure A2.20 till A2.22. In this alternative approach the results of ShorelineS match slightly better with XBeach (green line: original, red line :alternative), certainly for the lower blocking coefficients. But this approach is not realistic, as it neglects the effects of re-orientation of the coastline near the groin. Using the  $Dlt$  calculated in ShorelineS also gives less scatter (this is due to the deviation of  $Dlt$  theo and  $Dlt$  ShorelineS specially for very oblique waves, for which a larger  $\gamma$  would be more appropriate).

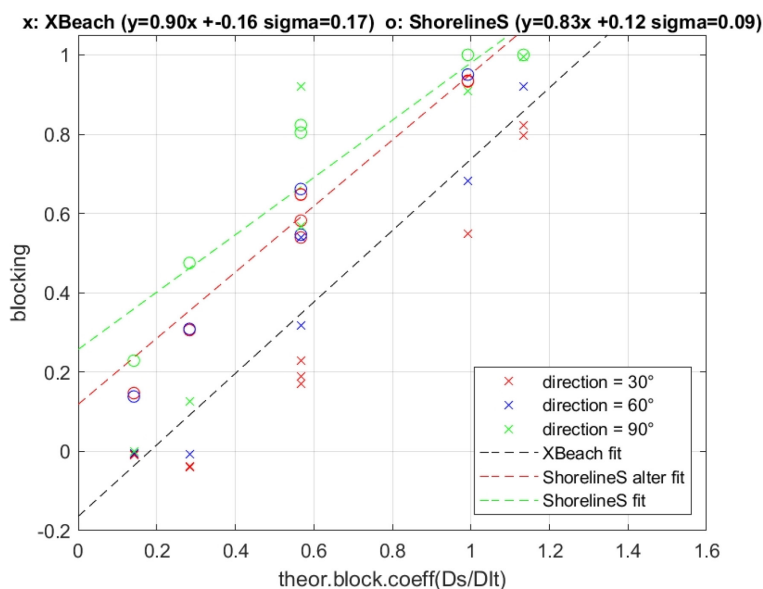


Figure A2.20 Blocking ratio in function of the theoretical blocking coefficient (ShorelineS:alternative approach) (green line: result original approach).

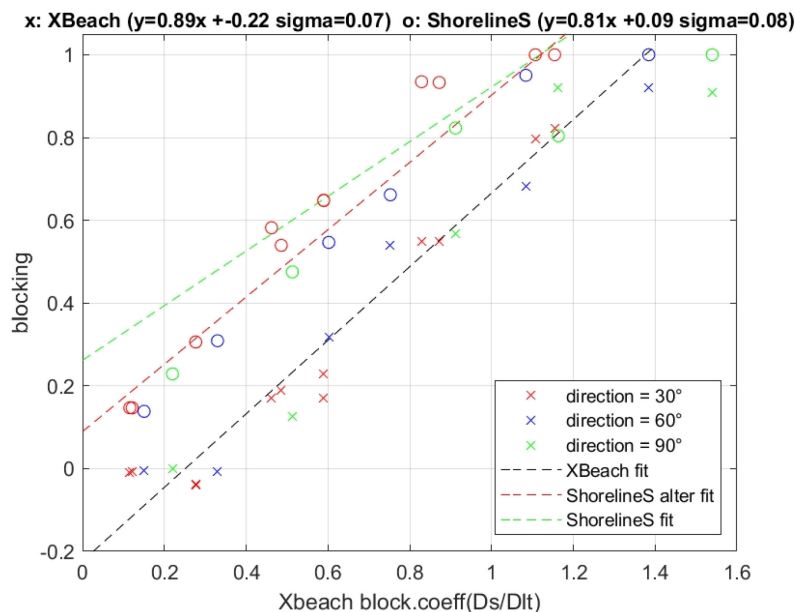


Figure A2.21 Blocking ratio in function of the blocking coefficient obtained by XBeach (ShorelineS: alternative approach) (green line: result original approach).

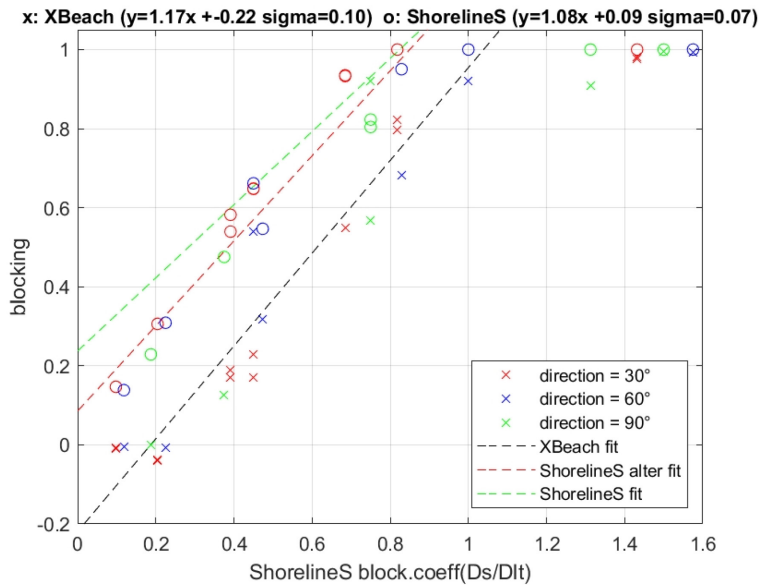


Figure A2.22 Blocking ratio in function of the blocking coefficient obtained by ShorelineS (alternative approach) (green line: result original approach).

In Figures A2.23 and A2.24 only simulations for 1 direction (resp. 30° and 60°) are shown. These figures show that there is no dependency of the fit/scatter on the wave height.

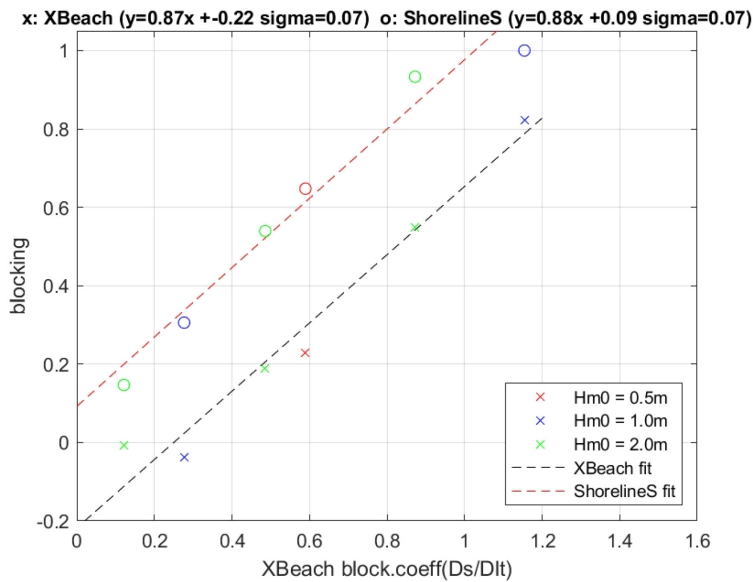


Figure A2.23 Wave direction 30° Blocking ratio in function of the blocking coefficient obtained by XBeach (ShorelineS: alternative approach).

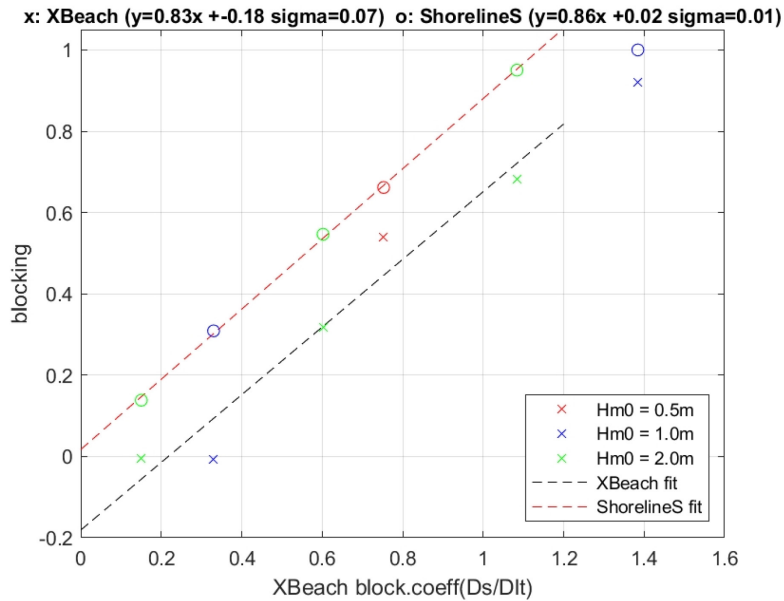
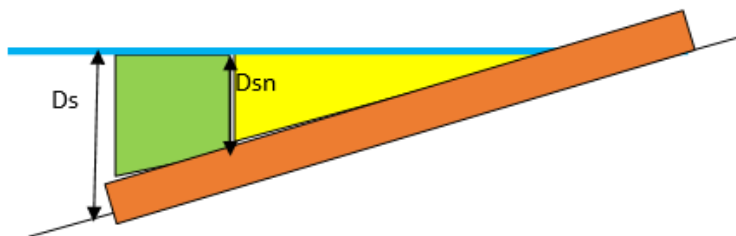


Figure A2.23 Wave direction 60° Blocking ratio in function of the blocking coefficient obtained by XBeach (alternative approach).

### Results for submerged groins

Only in XBeach submerged groins can be modelled. In the following figures the XBeach simulations with groins above water level are compared with groins with crest 1m above sea bed (following the beach slope). Figure 3-17 shows the results for all groins together ( $D_s = 0.5 // 2 // 3.5$ m). Figure 3-18 shows the results for  $D_s=0.5$ m. In that case, a 1m high groin is not submerged. The figure is just to show that the results correspond with the groin above water level (the absolute value of the crest is different, although both are above water level, but this can also influence the slope position).

In the next step a new  $D_s$  is calculated ( $D_{sn}$ ) such that the wet surface between  $D_s$  and  $D_{sn}$  is equal to the wet surface between the submerged groin and the water level (green surface = yellow surface) ( $D_{sn}=(D_s^2 - (D_s - h_{gr})^2)^{0.5}$ . ( $h_{gr}$ =height of the groin) (if  $h_{gr} > D_s$ ,  $D_{sn}=D_s$ ).



In the relationship between  $D_s/Dlt$  and the blocking for a groin above water level,  $D_s$  is replaced by  $D_{sn}$  (so a  $D_s$  value gives a reduced blocking) and this relation is compared with the results of the 1 and 2m high groin.

There are 3 combinations where the submersion of the groin is significant: groin up to -1.5m TAW ( $D_s=3.5$ ) with a groin of 1 m (depth reduction of about 28% at the offshore tip of the groin) or a groin of 2m (depth reduction 57%) and a groin up to 0m TAW ( $D_s=2$ m) with a groin of 1m height (depth reduction of 50%).

In Figure 3-19 till Figure 3-21 the results are shown for these groins with resp. 1 and 2m height. The green line shows the curve obtained with the XBeach results for a groin above water level for an adapted  $D_s$ . (so in theory, this green line can be used with as input the real  $D_s$  value (not taken into account the height of the groin (the equation of the green line depends on the height of the groin)). The larger the depth reduction at the offshore end of the groin, the better the green line fits the results

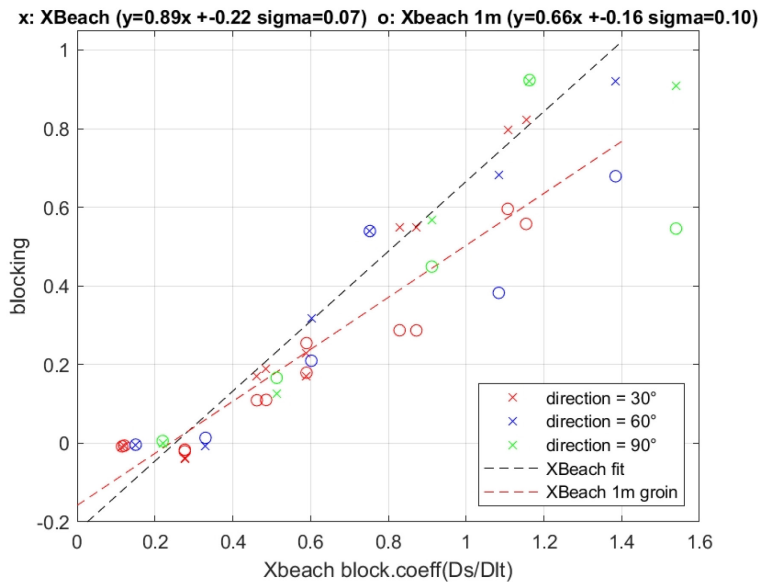


Figure A2.24 Effect of a submerged groin 1m high on the reduction in blocking (all groins) (Xbeach fit: XBeach results for a groin above water level//XBeach 1m groin: XBeach results for a 1m high groin).

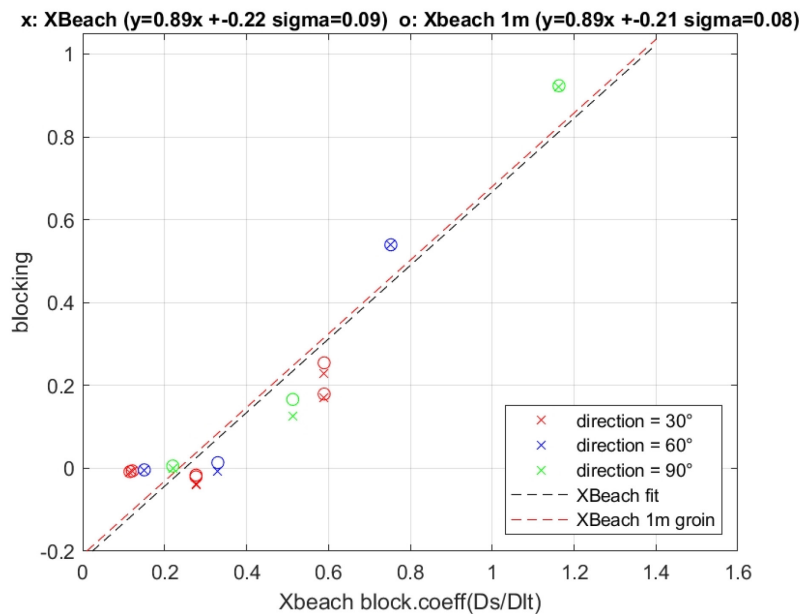


Figure A2.25 Effect of a submerged 1m high groin on the reduction in blocking (groin with tip at 1.5m TAW (( $D_s$ )=)0.5m below water level).

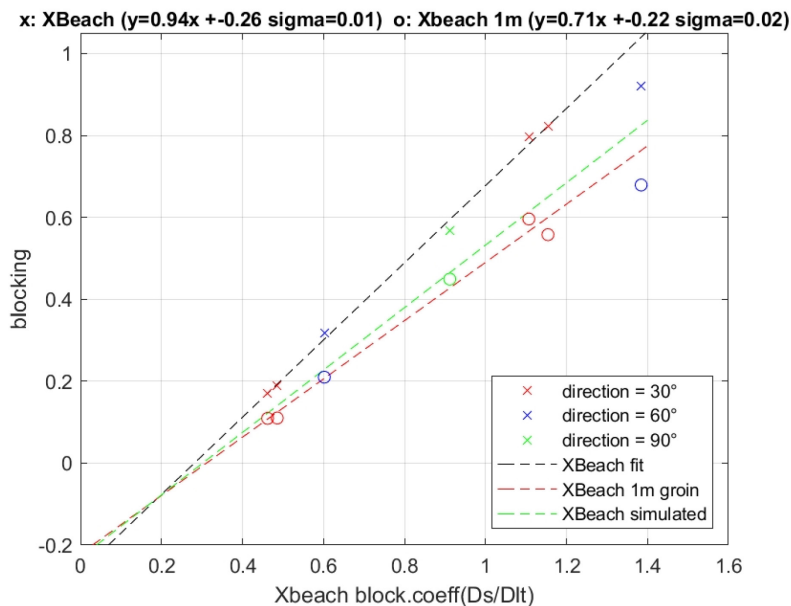


Figure A2.26 Effect of a submerged 1m high groin on the reduction in blocking (groin with tip at 0m TAW ((Ds=)2m below water level) ) (Xbeach fit: XBeach results for a groin above water leve//XBeach 1m groin: XBeach results for a 1m high groin, XBeach simulated: using results of a groin above water level and adapt Ds to simulate a 1m high groin).

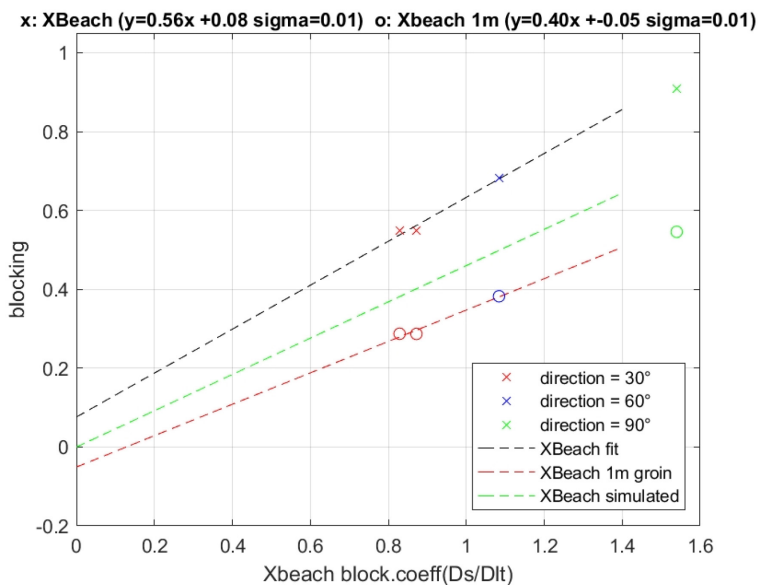


Figure A2.27 Effect of a submerged 1m high groin on the reduction in blocking (groin with tip at -1.5m TAW ((Ds=)3.5m below water level).

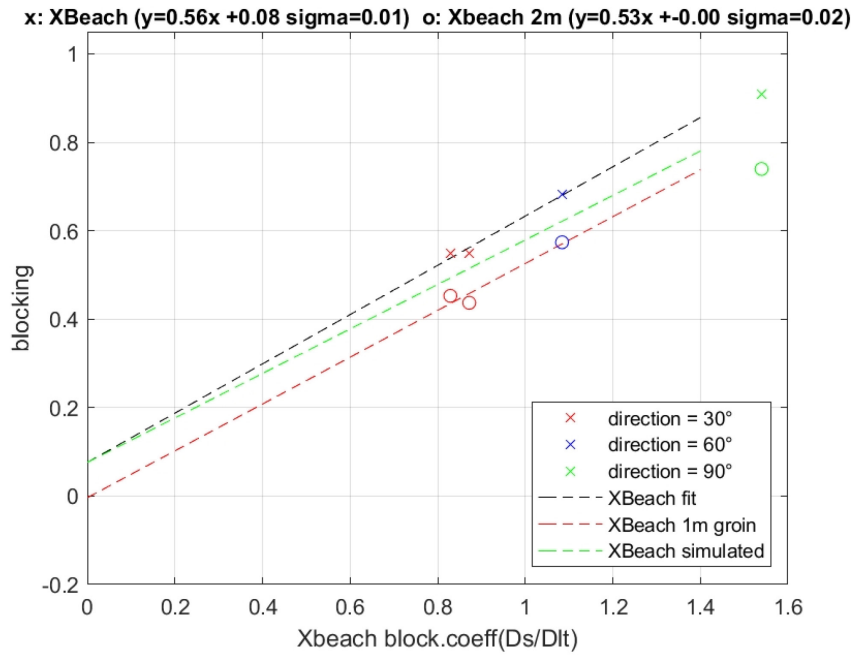


Figure A2.28 Effect of a submerged 2m high groin on the reduction in blocking (groin with tip at -1.5m TAW (( $D_s$ )=3.5m below water level).

### 3. Final XBeach calculations

In this chapter the results are shown for the final XBeach simulations. Groins are emerged (if present).

In all the simulations a Manning coefficient of 0.02 and the Soulsby Van Rijn transport formulation is used.

#### ***Cross shore profile adaptation***

With the aim of doing long term XBeach simulations, the evolution of the cross shore profile is tested.

BOI settings give much more stable cross shore profile compared to the original WTI settings (Figure A2.29). This also influences strongly the longshore transport distribution, which is much more constant in time using BOI (Figure A2.30).

The profile evolution with and without tide and for 2 different wave heights is shown in Figure A2.31.

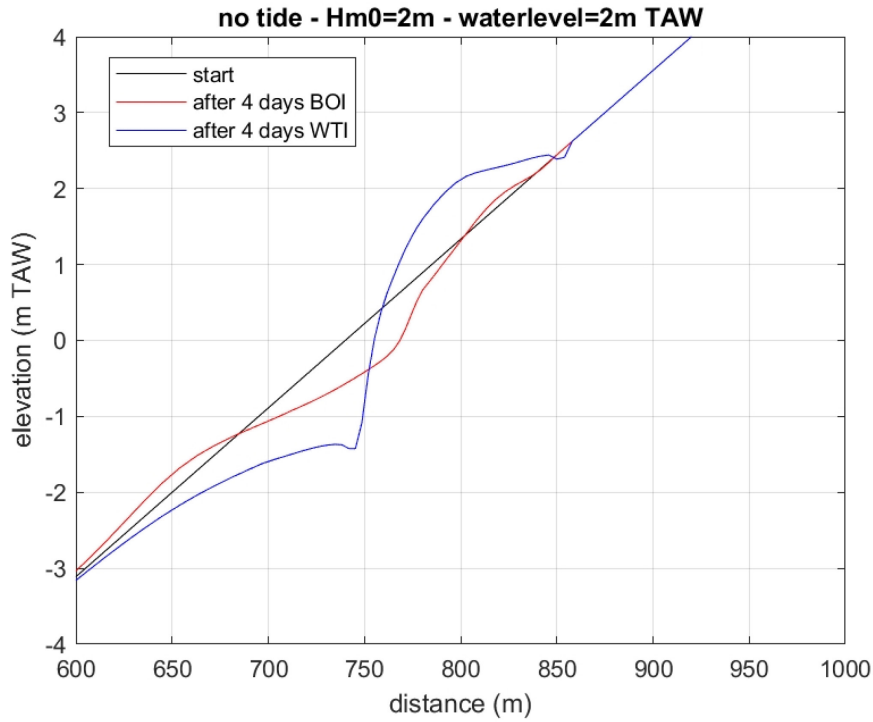


Figure A2.29 Evolution of the cross shore profile.

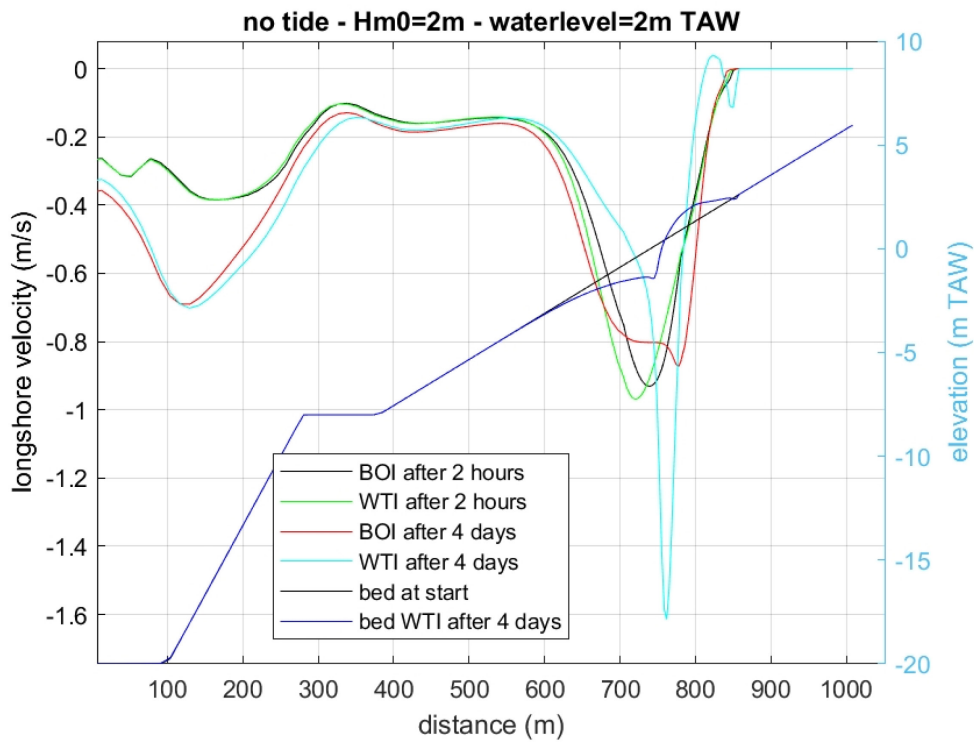


Figure A2.30 Longshore velocity.

All simulations done with BOI settings. The cross shore profile evolution is shown in the next figure:

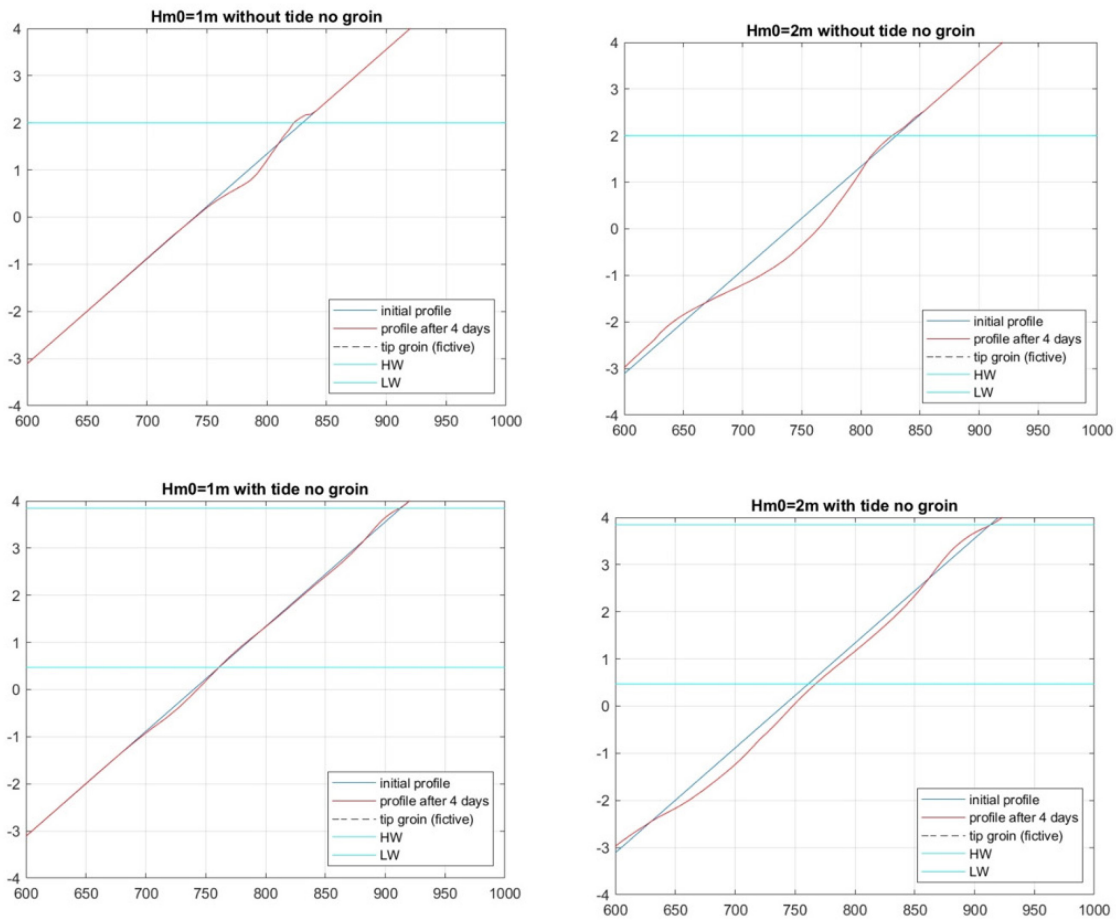


Figure A2.31 Evolution of the profile with and without tide for different wave heights

**Morphological evolution after 8 days with constant wave and tide conditions for emerged groins**

Simulations are done for 8 days (using morfacopt=0, morfac=2) with and without tide. The bed evolution for Hm0=1m is shown in Figure A2.32. As can be seen some minor sedimentation can occur downdrift the groin. For Hm0=2m (Figure A2.33) this sedimentation is much more extended, especially if tide is involved.

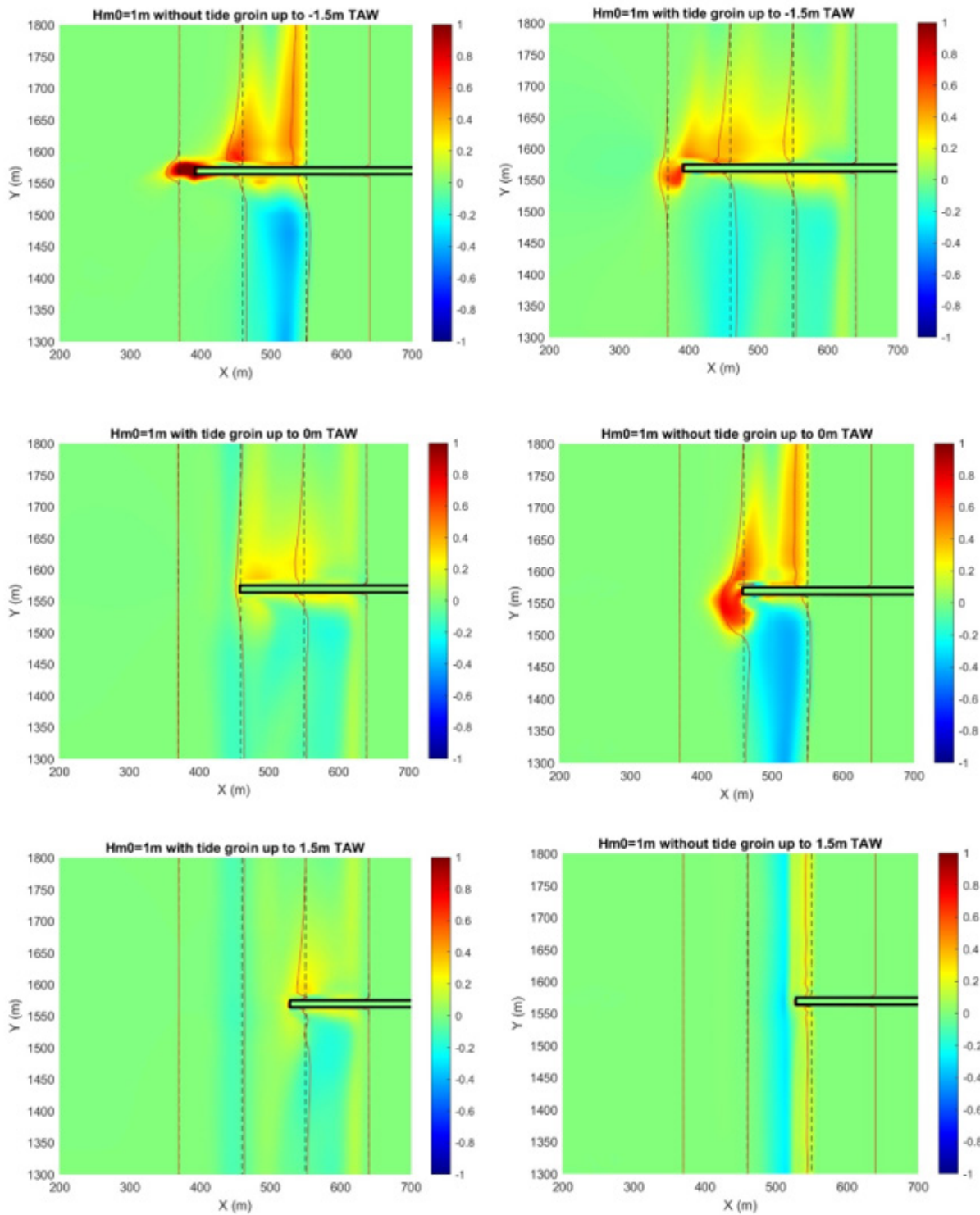


Figure A2.32 Morphological evolution (+:sedimentation in m) after 8 days with (left) and without (right) tide for  $H_{m0}=1\text{m}$  for 3 different groin lengths.

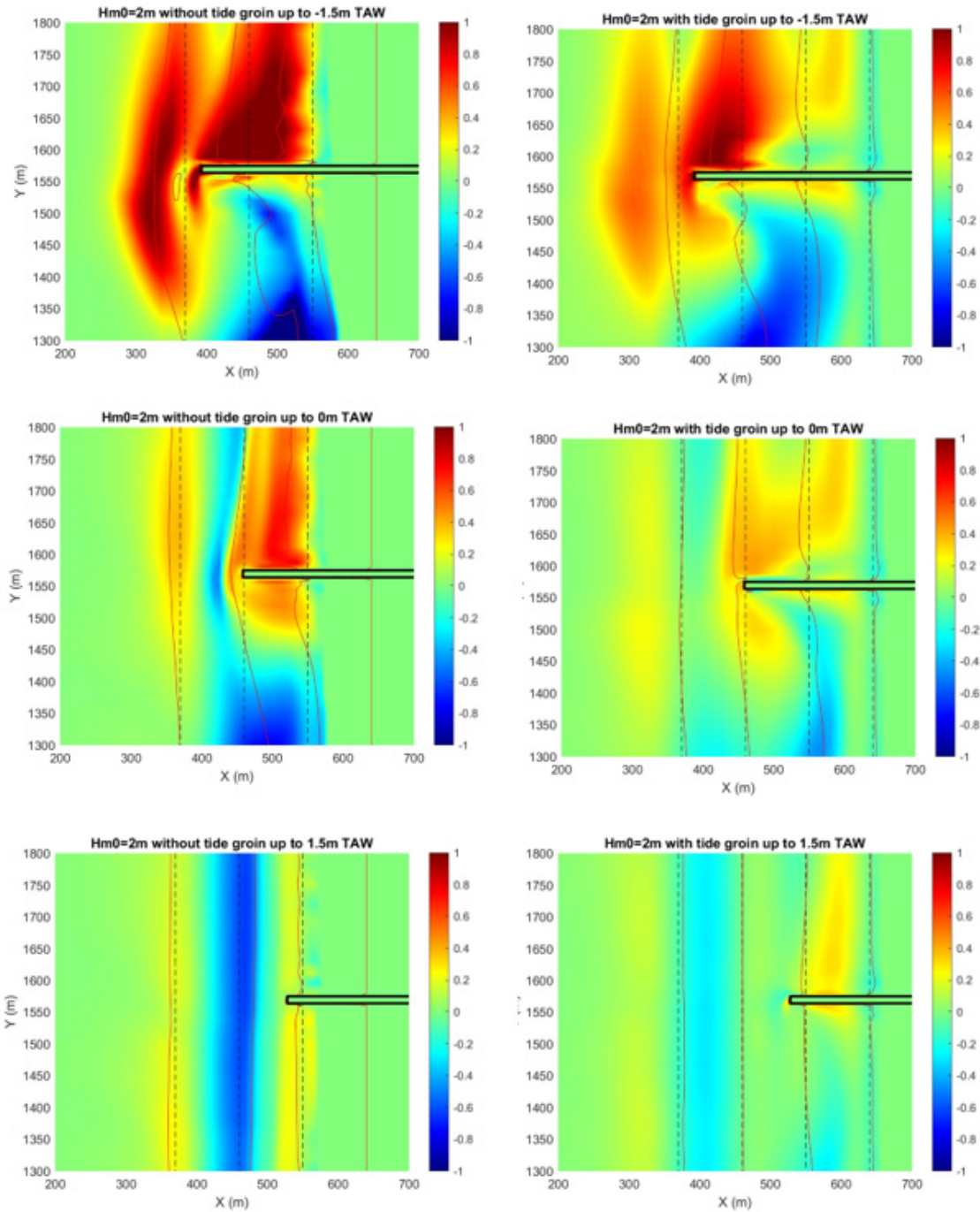


Figure A2.33 Morphological evolution (+:sedimentation in m) after 8 days with (left) and without (right) tide for  $H_{m0}=2m$  for 3 different groin lengths (emerged)

Figure A2.34 shows the time evolution of the blocking and sediment transport under tidal conditions. In some cases the blocking is larger than 1. This means that the direction of the transport changes due to the presence of the groin. The strong variation of this blocking, means this variation should also be implemented in ShorelineS.

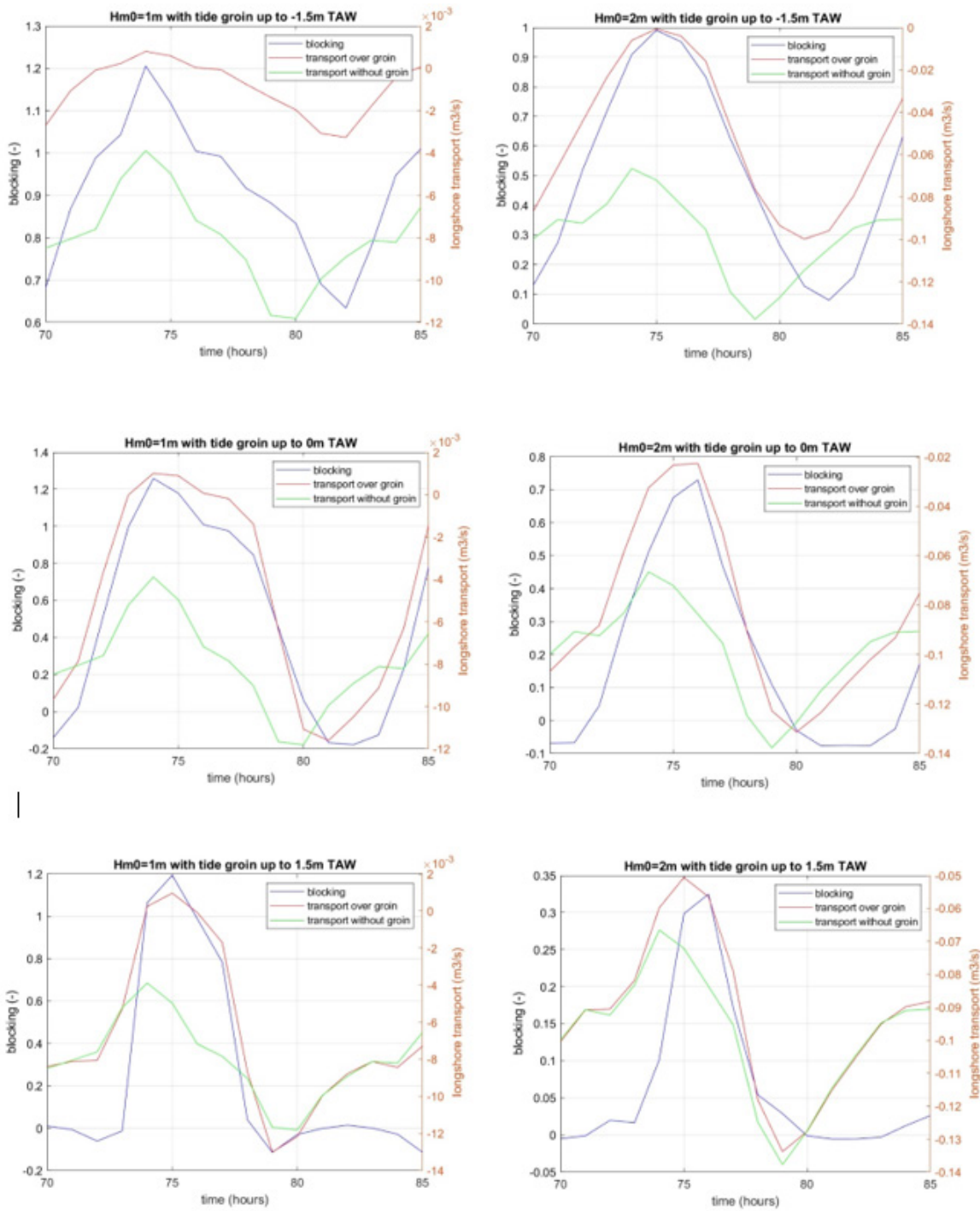


Figure A2.34 Evolution in time of the blocking and longshore transport under tidal conditions. HW at t=75h, LW at t=81h. At HW the tide induced current is opposite to the wave induced current.

Figure A2.35 shows that in general the blocking decreases slightly in time for the first 8 tidal cycles.

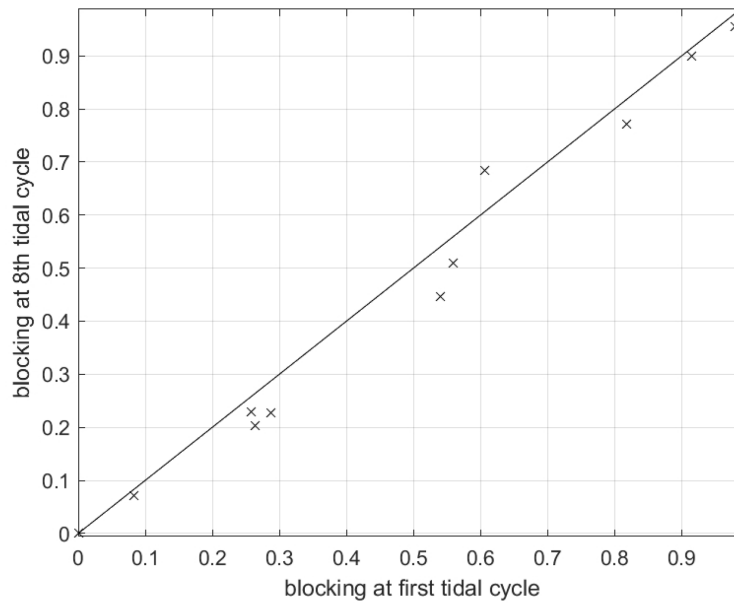


Figure A2.35 Averaged blocking at the 8<sup>th</sup> tidal cycle compared to the first tidal cycle.

#### 4. XBeach simulations with submerged groins

XBeach simulations are done for:

- Beach slope of 1:45
- Wave heights just seaward of the depth of closure: 0.5;1;2m
- Wave direction -30° ; 30° ;60°
- Directional spreading 5° (corresponding to ShorelineS) (\*)
- Constant water level of 2m TAW and tidal variation (LW at 0.5m TAW, HW at 4m TAW)
- Groins with offshore toe at a beach depth -3;-1.5;0;+1.5m TAW (for a water level of 2m, this gives a Ds of resp. 5;3.5;2;0.5m)
- Relative groin height of 0;1;2;3m + emerged groin
- Simulated time period : 26 hours (in order to have 2 tidal cycles). Earlier calculations with much longer duration (5 days) showed little variation in blocking coefficients)
- Use of the BOI settings and the Soulsby-Van Rijn transport formulation.

(\*) the directional spreading is of minor importance for the blocking, as illustrated in table below.

Hm0 (m)	Ds (m)	groin height above bed (m)	blocking			
			dir.spr. 30°	dir.spr. 15°	dir.spr. 5°	dir.spr. 15° with Van Thiel
1	2	1	0.57	0.49	0.51	0.54
1	2	emerged	0.78	0.72	0.70	0.73
1	5	2	0.88	0.83	0.82	0.84
1	5	emerged	1.00	0.99	0.99	0.99
2	5	2	0.39	0.40	0.45	0.50
2	5	emerged	0.80	0.79	0.74	0.78

Influence of the directional spreading (and transport formulation) on the blocking, for different wave conditions and wave heights

The results are shown in Figure A236. The effect of the (relative) groin height on the blocking is also visualized in Figure A2.36.

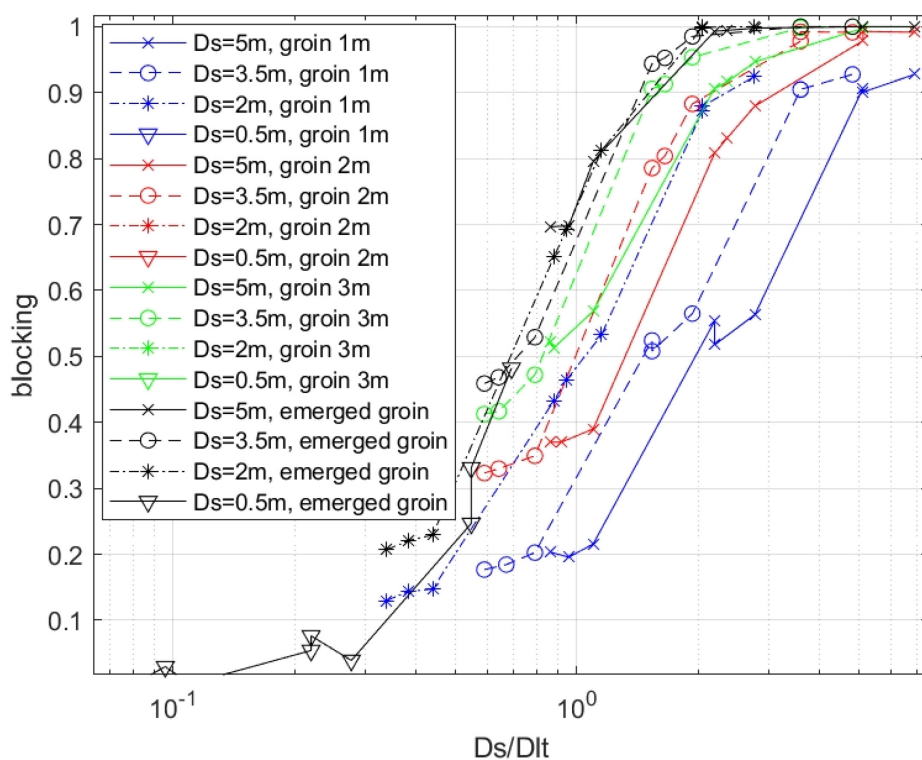


Figure A2.36 Blocking as function of Ds/Dlt for different values of Ds and groin height.

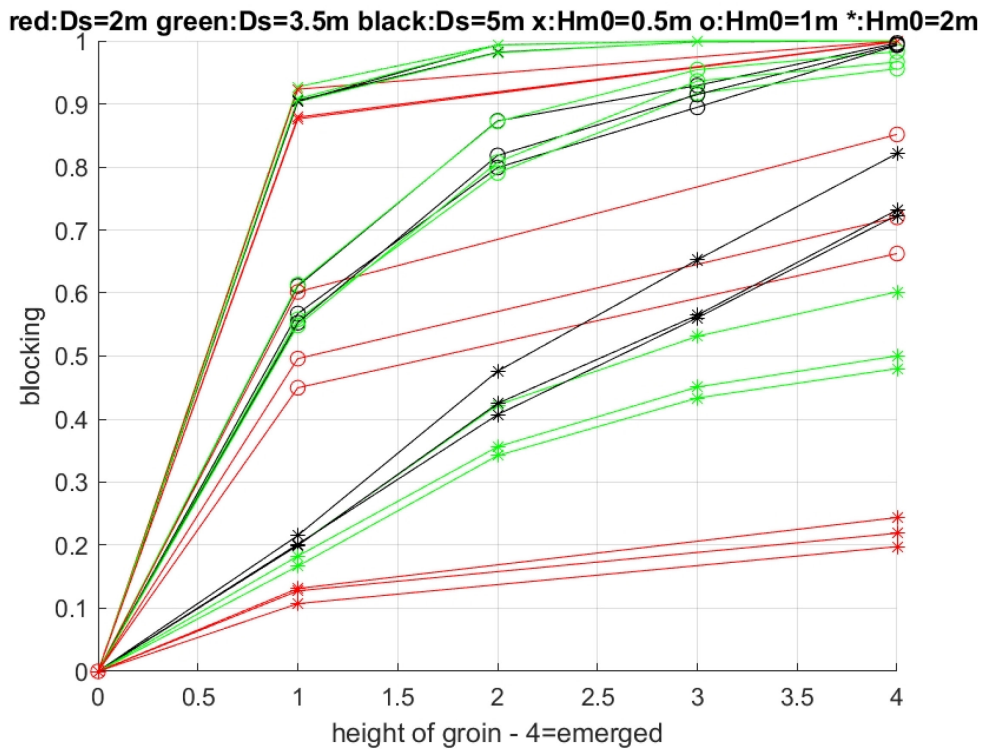


Figure A2.36 Visualisation of the effect of the relative grain height on the blocking

It was found  $D_s'/D_s$  and  $D_s/D_{lt}$  are the relevant parameters to describe the reduction of the blocking due to the lower grain. In Figures A2.37 and A238 it can be seen that this relation is quasi linear with (of course) saturation for values close to 1. However, also logarithmic relations are tested.

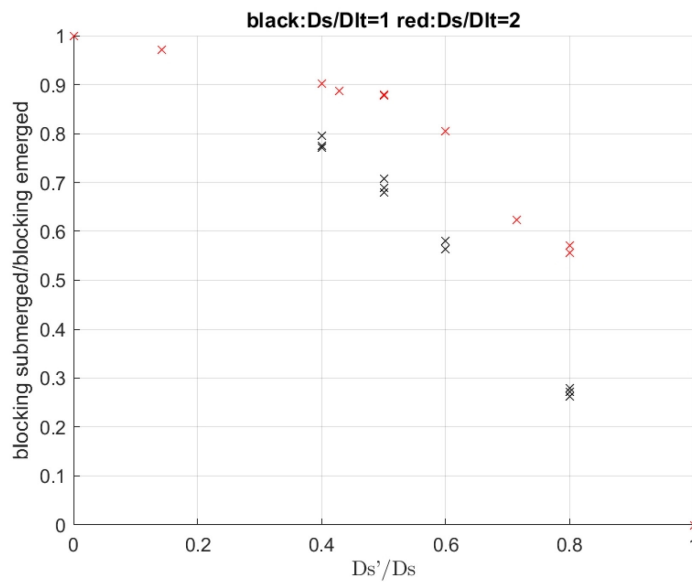


Figure A2.37 ratio of blocking for submerged grain (various heights) over blocking emerged grain in function of  $D_s'/D_s$ .

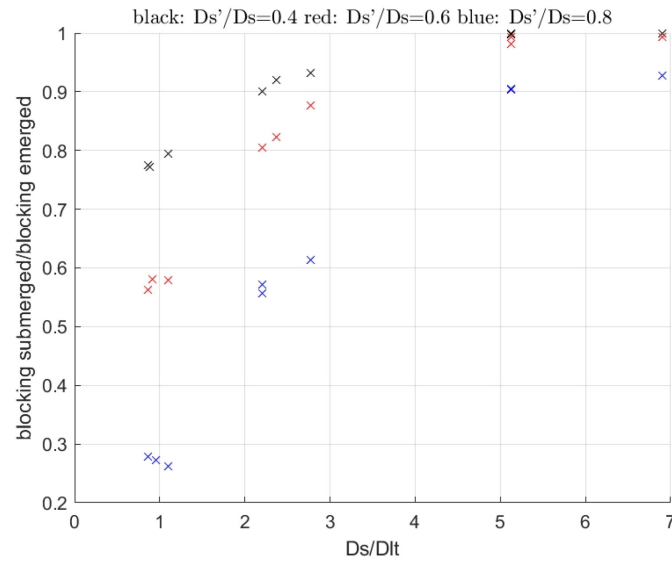


Figure A2.38 ratio of blocking for submerged groin (various heights) over blocking emerged groin in function of  $D_s/D_{lt}$ . Using curve fitting gives following reduction coefficient (redu) (ratio of blocking submerged groin over blocking emerged groin):

$$\text{Redu} = -0.973 \frac{D_s'}{D_s} + 0.1296 \frac{D_s}{D_{lt}} + 1.023.$$

The formula is valid for  $D_s'/D_s < 0.8$ . For very low groins in combination with high  $D_s/D_{lt}$  values, the reduction is overestimated. It is advised to interpolate between the obtained value for  $D_s'/D_s=0.8$  and 0 for  $D_s'/D_s=1$  (=no groin).

For all simulations with submerged groins, the reduction is applied on the blocking of the corresponding emerged simulation (=estimated blocking). This result is compared with the modelled (XBeach) reduction coefficient. The maximum error is 0.12, the standard deviation 0.05. The comparison is shown in Figure A2.39.

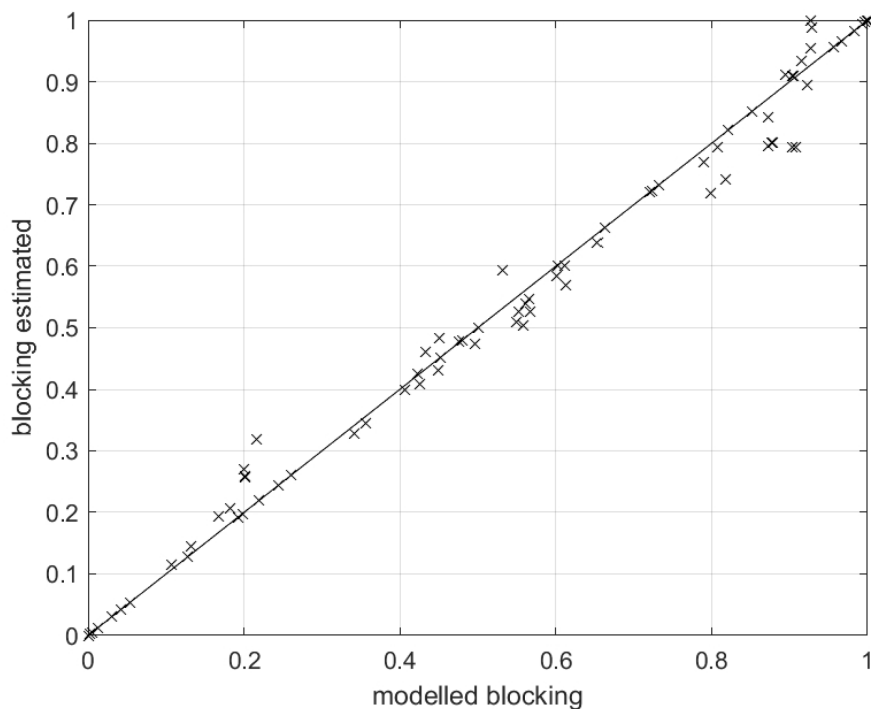


Figure A2.39 Comparison between modelled blocking and estimated (via formula) blocking

## 5. Use of ShorelineS with new groin formula

### Modifications

Following modifications are applied in ShorelineS

- Using of Manning coefficient instead of Chezy (cf. chapter 2)
- $Dlt$  is calculated based on the longshore velocity profile (obtained in tide\_wave\_transport.m) for 24 tidal phases
- $D_s$  varies with tidal water level (24  $D_s$  values)
- The longshore transport over the groin is calculated for each phase of the tide (24 values), using the 24 values of transport just upstream groin,  $D_s$  and  $Dlt$
- A new parameter  $groinele$  is introduced, it is the elevation of the offshore tip of the groin. With this parameter the depth at the tip of the groin can be calculated ( $D_s'$ )
- The reduction of the blocking is calculated, based on the formula of chapter 5.

The effect of the modifications is shown by comparing Figures A2.40 and A24.1 (simulations with emerged groin). For many points, the blocking in ShorelineS is far too high, which is much better after the modifications.

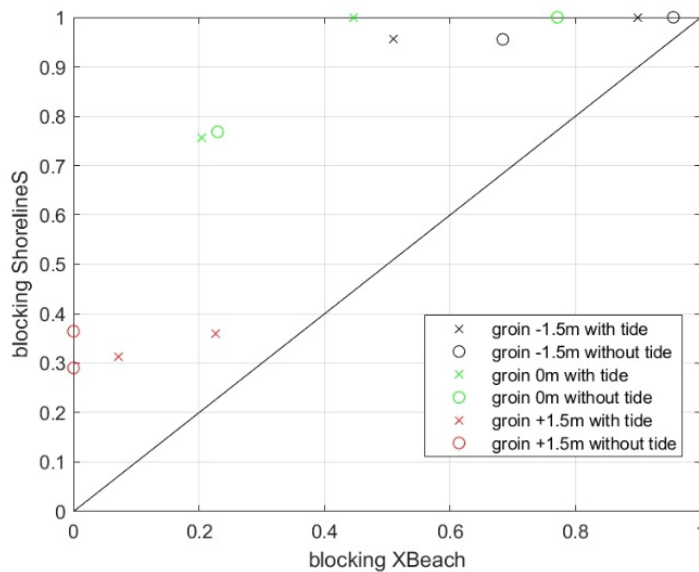


Figure A2.40 Comparison XBeach – ShorelineS before modification of ShorelineS ( $H_{mo}=1$  & 2m, direction  $30^\circ$ ).

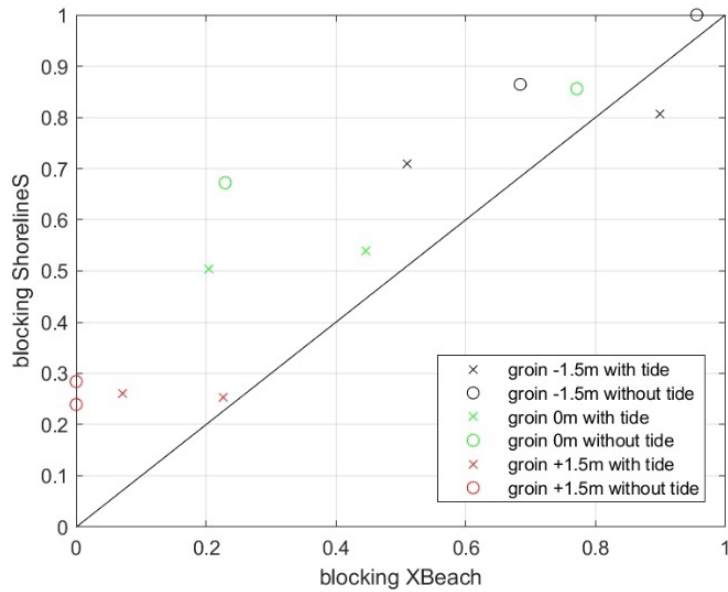


Figure A2.41 Comparison XBeach – ShorelineS after modification of ShorelineS (Hmo=1 & 2m, direction 30°).

The effect from the tide on the blocking is clear from Figure A2.42 (emerged groins): without modification (diamonds) there is of course no effect of the tide on the blocking. After modification, the effect is clear (triangles in SHorelineS, x for Xbeach) : the tide reduces the blocking. This is partly due to the offshore extension of the zone with sediment transport (increase of DLt). The other reason is that these cases are with a wave direction opposite to the flood direction. This means that at HW, when the groin is most effective, the longshore transport is reduced due to the tide. Most transport occurs near LW, when the groin is not effective (low blocking). Resulting, the blocking is reduced.

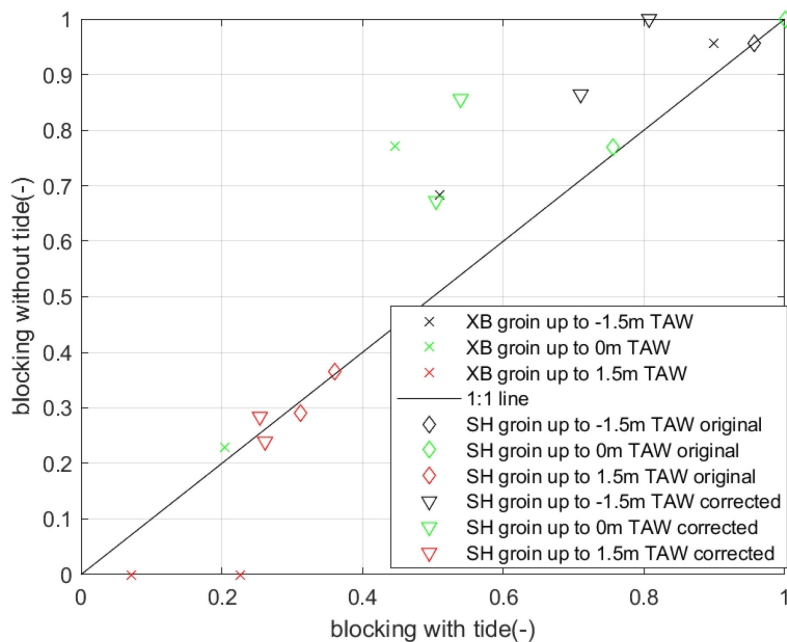


Figure A2.42 Comparison of the blocking for case with tide and without tide (wave direction opposite to flood direction)

If the wave direction is in the direction of the flood, the maximum transport occurs at higher water levels, making the groin more efficient (larger blocking). This is visible in Figure A2.43.

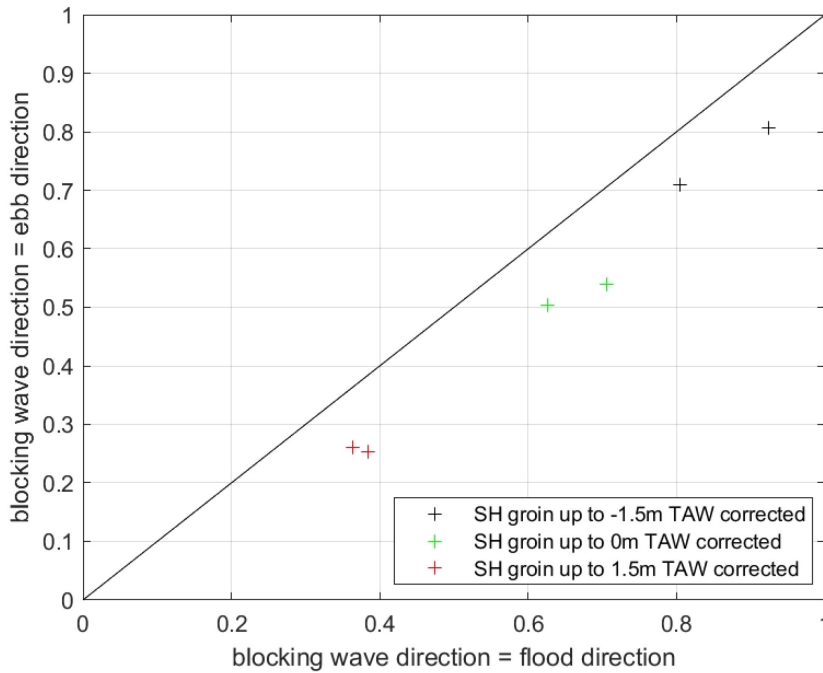


Figure A2.42 Effect of wave direction relative to the flood direction (ShorelineS simulations).

**Comparison with XBeach**

Blocking is calculated in XBeach and SHorelineS after 12h and after 24 hours. As can be seen the differences are small (Figure A2.43). For XBeach, even after 100hours, the differences are small.

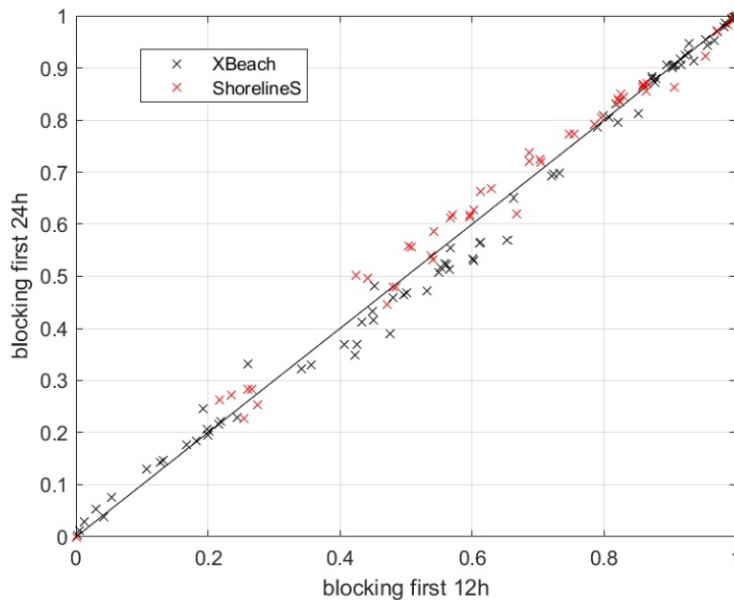


Figure A2.43 Time effect on the blocking.

Figure A2.44 shows that the agreement between modelled  $D_s/D_{lt}$  values in XBeach vs ShorelineS is very good.

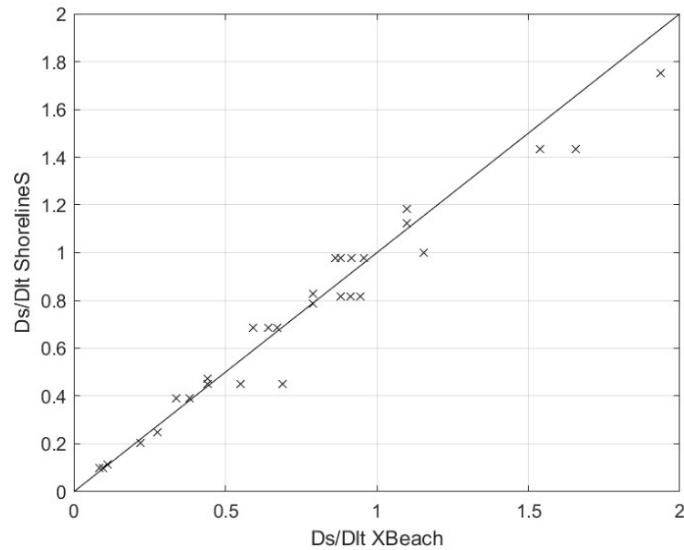


Figure A2.44 Comparison modelled  $D_s/D_{lt}$  values XBeach - ShorelineS

Figure A2.45 shows that the blocking in ShorelineS is higher than in XBeach. This is possibly partly because of the quick change in coastline orientation in ShorelineS. The initial blocking (as calculated at the first time step, with the original coastline) in ShorelineS is much closer to the XBeach values.

But, as can be seen, the results for the emerged groins are equal quality as the results of the submerged groins. This means that the new approach in ShorelineS is successful.

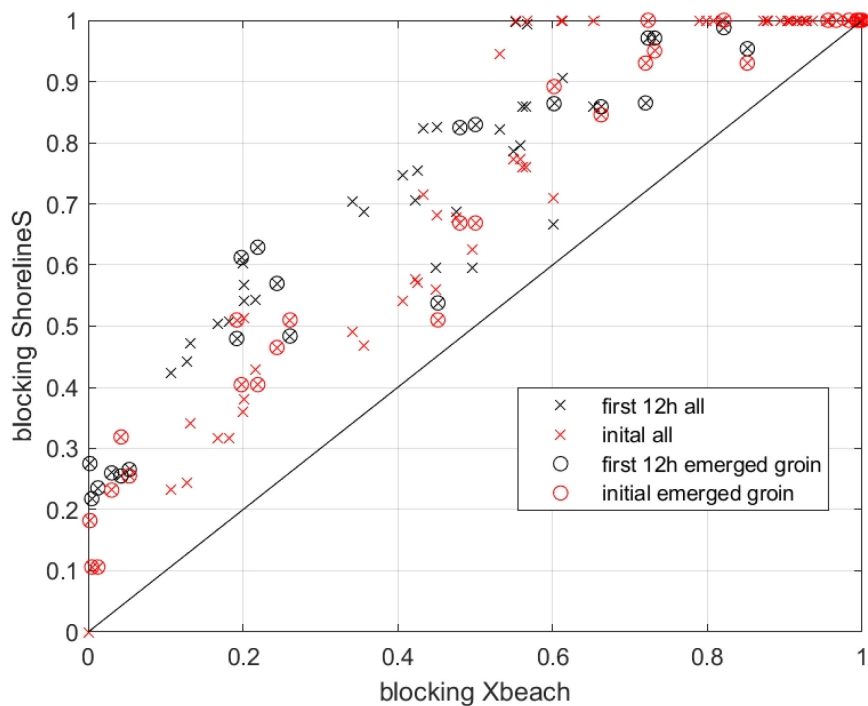


Figure A2.45 Comparison modelled blocking values XBeach – ShorelineS (conditions without tide).

In Figure A2.46 the same comparison is made for conditions with tide. Initial blocking is not presented, as this parameter varies in the tidal cycle. The conclusion is the same. It proves that the module with tidal conditions is working.

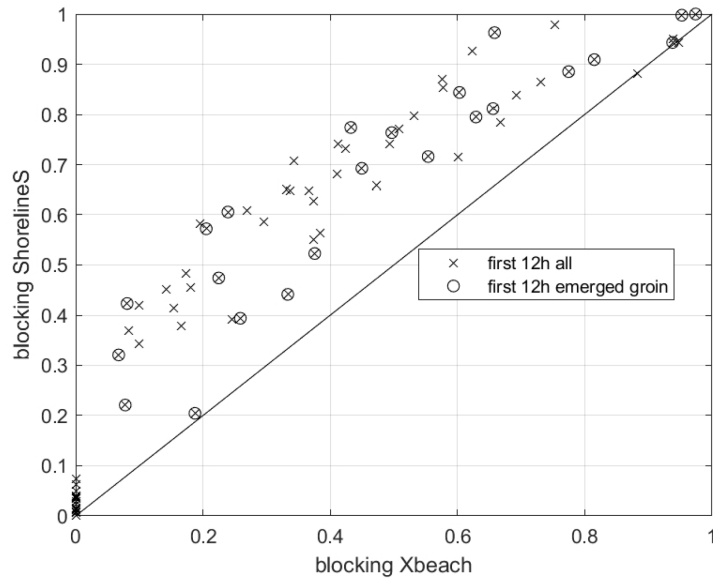


Figure A2.46 Comparison modelled blocking values XBeach – ShorelineS (conditions with tide).

## 6. Long term simulations

2 simulations are done. In both cases the wave direction is 30° towards the normal, the water level is constant and the groin is emerged.

In simulation 1 the wave height is 1m,  $D_s=2m$ .

In simulation 2 the wave height is 2m,  $D_s=3.5m$ . The used domain became too small after 8 days simulation. It should be noted that 8 days with a wave height of 2m near the beach involves already the expected transport after 1 year normal wave conditions. Before that time, already some instabilities in ShorelineS occurred (small periods with somewhat smaller blocking occurred). Both in XBeach and ShorelineS the blocking is rather constant (time output frequency is too small in XBeach to see the first 20 hours). Instabilities in ShorelineS are visible near 80 and 120h. The bed evolution is visible Figures A2.48 and A2.49.

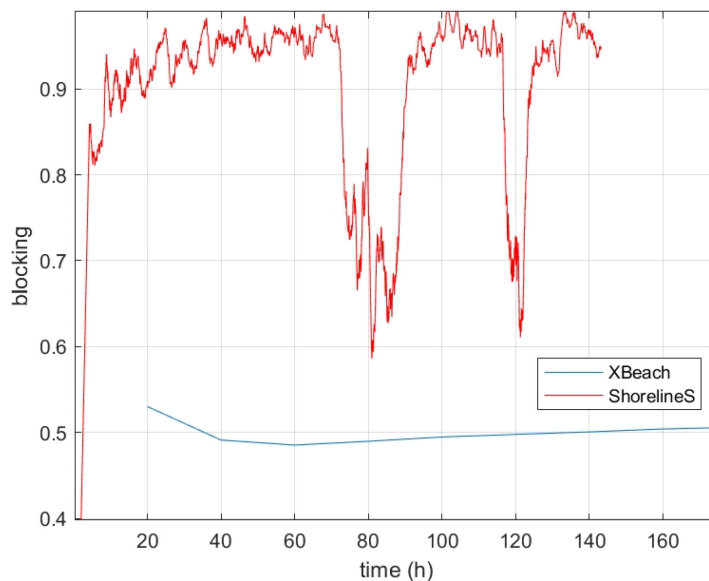


Figure A2.47 Time evolution of the blocking (simulation 2).

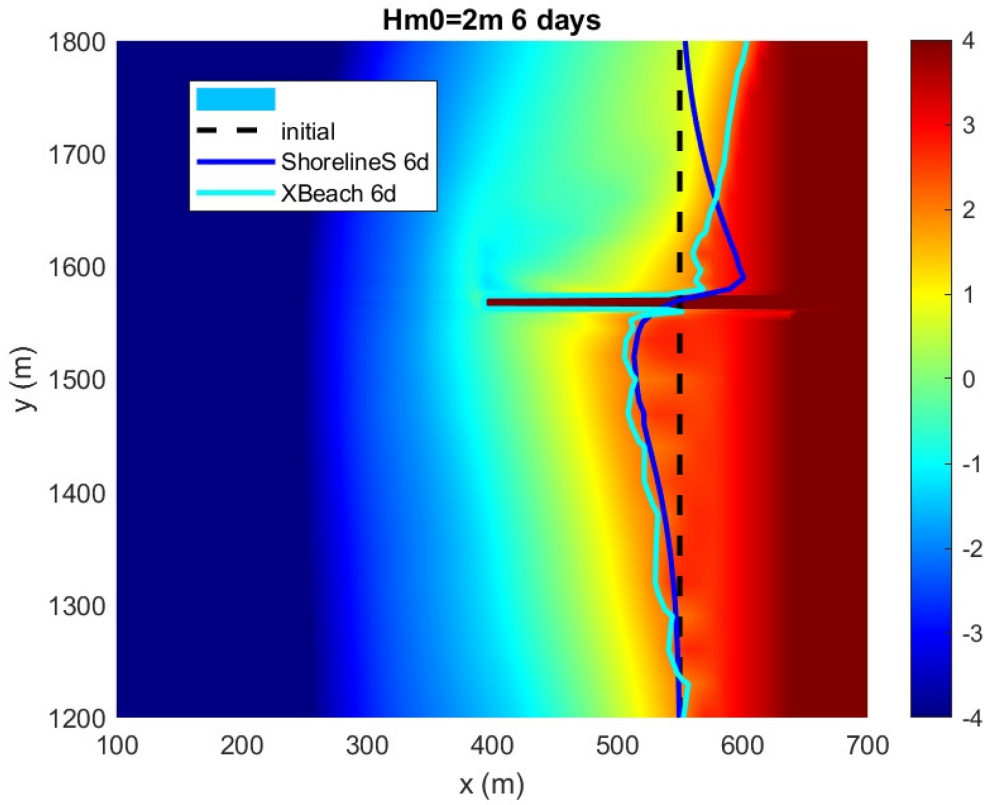


Figure A2.48 Bathymetry after 6 days + coastline (simulation 2) zoom.

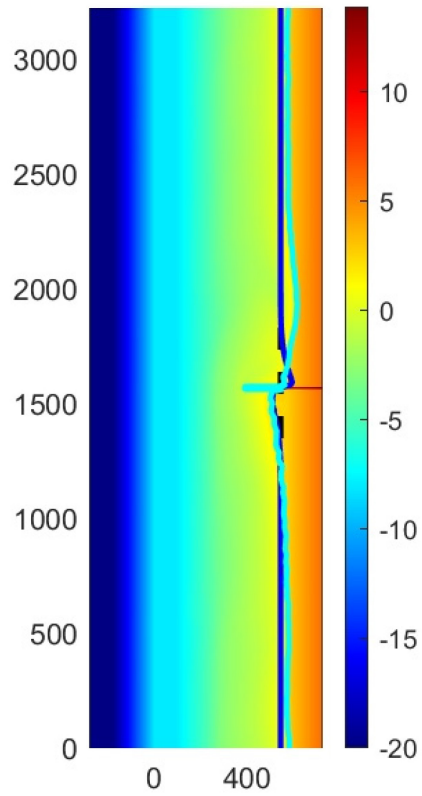


Figure A2.49 Bathymetry after 6 days + coastline (simulation 2).

## Conclusions and recommendations

- XBeach and ShorelineS compare very well on longshore velocity and sediment transport if for the ShorelineS model a Manning coefficient (0.02) is used for roughness (wave related) and if for Xbeach the WTI settings are used together with the Soulsby Van Rijn transport formulation
- The blocking is higher in ShorelineS compared to XBeach;
- The ration  $A_w/\gamma$  seems to depend on the wave direction. In ShorelineS this can be implemented by calculating the real offshore limit of the offshore transport (in the tidal module where the cross shore distribution of the longshore transport is obtained), or a relation representing this dependency could be build in;
- In ShorelineS the coastline near the groin change orientation already in the first time steps. This gives extra blocking (since the reorientation reduces the transport in the first upward cell). This might not happen that fast in XBeach.

Following modifications are applied in ShorelineS based on calculations with XBeach to identify the effect of a submerged groin on the sediment transport:

- Using of Manning coefficient instead of Chezy (cf. chapter 2);
- $Dlt$  is calculated based on the longshore velocity profile (obtained in `tide_wave_transport.m`) for 24 tidal phases;
- $D_s$  varies with tidal water level (24  $D_s$  values);
- The longshore transport over the groin is calculated for each phase of the tide (24 values), using the 24 values of transport just upstream groin,  $D_s$  and  $Dlt$ ;
- A new parameter `groinele` is introduced, it is the elevation of the offshore tip of the groin. With this parameter the depth at the tip of the groin can be calculated ( $D_s'$ );
- The reduction of the blocking is calculated, based on the formula of chapter 5.

Recommendations:

- Examine the higher blocking in ShorelineS vs XBeach. A solution can be the bypass factor, but it has to be figured out how this should be done in combination with the reduction factor for submerged groin and the effect of instabilities causing a reset of the bypass factor to 1;
- Further long term simulations.

# Appendix 3 Generation of tidal input files for ShorelineS

<b>Title :</b> Pre-processing: tide input file for ShorelineS	
<b>Type :</b> <input type="checkbox"/> Case study <input checked="" type="checkbox"/> Development	<pre>function make_tidefile(xystat,cZWL,vmean,xsdst,dps,varargin) % FUNCTION make_tidefile(xystat,wl) creates the tidefile for ShorelineS % This function computes M2 and M4 tidal components, given any % timeseries of waterlevels. % Then it creates the tidefile (in the present working directory) as % expected by the tide-module of ShorelineS % % INPUT: % xystat: [N x 2] matrix containing x- and y-coordinates of N tide % stations (measured or modelled). Minimal 2 stations should be % defined, and ordered in such a way that the sea is on the % lefthand side of the line (conform ShorelineS coastline % definition). % cZWL: {N x 1}[nT x 2] cell-array containing N waterlevel timeseries, % with timestamp and value in the columns of the matrix. The % number of timestamps (nT) can be different for each station (N) % vmean: [N x 1] vector containing the tidally averaged (residual) % alongshore velocity in the stations (if only a scalar is given, % it is repeated N times) % xsdst: [N x 1] cross-shore distance (m) % dps: [N x 1] bed level (m MSL) % &lt;varargin&gt; keyword-value pairs % latitude: switch for nodal correction, activated by vector "lat": % [N x 1] vector containing the latitude of the stations % (if only a scalar is given, it is repeated N times) % ssSwitch: switch for the computation of the alongshore surface slope: % either "harmonic" or "1D_analytical" (default) % Cf: bed friction coefficient (-) % hmin: minimum water depth (m) % tidefile: [char-array] name of outputfile % % NOTE: The number of timestamps (nT) can be different for each station % (N): e.g. different time intervals, but it is advisable that they % span the same period. Time should be expressed as MATLAB datenum. % Having NaN's in the timeseries should be avoided. % % OUTPUT: % tidefile containing xstat, ystat, etaM2, etaM4, detadsM2, detadsM4, % phiM2, phiM4, km2, km4, ss for every station % % DEPENDENCIES: % - t_tide.m (see Deltares' OpenEarthTools)</pre>
<b>Location :</b> <i>any</i>	
<b>Alignment with task :</b> <i>T1b: efficient wave, current and climate conditions – tidal currents</i> <i>T6: development of pre- and post-processing routines</i>	
<b>Organization :</b> <i>Antea Group Belgium</i>	
<b>People :</b> <i>Arvid Dujardin, Antea Group Belgium</i>	

## Introduction

This case aims at developing an easy-to-use method to generate tide boundary conditions for the ShorelineS model. A specific MATLAB function, in-line with the ShorelineS coding guidelines, will be developed to generate the tide file as expected by ShorelineS' tide-module. The user will need to provide measured or modelled water level time series together with meta-data of the stations location and an estimate of the residual alongshore component of the tidal current.

## Description

*Make\_tidefile.m* writes the tidefile in the format expected by ShorelineS tide-module, based on water level timeseries and tidally averaged alongshore current, for a series of stations (measured or modelled).

- The user needs to provide water level time series for at least 2 stations along the ShorelineS models boundary. The meta-data for the stations are: its X- and Y-coordinates, its distance from the shore and the bed level at the location in respect to Mean Sea Level. Also an estimate of the tidally averaged (residual) alongshore velocity needs to be given.
- Optional inputs are the latitude of the stations, the bed friction coefficient  $C_f$ , the minimum water depth  $h_{min}$  and the name of the output file. If the latter three are not user defined, the ShorelineS default values are used for  $C_f$  and  $h_{min}$ ; the default output filename is *tidefile.txt*.
- From the water level timeseries the M2 and M4 harmonic components are derived by the function *t\_tide.m* (Pawlowicz, 2002) as included in Deltares' OpenEarthTools. If the optional input latitude is given, *t\_tide.m* will perform a nodal correction on the harmonic components.
- For compatibility reasons it makes use of *tide\_1d\_ana\_anycomp.m* as included in the ShorelineS code-base itself, to calculate the mean longshore surface slope. This option can be switched off by setting the *ssSwitch*-keyword to harmonic.
- Calculated variables are written to *tidefile.txt*

## Methodology

An example on how to compute and implement tidal boundary conditions was made available by Dano Roelvink for the Flanders Hydraulics Knokke testcase. Results from a Delft3D 4suite model, a MATLAB script and resulting tidal boundary file for ShorelineS were shared. *Make\_tidefile.m* was used on the same Delft3D history-output to generate a new ShorelineS' tidal boundary file. The resulting *tidefile.txt* was compared to the tidal boundary file as provided by Roelvink to check consistency.

## Results

Small differences between the obtained amplitudes of the tidal components (order of magnitude: centimeters), as well as in the mean longshore surface slope ( $10^{-5}$ ) were observed. Observed differences between the obtained alongshore phase difference gradients are also small (order of magnitude:  $10^{-6}$ ). Large differences between the phase angles for the tidal components are explained by a different reference time used for *t\_tide.m* and Roelvinks script. This is however not a problem since the phase angle only defines the reference start time within the tidal cycle, while the alongshore phase difference is affecting the surface slope.

A comparison between the results of a ShorelineS model ran with a) Dano Roelvinks initial tide boundary file and b) the new *tidefile.txt* should still be done, to get an estimate of the importance of the observed differences between both input files.

## Conclusion

*Make\_tidefile.m* provides a more user friendly way to generate tide boundary conditions for ShorelineS. The use of optional inputs (*varargin*) facilitates the implementation of new functionalities to the routine.

## Appendix 4 Kustlijnveranderingen te Knokke-Heist in de afgelopen 50 jaar – Memo (deel 1)

In deze memo worden de kustlijnveranderingen te Knokke-Heist in de afgelopen ca. 50 jaar beschreven. Deze data-analyse is ter voorbereiding van de opmaak van een ShorelineS kustlijnmodel voor deze zone.

### **Kustlijnprogradatie**

De grootste kustlijnverandering die heeft plaatsgevonden was in 1977-79 toen de grootste strandsuppletie tot nu toe aan de Belgische kust werd uitgevoerd (ca. 8,5 miljoen m<sup>3</sup> zand aangebracht over een kuststrook van ca. 9 km, dwz ca 950 m<sup>3</sup>/m). Deze werken verliepen gelijktijdig met de uitbouw van de oostdam van de voorhaven van Zeebrugge die gerealiseerd werd in de periode 1977-1986 [Houthuys et al, 2022].

In de jaren na deze grote werken zijn ook kustlijnveranderingen opgetreden maar minder omvangrijk. Grosso modo is :

- de kustlijn die eind de jaren '70 is aangelegd in de decennia erna in stand gehouden door de uitvoering van onderhoudssuppletiewerken (vooral in het kustdeel Knokke-Zoute waar sterke kustlijnerosie optrad). De progradatie door de suppletie van 1977-79 bedroeg ca. 80 m ;
- de kustlijn in Heist-Duinbergen(-Albertstrand) verder zeewaarts geëvolueerd door een combinatie van suppletiewerken en sedimentatie in de luwte van de voorhaven van Zeebrugge. De progradatie bedraagt er meer dan 100 m ;



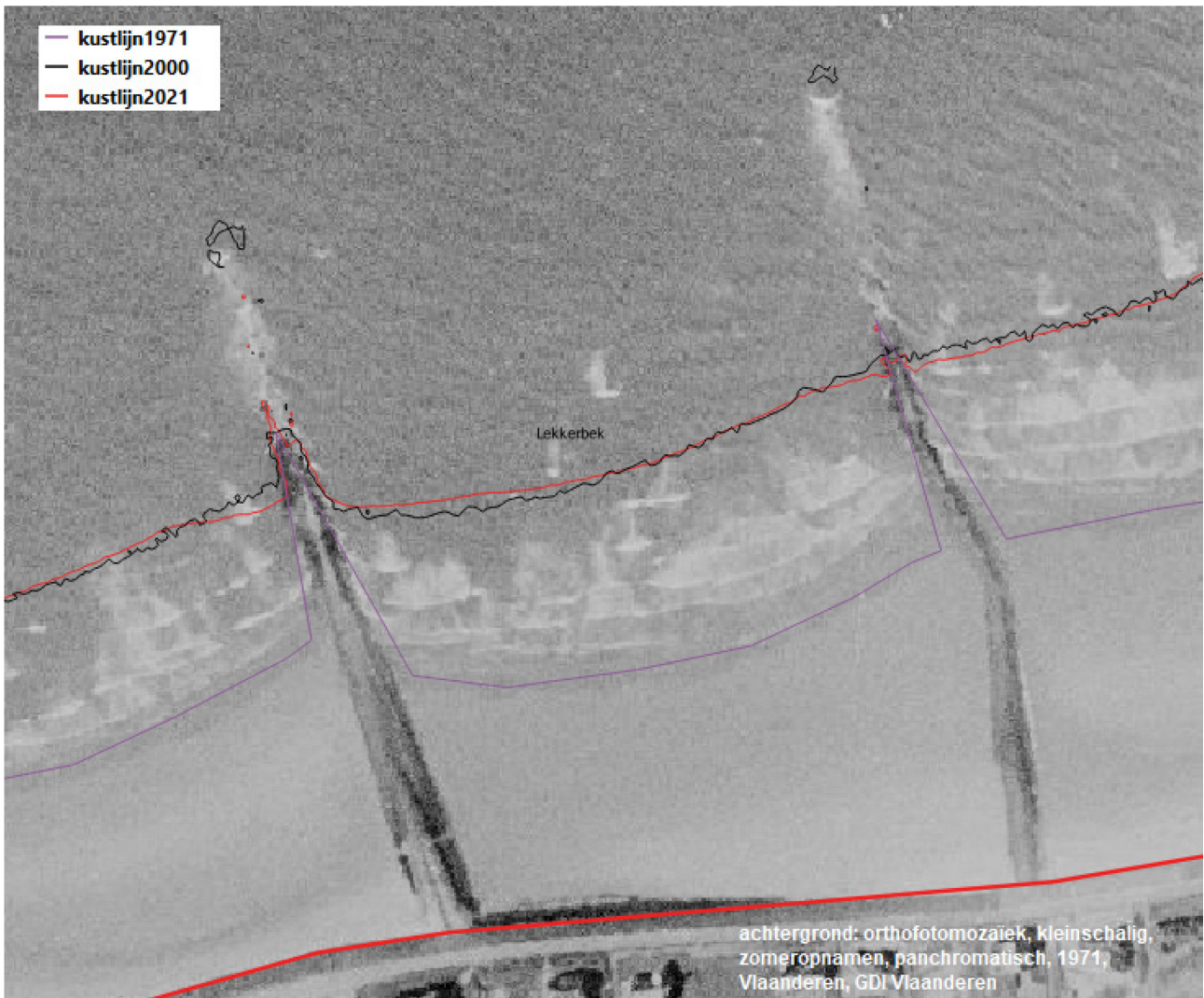
Figuur A4.1 De evolutie van de kustlijn (ca. +1.39 m TAW contour) te Knokke-Heist in de periode 1971-2021.

De kustlijnen op Figuur A4.1 illustreren de genoemde veranderingen.

De kustlijnen anno 2000 en anno 2021 zijn gebaseerd op de nauwkeurige DEMs (2 m x 2 m resolutie) die afgeleid zijn van de LIDAR data van de kustmonitoring die uitgevoerd wordt door afdeling Kust. De positionele nauwkeurigheid hiervan is ca. 1 m.

De kustlijn anno 1971 is veel minder nauwkeurig want bekomen door digitalisatie van de overgang tussen droog en nat op kleinschalige orthofoto's (celgrootte 1 m x 1 m) beschikbaar voor Vlaanderen (te downloaden via [Kaart | Geopunt Vlaanderen](#)). De waterstand tijdens deze opname is geschat op 1.35 m TAW +/- 0.05 m (zie bijlage). De positionele nauwkeurigheid bedraagt 10 m (of meer) hetgeen bepaald wordt door de onzekerheid bij het digitaliseren van de land-water overgang. Figuur A4.2 illustreert dit.

Essentieel voor de onderlinge vergelijking in het licht van de morfologische evolutie is dat de drie kustlijnen dezelfde hoogtecontour weergeven, namelijk +- de 1.39 m TAW. Dit feit wordt bevestigd door de samenvallende ligging van deze kustlijnen ter plaatse van de uiteinden van de strandhoofden. Zie ter illustratie Figuur A4.2.



Figuur A4.2 De samenvallende ligging van de drie kustlijnen 1971, 2000, 2021 ter hoogte van de uiteinden van de strandhoofden bevestigt dat ook de 1971-kustlijn representatief is voor de +1.39 m TAW contour. Hier een voorbeeld te Lekkerbek. De afstand tussen de twee strandhoofden is ca. 250 m.



Figuur A4.3 Overzicht van de uitgevoerde suppleties in de periode 1977-2021.

### ***Uitgevoerde suppletiewerken***

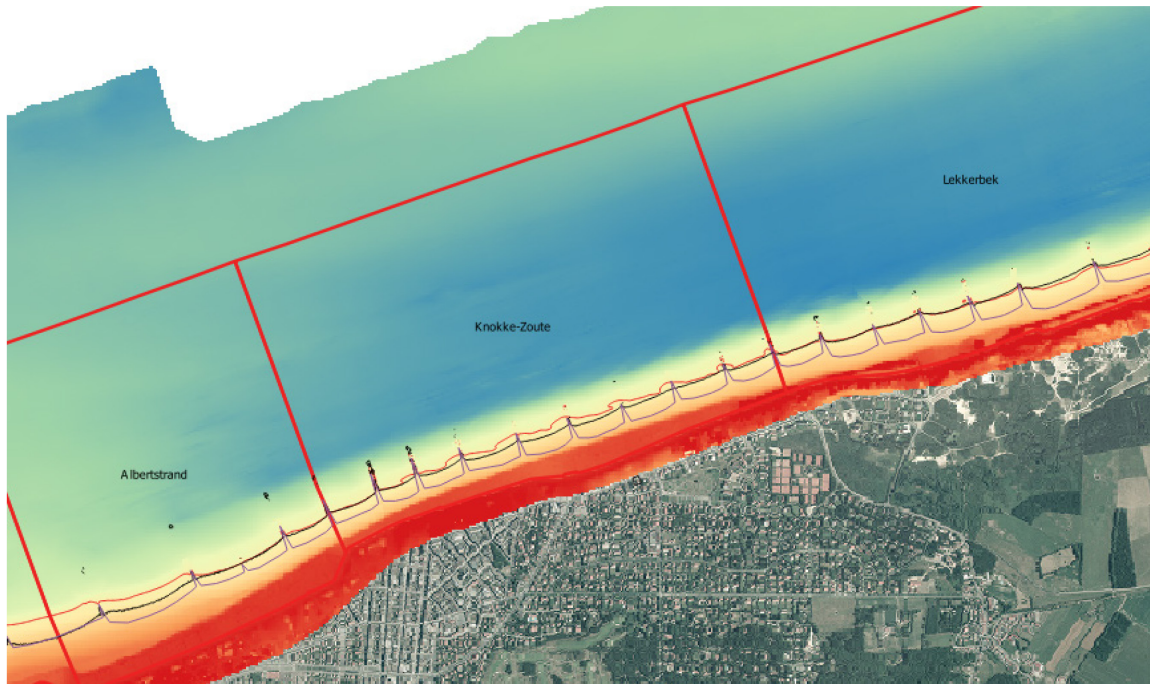
Gegevens uit Houthuys et al, 2022 werden aangevuld met de cijfers voor 2020 en 2021 bekomen van afdeling Kust (GIS-bestanden “zandaanvoer” waarin per jaar cijfers over zandwerken zijn gedocumenteerd). Een overzicht van de uitgevoerde suppletiewerken sinds 1977 wordt gegeven op Figuur 3.

Globaal kan men onderscheid maken tussen:

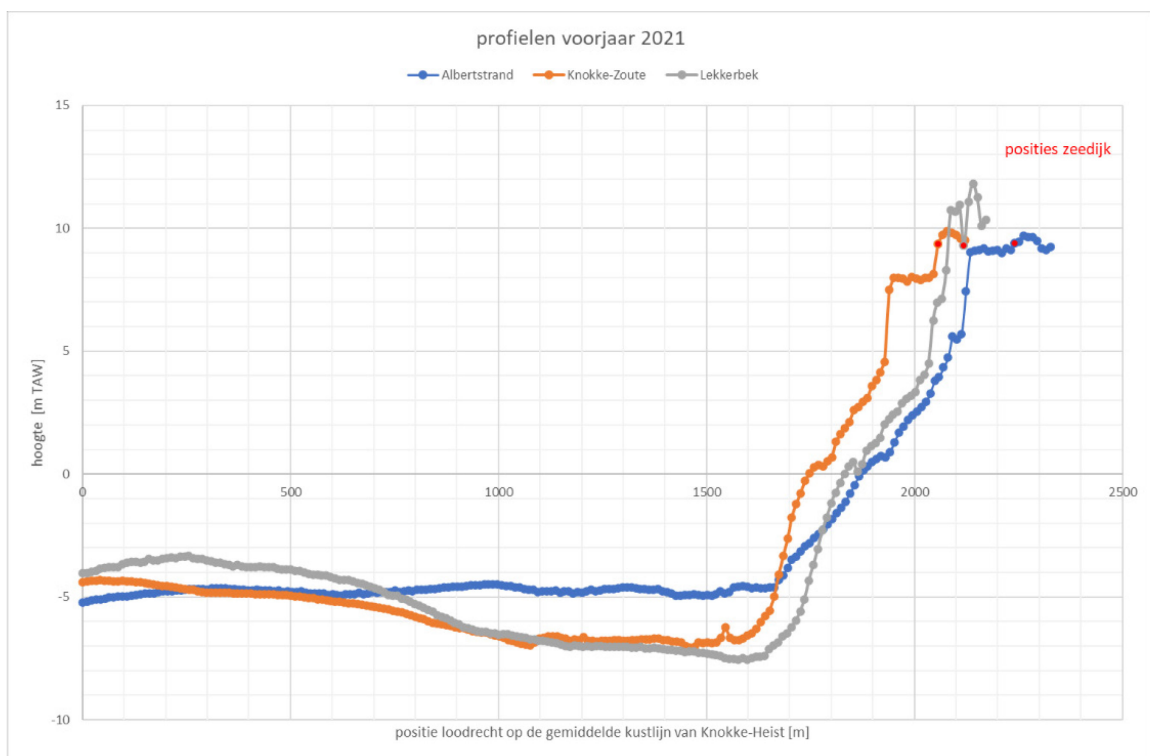
- de suppletie van 1977-79, met de grootste intensiteit (950 m<sup>3</sup>/m), en met de grootste uitgestrektheid (heel het studiegebied uitgezonderd thv het Zwin; een kustlengte van ca. 9 km). Hiermee werd de huidige kustlijn van Knokke-Heist gerealiseerd;
- zandaanvoer in het kustdeel Heist, door enkele suppleties in de periode 1986-2012, met een significante totale intensiteit (658 m<sup>3</sup>/m over een kustlengte van 972 m). Deze aanvoer versnelde de natuurlijke accumulatie in het sedimentatiegebied in de luwte van de oostdam;
- zandaanvoer in de regio rond Duinbergen (deels in kustdeel Duinbergen, deels in kustdeel Alberstrand), door enkele suppleties in de periode 2003-2021, met een significante totale intensiteit (444 m<sup>3</sup>/m over een kustlengte van 2400 m);

intense zandaanvoer in het kustdeel Knokke-Zoute (en soms aangrenzende secties), met een intensiteit per jaar van gemiddeld 37 m<sup>3</sup>/m/jaar over een kustlengte van 2237 m gedurende de afgelopen 41 jaar (dit is in het totaal 1500 m<sup>3</sup>/m over een kustlengte van 2237 m). Hiermee werd de kustlijnerosie sinds 1980 in dit kustdeel tegengegaan. In dit kustdeel is veruit het meeste zand aangevoerd van het hele studiegebied. De belangrijkste reden hiervoor is wellicht de vooruitgeschoven ligging van dit kustdeel waardoor langtransportverlies naar de naburige kustdelen optreedt. De relatief sterke getijstromingen door de nabijheid van de Appelzak hebben daarbij een significant effect op het langtransport. Een ander stuk van de verklaring is dwarstransportverlies naar de Appelzakgeul. Deze geul bevindt zich het dichtst bij het strand in het kustdeel Knokke-Zoute en in het kustdeel Lekkerbek. Ter illustratie Figuren A4.4, A4.5 en A4.6.

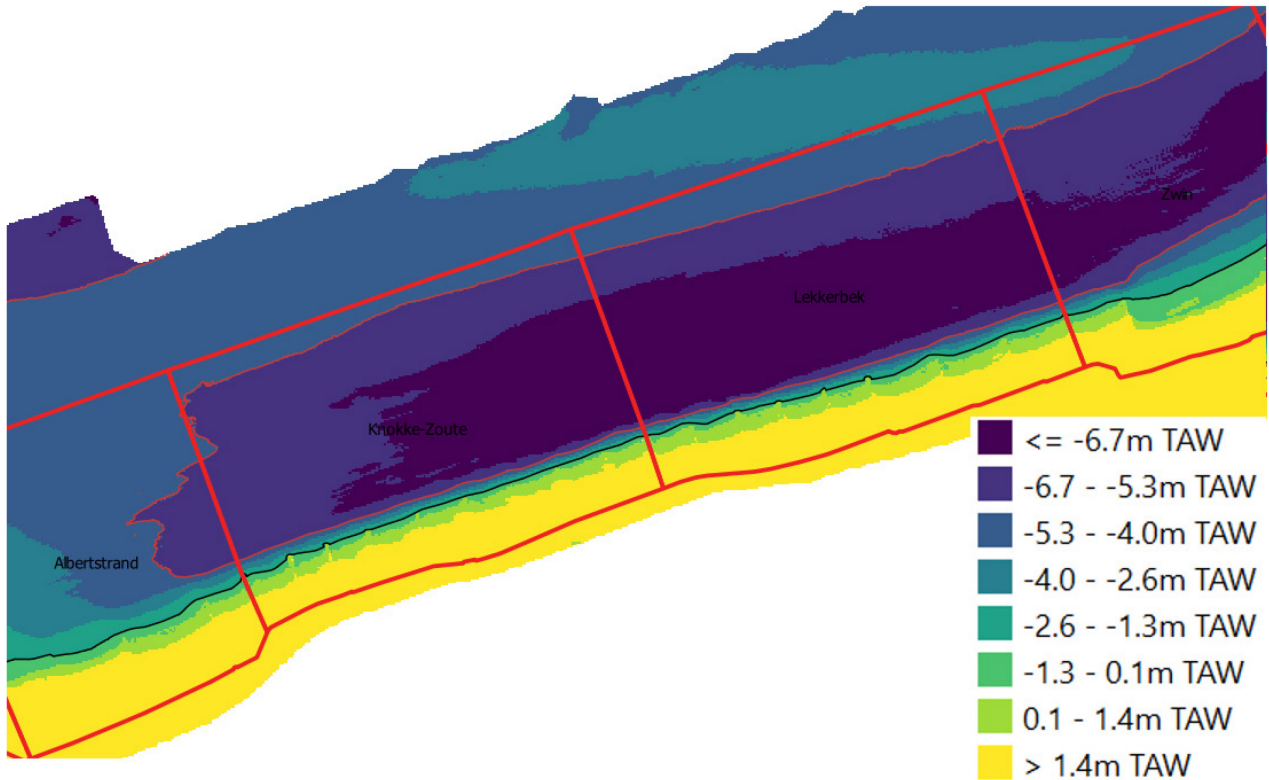
Door hindcasting met een ShorelineS kustlijnmodel zal het relatieve aandeel van de twee genoemde processen onderzocht worden (enerzijds differentieel langsport, anderzijds dwarstransport). Ook zal het relatief belang van de getijstromingen tov het golfklimaat voor het langtransport onderzocht worden.



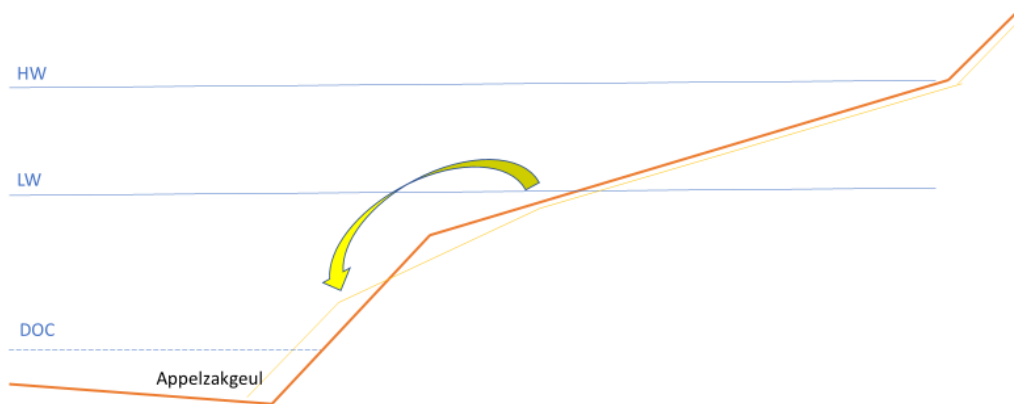
Figuur A4.4 Het kustdeel Knokke-Zoute heeft een vooruitgeschoven ligging tov de naburige kustdelen. In dit kustdeel ligt de Appelsakgeul het dichtst bij het strand.



Figuur A4.5 Profielen genomen in het midden van de kustdelen Albertstrand, Knokke-Zoute en Lekkerbek, van het DEM voorjaar2021 (g\_vo2021\_1). De landwaartse rand van de Appelsakgeul is gesitueerd rond  $x=1600$  à  $1700$  m. De zeedijk in het kustdeel Knokke-Zoute bevindt zich rond  $x=2060$  m, significant meer zeewaarts dan in de naburige kustdelen ( $x=2120$  m in Lekkerbek en  $x=2240$  m in Alberstrand). Analoog voor de zeewaartse rand van de droogstrandberm (in Knokke-Zoute rond  $x=1940$  m; in Lekkerbek ca. 100 m meer landwaarts, in Alberstrand ca. 200 m meer landwaarts). In kustdeel Lekkerbek bevindt er zich een duin voor dijk. In de andere twee kustdelen een horizontaal strandplateau. In de kustdelen Knokke-Zoute en Lekkerbek is de helling van de vooroever steiler dan de helling van het intertidaal strand; dit lijkt een gevolg van een tendens van de Appelsakgeul om er landwaarts uit te breiden.



Figuur A4.6 Morfologie van de kust nabije zeebodem in het oostelijke deel van het studiegebied (DEM voorjaar 2021, g\_vo2021\_1). Het diepste deel van de Appelszak (< -6.7 m TAW) bevindt zich in de kustdelen Knokke-Zoute, Lekkerbek, Zwin (en verder in NL).



Figuur A4.7 Veronderstelde mechanisme van dwarstransport verlies uit de actieve zone naar de Appelszakgeul, in kustdelen Knokke-Zoute en Lekkerbek. Nadat materiaal in de Appelszakgeul beland is, wordt het door de langse getijstroomingen in de geul weggevoerd naar elders. Dit proces veroorzaakt kustlijnachteruitgang in de kustdelen Knokke-Zoute en Lekkerbek. De omvang van dit proces is echter onbekend. De precieze mechanismen zijn niet bekend maar men kan aannemen dat de golfwerking de drijvende kracht is achter dit dwarstransport.

De steilste helling van de lagere vooroever (tussen -1.3 m TAW en -5.3 m TAW) bevindt zich op de grens van de kustdelen Knokke-Zoute en Lekkerbek. De “morfologische interactie” tussen de Appelszak en de strandzone lijkt even sterk te zijn in beide deze kustdelen, geleidelijk afnemend wanneer de afstand tot de grens van beide kustdelen groter wordt. Het feit dat er in Lekkerbek relatief t.o.v. Knokke-Zoute geen al te grote suppletie-inspanningen zijn geleverd moeten worden in de afgelopen decennia om de kustlijn in stand te houden doet vermoeden dat het mechanisme van zandverlies door dwarstransport over de grens van de “depth of closure” (rond de - 5 m TAW) van secundair belang is als proces relatief t.o.v. het proces van differentieel langstransport. Het mechanisme van dwarstransportverlies wordt verondersteld het gevolg te zijn van de steile helling van de vooroever ( $\sim 1/15$ ), die veroorzaakt wordt door de aanwezigheid van de

Appelzak getijdegeul en die maakt dat er een onbalans is tussen enerzijds de cross-shore landwaartse processen en anderzijds de cross-shore zeewaartse processen. In een evenwichtsprofiel zijn beide processen van gelijke grootte zodat er geen netto dwarstransport plaatsvindt, maar in casu is een netto verlies zeewaarts plausibel. Het veronderstelde mechanisme wordt geïllustreerd op Figuur A4.7.

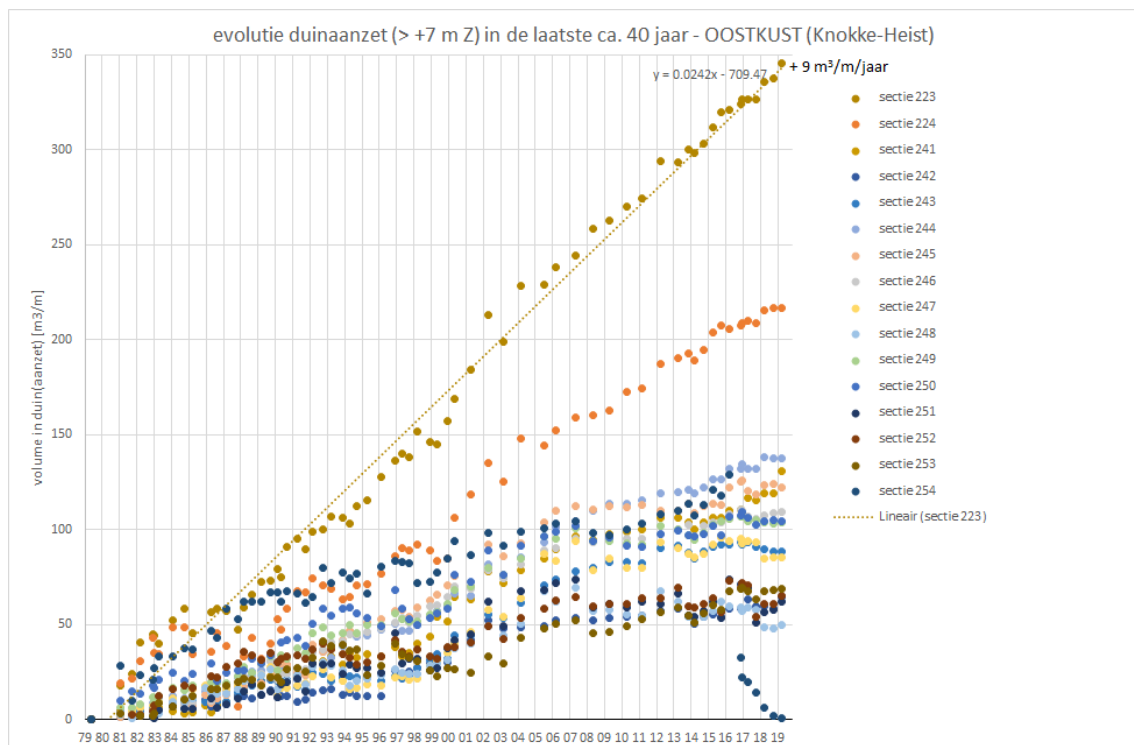
### Duingroei

In twee deelgebieden is er een duingroei opgetreden in de laatste 40 jaar:

- een kleine zone te Duinbergen (secties 223-224)
- een langere zone van Lekkerbek tot aan het Zwin (secties 241-254)

Deze duingroei is kunnen gestaag doorgaan dankzij de beschikbaarheid van zand (vooral via de uitgevoerde suppletiewerken; deels ook via natuurlijke aanvoer nl in de luwte van de oostdam).

De evolutie in de tijd hiervan is getoond op Figuur A4.8.



Figuur A4.8 Duingroei in twee deelgebieden 1) Duinbergen (secties 223-224) en 2) Lekkerbek-Zwin. NB de afname voor sectie 254 vanaf 2017 is veroorzaakt door het weggraven van duin als deel van de uitbreiding van het Zwin.

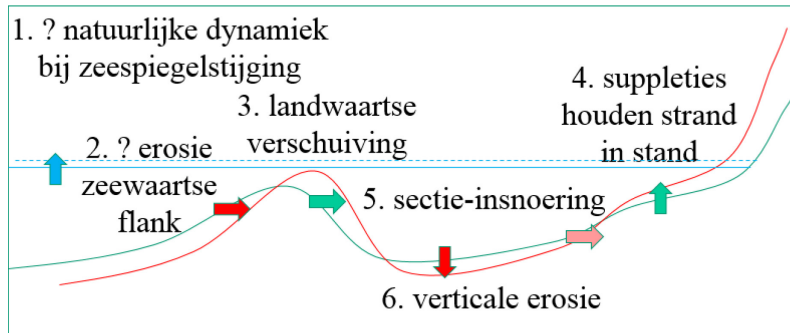
Bij deze duingroei is zand onttrokken aan de strandzone, dit wil zeggen kustlijnachteruitgang als gevolg. Een duingroei van b.v. 9 m<sup>3</sup>/m/jaar resulteert in een kustlijnachteruitgang van ca. 0.9 m/jaar (rekening houdend met een actieve hoogte van 10 m). Dit effect gaat dus over decimeters per jaar kustlijnachteruitgang.

### Effect zeespiegelstijging op kustlijnachteruitgang

Volgens de hypothese uit de Bruun regel dat een evenwichtsprofiel in de actieve zone meegroeit met de zeespiegel zou ten gevolge van de 2.4 mm/jaar zeespiegelstijging gedurende de afgelopen 40 jaar de kustlijn achteruit gaan, moesten er geen andere processen en ingrepen gebeurd zijn. De mate van achteruitgang is evenredig met de snelheid van zeespiegelstijging en omgekeerd evenredig met de helling van het actieve

profiel. Met een (gemiddelde) helling 1/30 komt een kustlijnachteruitgang overeen van 0.07 m/jaar. Dit effect gaat dus over centimeters per jaar kustlijnachteruitgang. Het zal belangrijker worden igv een doorgaande versnelling van de zeespiegelstijging.

Belangrijker wellicht voor het risico van kustlijnachteruitgang te Knokke-Heist is het feit dat in hypothese een verdere verdieping en landwaartse beweging van de Appelzak verwacht wordt. Mogelijks is dit een gevolg van de zeespiegelstijging, mogelijks ook niet. In elk geval volgt uit de observaties van de afgelopen decaden dat de Appelzakgeul verdiept en een tendens heeft om landwaarts te bewegen, gelinkt met een landwaartse beweging van de Paardemarkt zandbank. De gemeten verdieping van de Appelzak in kustdelen Knokke-Heist en Lekkerbek bedraagt orde van grootte 1 m in de laatste 30 jaar. Figuur A4.9 uit Houthuys et al, 2022 ter illustratie.



Figuur A4.9 Hypothese van trage morfodynamiek van de geul-bank complexen langs de Belgische kust. De trage morfodynamiek van Appelzakgeul – Paardemarkt bank is mede bepalend voor de kustlijndynamiek in Knokke-Heist.

### **Besluit**

Het kustdeel Knokke-Zoute is een hot spot van structurele kusterosie aan de Belgische kust, sinds de grote werken van havenuitbreiding en stranduitbreiding eind de jaren '70 – begin de jaren '80 van de vorige eeuw.

Dit kan in eerste instantie worden verklaard door de zeewaartse ligging van de kustlijn in dit kustdeel, wanneer we deze vergelijken met de ligging in de naburige kustdelen. Immers, dergelijke zeewaartse ligging veroorzaakt zandverlies naar de omgeving ten gevolge van gradiënten in langtransport.

Een tweede, minder belangrijk veronderstelde oorzaak is het optreden van dwarstransportverlies van de actieve zone richting zee, hetgeen veroorzaakt wordt door de nabijheid van de Appelzakgeul. Deze geul heeft het strand- en vooroeverprofiel verstoord, namelijk de diepere vooroever is versteild.

De trage evolutie van verdieping van de Appelzakgeul (gelinkt met een landwaartse trend van de Paardemarkt zandbank) versterkt beide bovengenoemde processen. Er wordt verwacht dat hierdoor de suppletiebehoefte in de komende decennia zal toenemen, additioneel t.o.v. wat nodig zal zijn om mee te groeien met de zeespiegel (~ Bruun regel).

### **Evaluatie in het kader van adaptatie aan zeespiegelstijging (Kustvisie)**

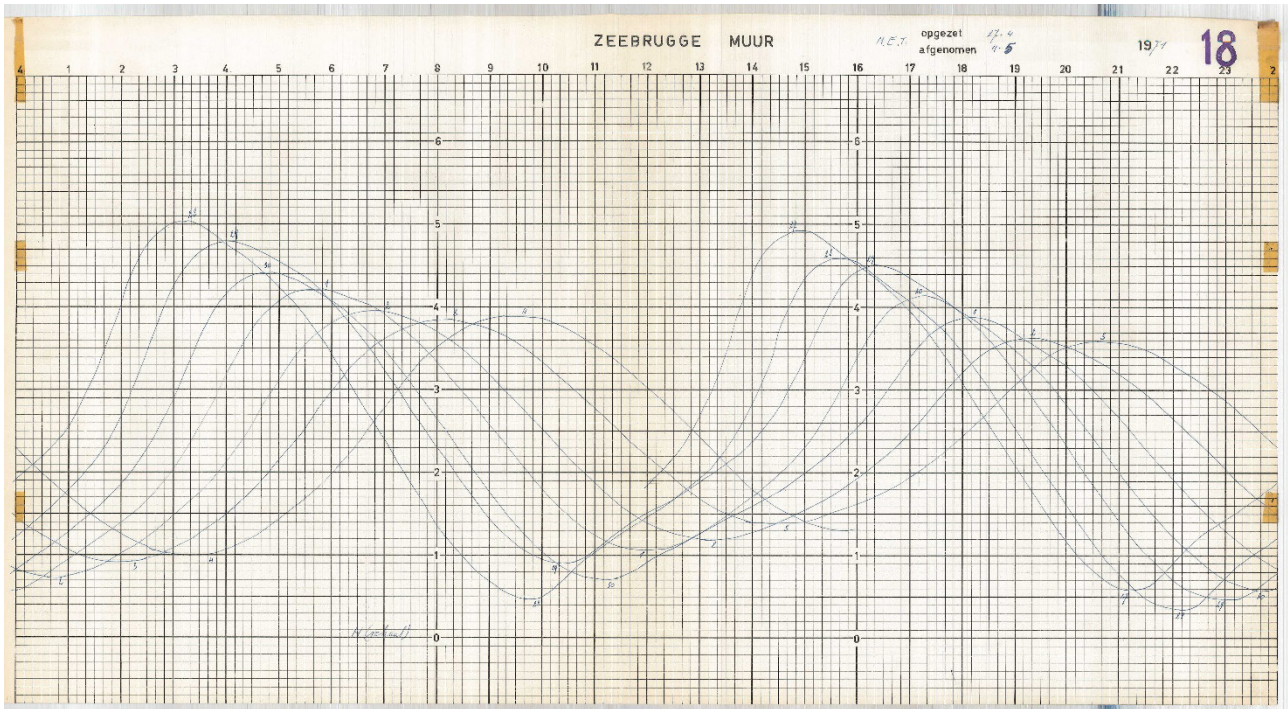
Omdat Knokke-Zoute een hot spot is van kustlijnerosie kan worden aanbevolen om in dit kustdeel Knokke-Zoute de target kustlijn minder sterk te doen afwijken van de target kustlijnen in de naburige kustdelen. In concreto kan dit betekenen om "hold the line" te ambiëren voor Knokke-Zoute ("kustlijn 2"), terwijl in de naburige kustdelen progradatie geambieerd wordt ("kustlijn 3").

Beschouwen we in het volledige studiegebied de suppletie van 1977-79 als een case van kustlijnadaptatie ("kustlijn 3"), dan kunnen we hiervoor stellen dat voor deze progradatie met orde van grootte 100 m een initiële zandaanvoer nodig was van orde van grootte ca. 1000 m<sup>3</sup>/m en dat dit in stand gehouden diende te worden door een gemiddeld onderhoud ten bedrage van ca. 500 m<sup>3</sup>/m over 41 jaar (gemiddeld 12

m3/m/jaar). De zeespiegelstijging opgetreden in de afgelopen 41 jaar bedroeg ca. 2.4 mm/jaar [Monbaliu et al, 2020].

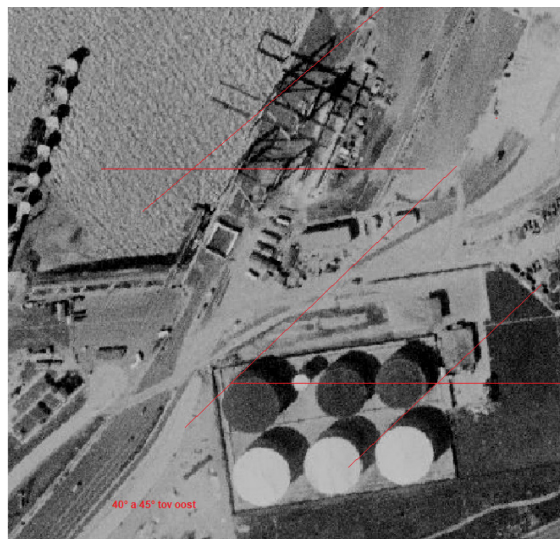
### Schatting van de waterstand tijdens de opname van de luchtfoto's op 2/5/1971

Het verloop van de waterstand op die dag is gekend dankzij de registratie door de maregraaf in de haven van Zeebrugge.

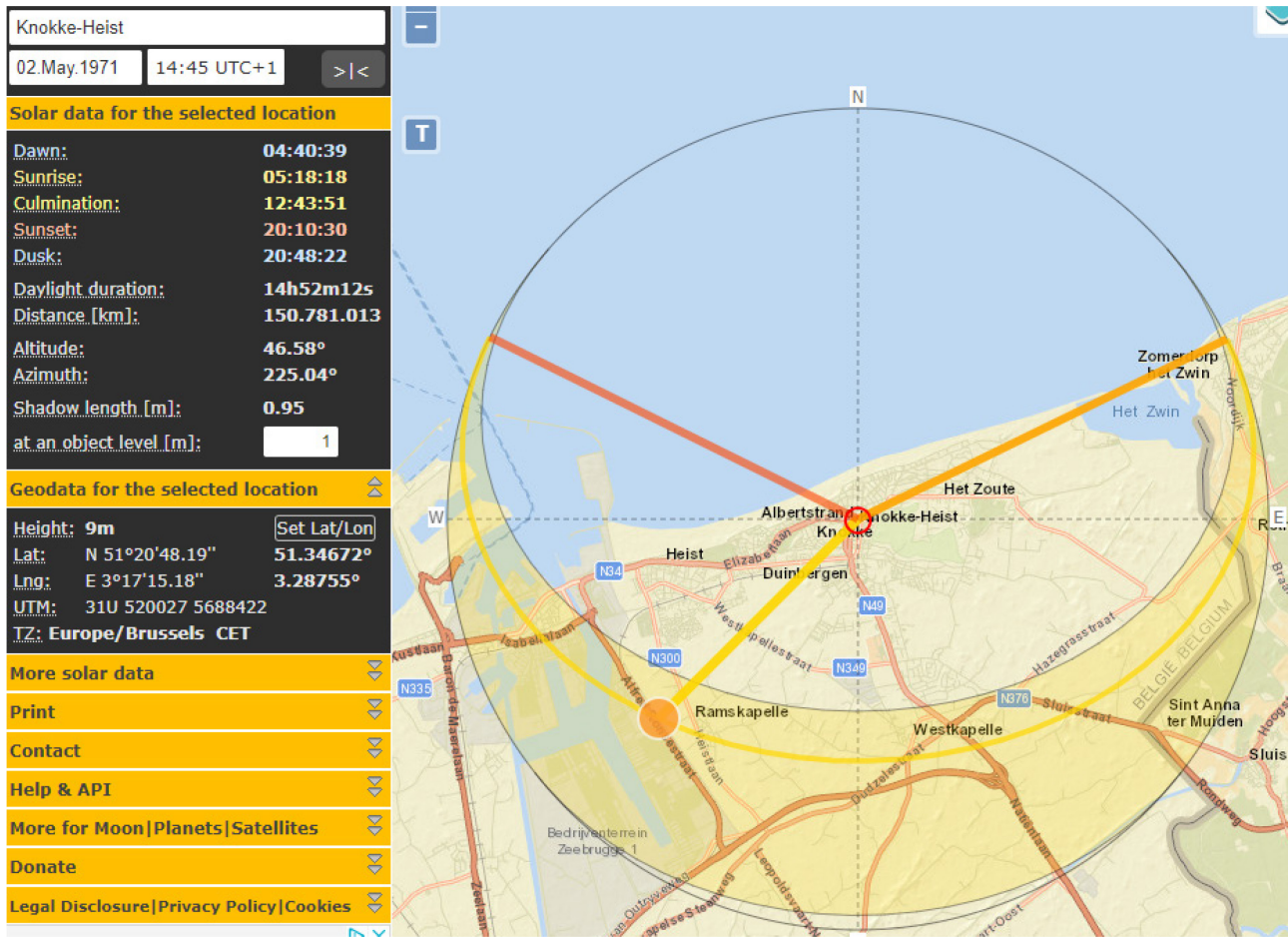


Figuur A4.10 Maregraafblad Zeebrugge.

Het tijdstip van de opname van de luchtfoto's kan geschat worden door de horizontale richting van de zonnestrallen te meten aan de hand van de richting van de schaduw die hoge verticale objecten werpen op het maaiveld (horizontaal). Hierbij is gebruik gemaakt worden van de tool op [www.suncalc.org](http://www.suncalc.org) waarin voor een willekeurige positie op aarde de richting van de zonnestrallen ivf de tijd gegeven wordt. Ter illustratie van de procedure hieronder een voorbeeld voor een beeld van de haven van Zeebrugge.



Figuur A4.11 Bepaling van de horizontale richting van de zonnestrallen voor de locatie "haven Zeebrugge". Resultaat in dit geval: 40° à 45° tov oost.



Figuur A4.12 Bepaling van het tijdstip horend bij een gegeven horizontale richting van de zonnestrallen ([www.suncalc.org](http://www.suncalc.org)) te Knokke-Heist.

Resultaat in het geval van de locatie “haven Zeebrugge”: 14u45 à 15u00 UTC+1

Deze werkwijze werd gevolgd voor verschillende andere locaties in het studiegebied. De luchtfoto's in het studiegebied zijn immers niet allemaal op hetzelfde moment genomen.

Overzicht van de resultaten:

locatie	Richting zonnestrallen	Tijdstip
Haven Zeebrugge	40° à 45° tov oost	14u45 à 15u00 UTC+1
Duinbergen-Albertstrand	38° tov oost	15u10 UTC+1
Knokke-Zoute	39° tov oost	15u05 UTC+1

Samengevat, de foto's zijn genomen in de periode 14u45 à 15u15 UTC+1.

Op de getijcurve komt dit overeen met een waterstand van 1.5 à 1.6 m H = 1.3 à 1.4 m TAW (NB: UTC+1=MET en het H-vlak ligt 19 cm onder het TAW-vlak te Zeebrugge). Het was opkomend tij.

Deze kustlijn is dus quasi dezelfde contour als de +1.39 m TAW kustlijn.

## Appendix 5 Kustlijnveranderingen te Knokke-Heist in de afgelopen 50 jaar – Memo (deel 2)

In deze memo worden de kustlijnveranderingen te Knokke-Heist beschreven. Deze data-analyse is ter voorbereiding van hindcasting van relatief korte periodes met ShorelineS.

### **Beschikbare data**

Als eerste is de periode 1999-2004 geselecteerd omdat 1) het een periode betreft met relatief weinig zandwerken in het gebied en 2) relatief veel beschikbare topobathymetrische data.

In maart-mei 1999 werd te Knokke-Zoute (secties 233-243) een onderhoudssuppletie uitgevoerd ten bedrage van 413500 m<sup>3</sup> effectief in-situ. In juni 2004 werd in ongeveer hetzelfde gebied (secties 232-243) 331400 m<sup>3</sup> effectief in-situ aangebracht. In de tussenperiode werd in het studiegebied (Knokke-Heist) slechts zeer beperkte zandwerken uitgevoerd. Enkel in Duinbergen-centrum (secties 224-226) werd het droog strand in stand gehouden door jaarlijkse zandwerken in het voorjaar (badstrandverhogingen): in de periode 1999-2003 was het zand voor de badstrandophoging afkomstig van afgraving nabij de laagwaterlijn; in de periode 2003-2004 werd extern zeezand aangevoerd. Deze zandwerken beïnvloeden de ligging van de kustlijn in deze zone van Duinbergen-centrum waardoor het niet mogelijk is om de output van de kustlijnmodellering te vergelijken met de opgemeten kustlijnen in dit gebied. Ref: Houthuys et al, 2022.

Strandopnames zijn uitgevoerd enerzijds door Eurosense en anderzijds door VITO. De als DEM beschikbare data zijn opgelijst in onderstaande tabel.

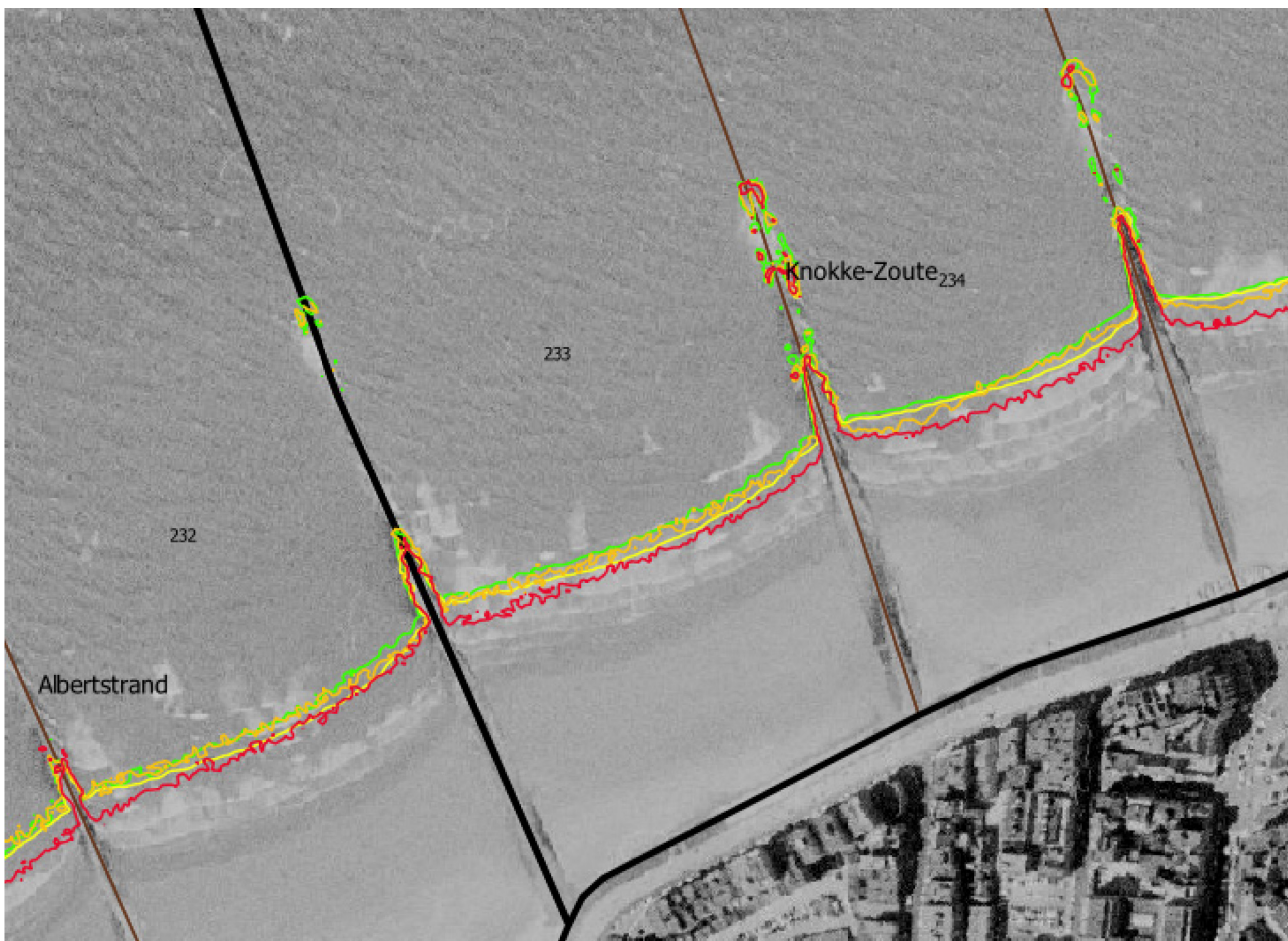
Datum opname	Uitvoerder	DEM
06-06-1999	Eurosense	Puntenwolk beschikbaar bij aKust
11-01-2000	Eurosense	Puntenwolk beschikbaar bij aKust
16-6-2000	Eurosense	Puntenwolk beschikbaar bij aKust
11-09-2000	VITO	G_2000_2 <sup>E</sup>
10-05-2001	Eurosense	G_2001_1 <sup>E</sup>
28-09-2001	VITO	G_2001_2 <sup>E</sup>
12-05-2002	Eurosense	Puntenwolk niet beschikbaar
18-12-2002	VITO	G_2002_2 <sup>E</sup>
14-04-2003	Eurosense	Puntenwolk niet beschikbaar; wel hoogtelijnen (DXF bestand)
17-04-2004	Eurosense	Puntenwolk niet beschikbaar

### Kustlijnevolutie

Voor alle beschikbare DEMs (1 m x 1 m rasters) werd de +1,39 m TAW kustlijn bepaald.

De evolutie in de tijd van deze karakteristieke kustlijn is niet-monotoon. Dat is het gevolg van enerzijds de seizoensale profieldynamiek (in de winter afslag op het droog strand en aangroei nabij de laagwaterlijn; in de zomer het omgekeerde) en anderzijds -vooral in de beginperiode- een aanpassing van het suppletieprofiel naar een meer natuurlijk profiel.

De kustlijnen afgeleid van de VITO-DEM's hebben een meer onregelmatig karakter in vergelijking met de kustlijnen afgeleid van de Eurosense-DEM's. Schaalniveau van deze onregelmatigheden is 1 à 10 m. Voor analyse van de kustlijnevolutie op tijdschaal jaren zijn gesmoothened kustlijnen gewenst, omdat morfologische variaties op schaalniveau 1 à 10 m buiten scope zijn van deze analyse. Zie ter illustratie onderstaande figuur: gele kustlijn (2001) op basis van Eurosense-data, versus groene (2000), oranje (2001) en rode (2002) kustlijnen op basis van VITO-data.

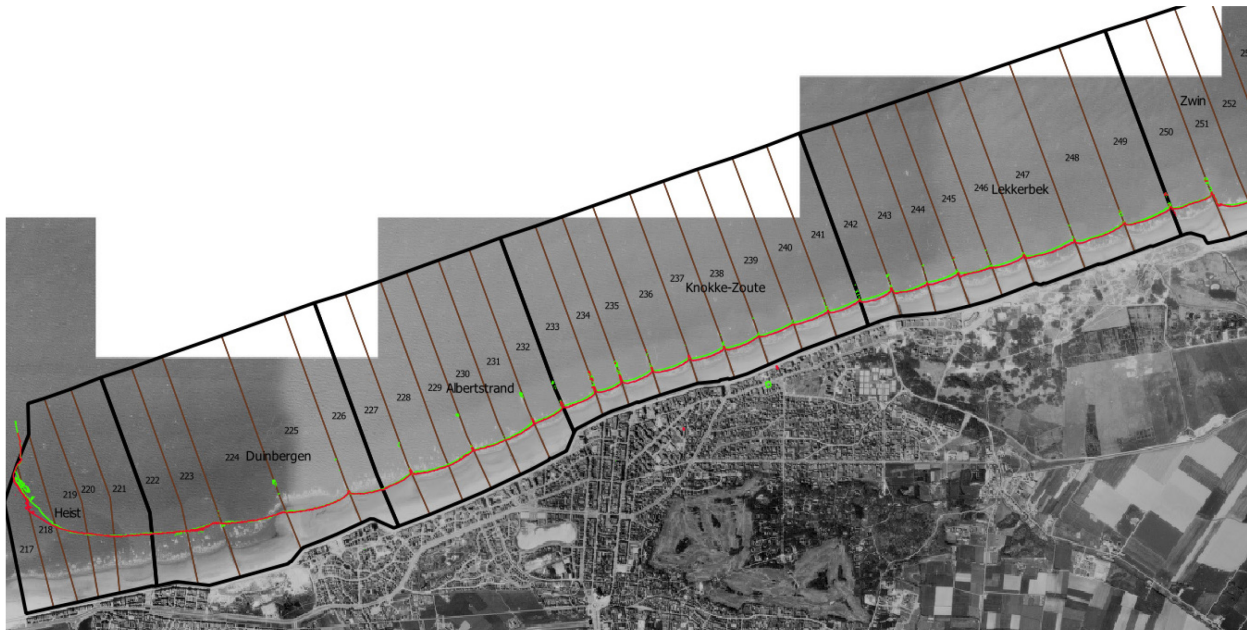


Op bovenstaande figuur merkt men ook op dat de kustlijn in een sectie tussen twee strandhoofden een boogvorm heeft (typisch bevindt zich de kustlijnpositie ter hoogte van strandhoofden 10 à 30 m meer zeewaarts dan in het midden tussen twee strandhoofden).

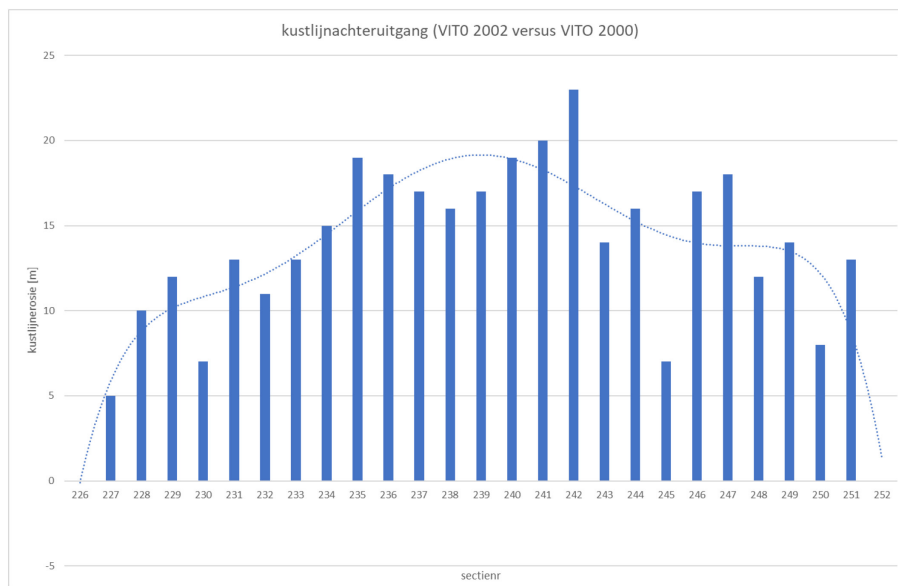
Op basis van het verschil in kustlijnligging van de VITO-data uit enerzijds 2000 en anderzijds 2002 (zie figuur hieronder), blijkt er in die periode van 2 jaar kustlijnerosie opgetreden te zijn te:

- lokaal vlak tegen de oostelijke havendam (secties 217-218)
- in een groot gebied thv de kustdelen Albertstrand, Knokke-Zoute en Lekkerbek

In de overige zones bleef de kustlijn ongeveer op positie (~stabiliteit).

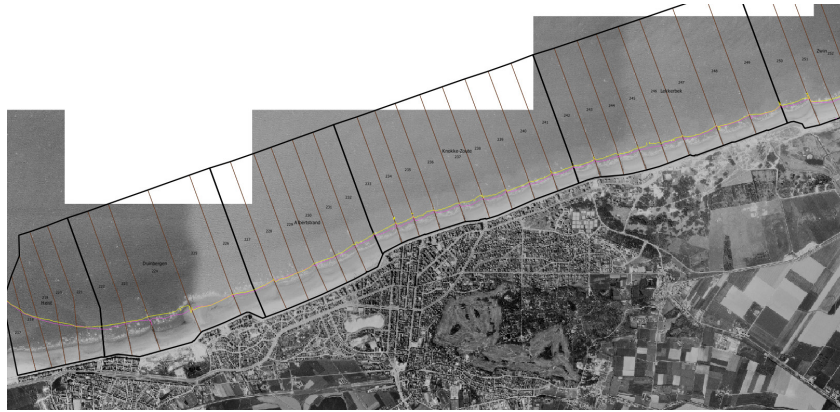


De grootte van deze kustlijnachteruitgang 2000-2002 in het gebied Albertstrand-Knokke-Zoute-Lekkerbek varieert. Zie onderstaande figuur.

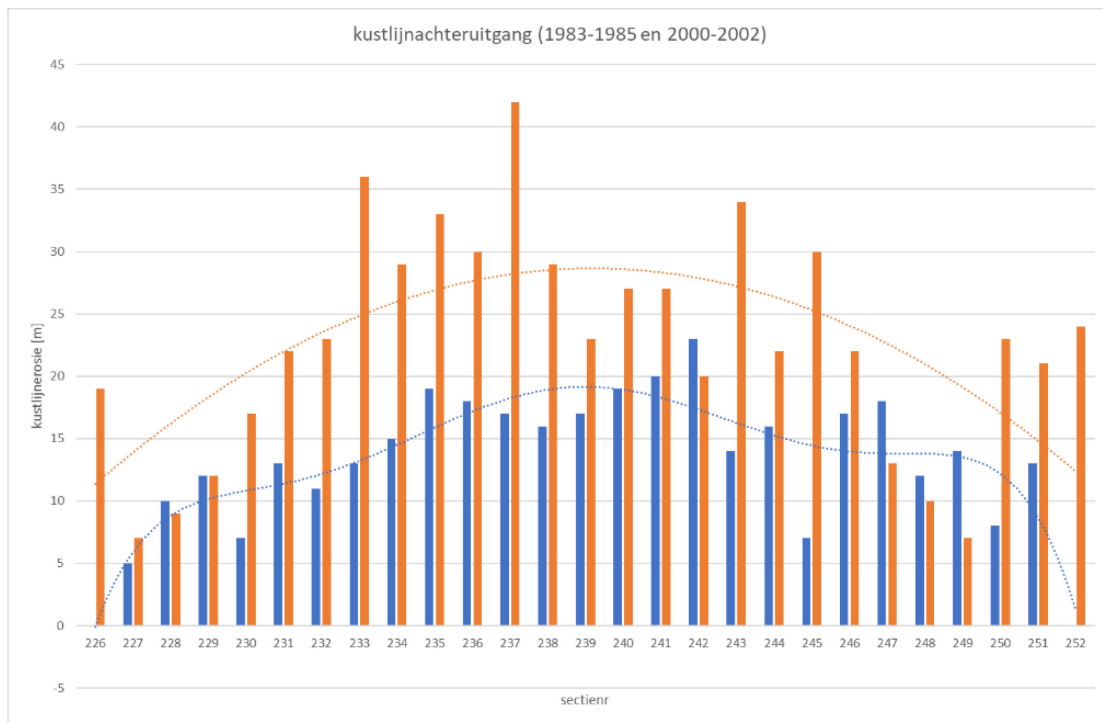


De grootste kustlijnachteruitgang trad op in de zone 234-247 (~kustdeel Knokke-Zoute + gedeelte Lekkerbek).

Ter vergelijking wordt de kustlijnevolutie in de periode 1983-1985 (ook 2 jaar) hieronder weergegeven (gebaseerd op twee voorjaarsopnames door Eurosense). In deze periode waren er geen zandwerken in het studiegebied uitgezonderd mogelijks zandaanvoer vlak tegen de oostdam ikv de uitbouw van de voorhaven. De grote suppletie van 1977-79 was ca. 5 jaar eerder.



Men merkt in 1983-1985 een kustlijnachteruitgang in het gebied Albertstrand-Knokke-Zoute-Lekkerbek die min of meer vergelijkbaar is met wat hiervoor te zien was voor de periode 2000-2002 in hetzelfde gebied. Zie onderstaande grafiek.



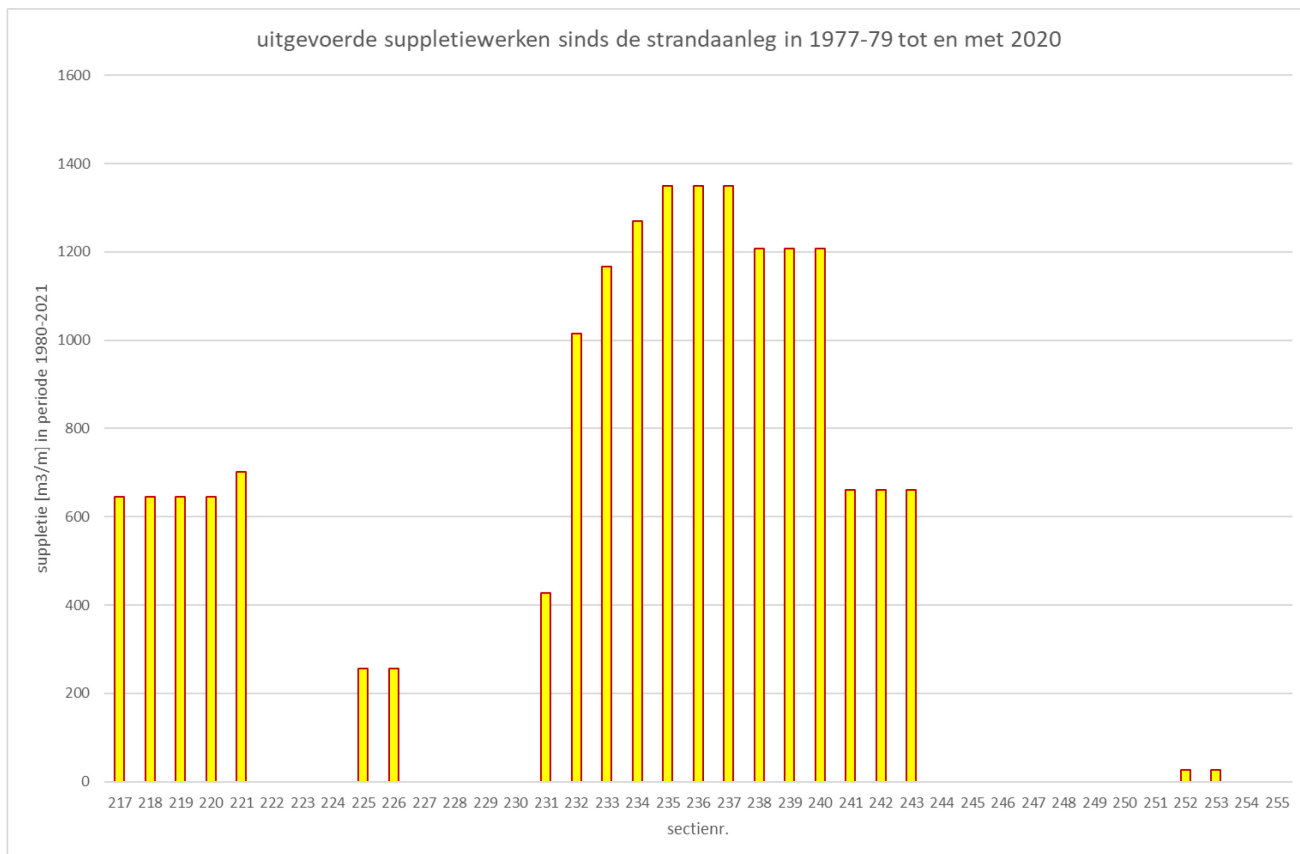
In de andere kustdelen Heist-Duinbergen en Zwin was er ook enige kustlijnachteruitgang in 1983-1985 (maar minder groot dan in Albertstrand-Knokke-Zoute-Lekkerbek), in tegenstelling tot +/- stabiliteit in deze zones in 2000-2002.

Mogelijk is er in de periode 1983-1985 een effect van ca. 10 m kustlijnachteruitgang in heel Knokke-Heist te wijten aan een dwarsprofiel-verandering t.g.v. de zomer-winter seizoenale cyclus.

De kustlijnachteruitgang was het grootst in de zone 233-245 (~kustdeel Knokke-Zoute + gedeelte Lekkerbek).

De zone met de grootste waargenomen kustlijnachteruitgang in zowel 2000-2002 als 1983-1985 komt grotendeels overeen met de zone waar er het meest gesuppleerd is in de periode nà 77-79 tot en met 2020.

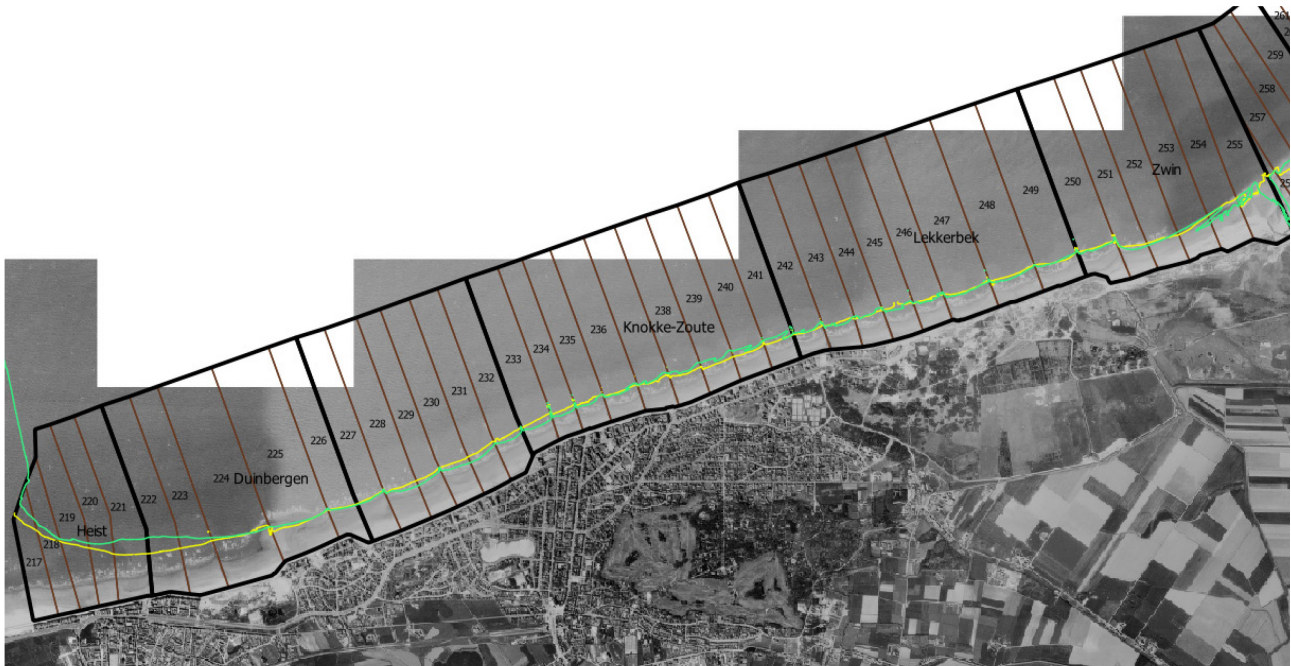
Er is het meest gesuppleerd in de zone 232-240 (~kustdeel Knokke-Zoute). Zie onderstaande grafiek.



Uiteraard hebben de uitgevoerde suppleties te kustdeel Knokke-Zoute ook de naburige kustdelen Albertstrand en Lekkerbek gevoed.

Het verschil in kustlijnen tussen enerzijds 4/2/1983 (gele lijn op figuur hieronder) en anderzijds 18/11/2020 (groene lijn op figuur hieronder) geeft aan dat er in deze periode netto :

- kustlijnprogradatie (~50 m) te noteren is in Heist + westelijk stuk Duinbergen ;
- kustlijnstabiliteit in oostelijke stuk Duinbergen ;
- kustlijnachteruitgang (~30 m) te noteren is in Albertstrand + westelijke stuk Knokke-Zoute ;
- kustlijnprogradatie (~30 m) te noteren is in oostelijke stuk Knokke-Zoute ;
- kustlijnstabiliteit in Lekkerbek-Zwin ;



#### Interpretatie:

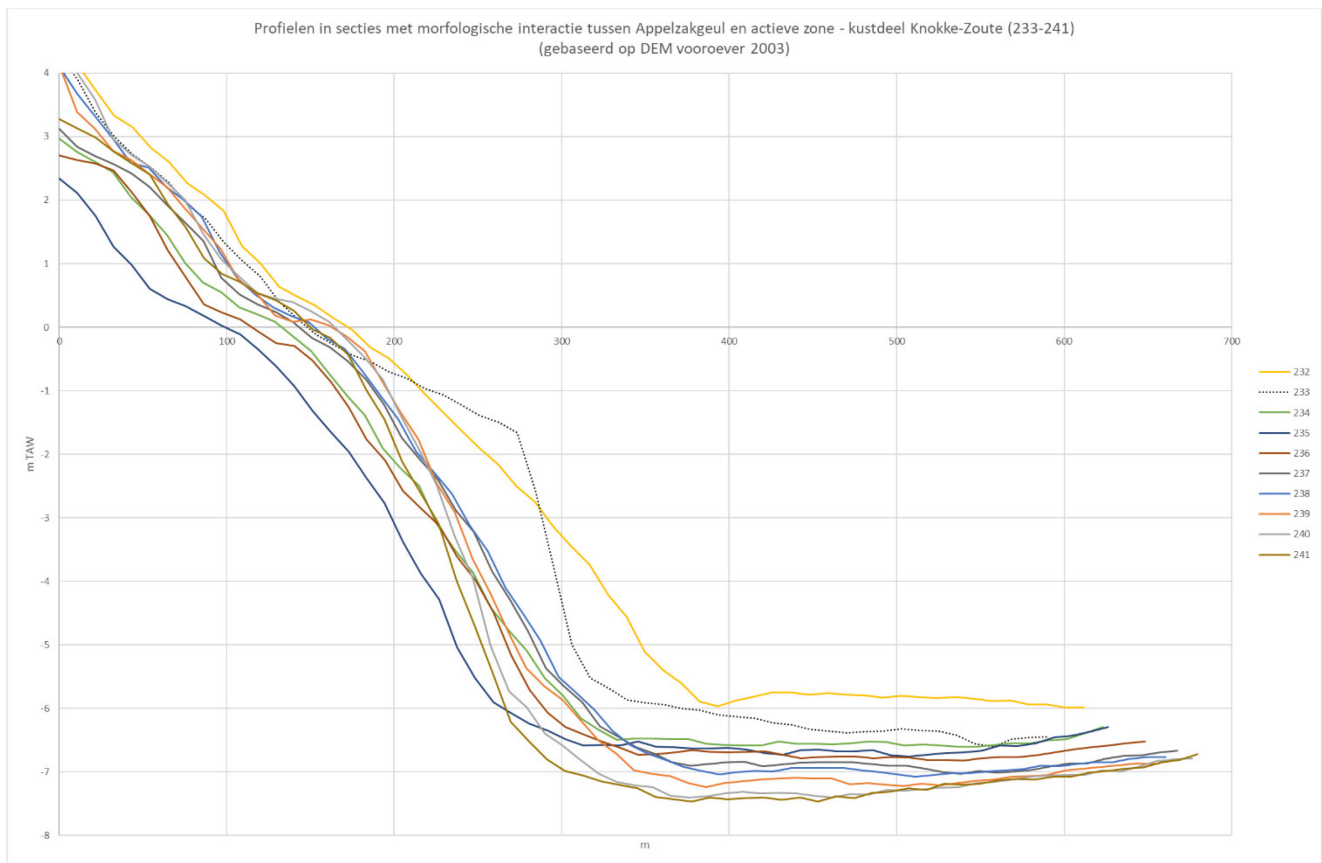
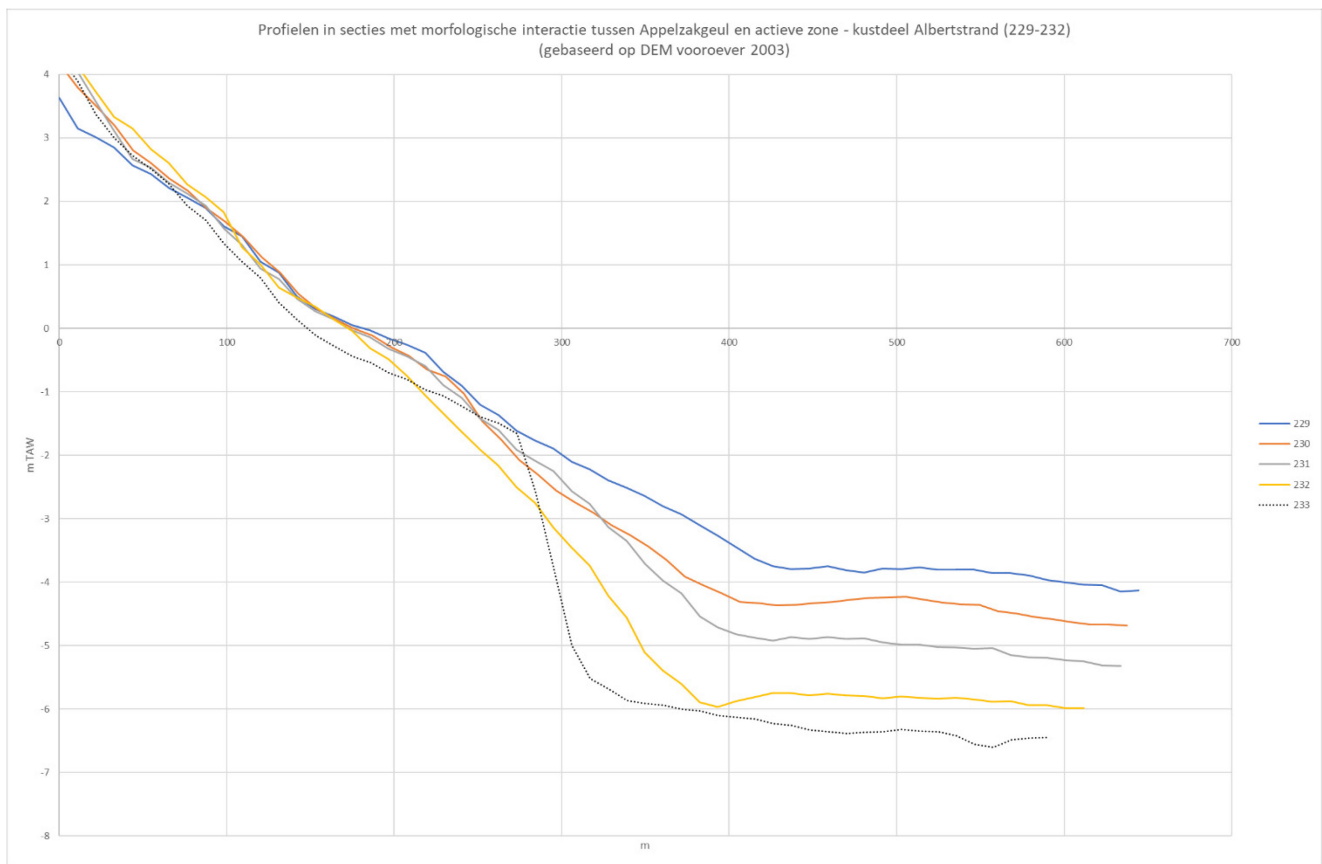
- de kustlijnvoortgang in de zone baai van Heist (~50 m) komt orde van grootte overeen met de uitgevoerde suppletiewerken in die zone (~650 m<sup>3</sup>/m) gedeeld door de actieve hoogte van het profiel (~10 m) ;
- de kustlijnachteruitgang in Albertstrand kan verklaard worden door de gradiënten in langtransport in die zone (dwarsverlies richting zee niet relevant in deze zone !) die niet voldoende gecompenseerd werden door voeding door suppletiewerken in de omgeving (Knokke-Zoute) ;
- het gemengd beeld in Knokke-Zoute is het netto resultaat van enerzijds 1a) gradiënten in langtransport 1b) dwarsverlies richting Appelzak en anderzijds 2) uitgevoerde suppletiewerken ;
- de stabiliteit in Lekkerbek is opmerkelijk: de langs- en dwarstransportverliezen werden grosso modo gecompenseerd door voeding door suppletiewerken in de omgeving (Knokke-Zoute) ;
- het gros van het zand van de onderhoudssuppletiewerken uitgevoerd thv Knokke-Zoute (1300 m<sup>3</sup>/m) is uit het studiegebied verdwenen ;

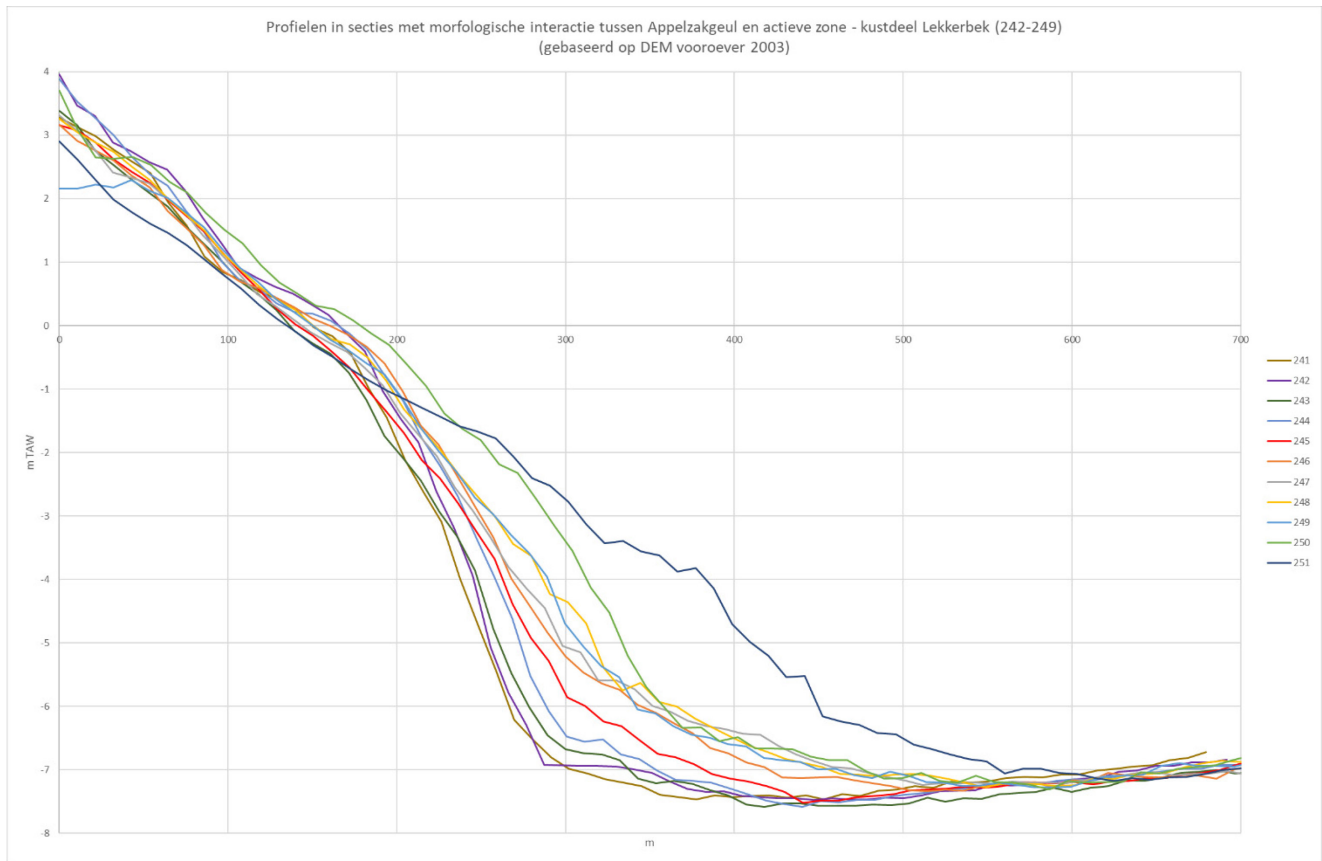
#### **Morfologische interactie met de Appelzakgeul**

Dwarsverlies uit het actieve profiel is te verwachten in de zones waar de diepere vooroever steiler is geworden dan het hoger gelegen deel van het actieve profiel, als gevolg van de morfologische interactie van de Appelzakgeul en de actieve zone.

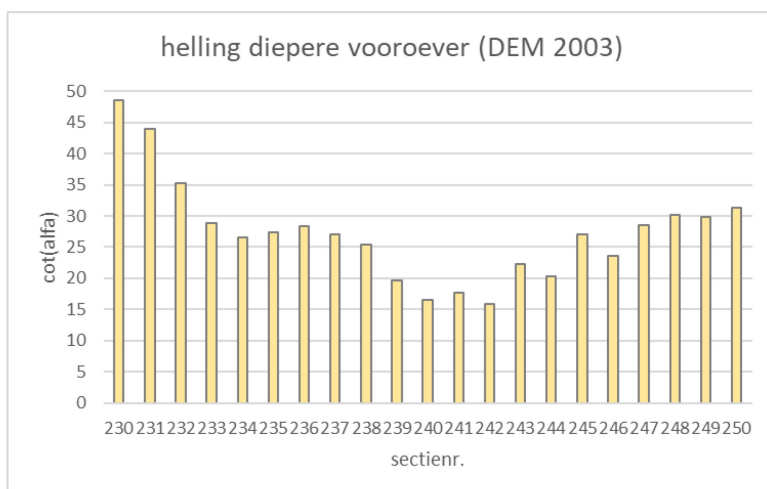
De vooroeverloding van 2003 (14/4/2003) is geselecteerd om te bepalen in welke zones deze morfologische interactie en dus verlies door zeewaarts dwarstransport te verwachten is. Deze opname is midden in de periode van na 1977-79 tot 2020 en ook 4 jaar na een suppletie (in 1999) en daarom is dit de beste opname om te gebruiken voor dit doeleinde.

In elke sectie is in het midden een cross-sectie getrokken door het vooroever-DEM en al deze profielen zijn geanalyseerd. Merk op dat er geen gebruik is gemaakt van het vooroever-DEM nabij strandhoofden omdat in deze zones de morfologie beïnvloed is door de strandhoofden hetgeen niet geregistreerd werd door de single-beam vooroeverlodingen. De profielen zijn getoond op onderstaande 3 figuren (Albertstrand, Knokke-Zoute, Lekkerbek).





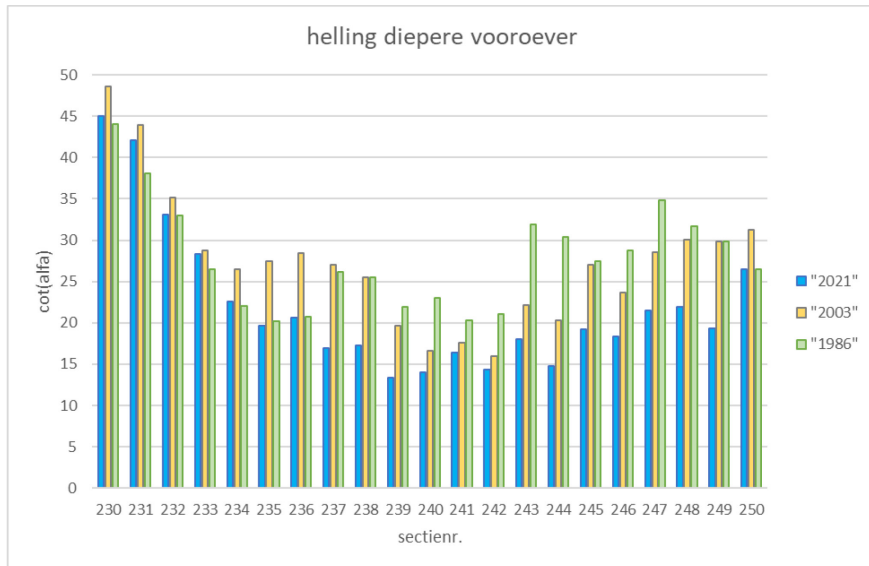
In de secties 230 tot en met 250 is er een steilere diepere vooroever zichtbaar in vergelijking met de helling van het hogere profiel. Een knikpunt tussen beiden bevindt zich rond -0.5 m TAW. Er kan aangenomen worden dat hoe steiler de diepere vooroever is hoe groter het dwarsverlies richting Appelzakgeul is. Deze helling varieert over het gebied en is het steilsth v de grens van kustdelen Knokke-Zoute en Lekkerbek. Zie onderstaande figuur (hellingen bepaald tussen -0.5 m TAW en -4 m TAW).



Op basis van deze informatie kan geconcludeerd worden dat dwarsverlies naar de Appelzakgeul :

- ongeveer even groot is in de kustdelen Knokke-Zoute en Lekkerbek
- van beperkt belang is in kustdelen Albertstrand en Zwin

Een verdieping en/of landwaartse verplaatsing van de Appelsakgeul, waardoor de helling van de diepere vooroever versteilt, zal een toename van het dwarsverlies naar de Appelsakgeul veroorzaken. Een indicatie van het belang hiervan wordt gegeven door de evolutie van de helling van de diepere vooroever te beschouwen in de afgelopen 40 jaar. De hoger bepaalde hellingen anno 2003 worden vergeleken met cijfers op basis van de vooroeverlodingen anno 2021 (G\_VO2021\_1) en anno 1986 (G\_1986V1\_Knok).



Men merkt op dat er in de periode 1986-2021 een versteiling is opgetreden van de diepere vooroever in het kustdeel Lekkerbek en het oostelijke stuk van het kustdeel Knokke-Zoute, waarmee een geleidelijke verhoging van het dwarsverlies gepaard is gegaan. Het is niet geweten hoe sterk de relatie tussen oversteilte en dwarsverlies bedraagt maar tentatief kunnen we als orde van grootte een factor 2 vergroting van het totale dwarstransportverlies in het gebied in 2021 versus in 1986 inschatten.

DEPARTMENT **MOBILITY & PUBLIC WORKS**  
Flanders hydraulics

Berchemlei 115, 2140 Antwerp

**T** +32 (0)3 224 60 35

**F** +32 (0)3 224 60 36

[flanders.hydraulics@vlaanderen.be](mailto:flanders.hydraulics@vlaanderen.be)

[www.flandershydraulics.be](http://www.flandershydraulics.be)